

**MODELING TRANSPORT PHENOMENA IN THE DRYING PROCESS
OF FERMENTED CACAO BEANS**

By

EVANDRO SENA PEREIRA

**A DISSERTATION PRESENTED TO THE GRADUATE SCHOOL
OF THE UNIVERSITY OF FLORIDA IN PARTIAL FULFILLMENT
OF THE REQUIREMENTS FOR THE DEGREE OF
DOCTOR OF PHILOSOPHY**

UNIVERSITY OF FLORIDA

2005

UNIVERSITY OF FLORIDA LIBRARIES

This dissertation is dedicated to my beloved wife, Ann Marie,
and children, Chaps, Chaps, and Ysa - with affection

ACKNOWLEDGMENTS

I would like to express my sincere gratitude to my supervisor, Dr. Klio Y. Chen, for his commendable guidance and advice, throughout my studies at the Agricultural and Biological Engineering Department. I am indebted to Dr. Maria Balaban for the opportune suggestions on how to approach the problems I had to face at the time of my qualifying exam. I am also grateful to the other members of the advisory committee, Dr. C. David Gaid, Dr. A. Tuzman and Dr. S. Iyengar, for their contribution to this project and my progress of study.

The experimental work was carried out at the Brazilian-Chinese Research Center (CBPDC). Therefore, I would like to express my appreciation to Dr. Edna Luz for the support received. I am much obliged to my friends and colleagues: Mauro, Mauro, Angélica S. Mendonça, Rita de Cássia Loureiro, Soraia M. Sousa, Márcio A. Berra, Selma Gesteira, Maria-da-Graça Saviol and Miriam (Raimundo M.) Silva, Antônio W. Silva, Carlos A. Conceição, Ireni B. Sousa, Vera M. Correia and Rosival F. Silva. Their help and collaboration during the hard times of execution of the studies, experiments and laboratory analyses were inestimable.

I am indebted to the Brazilian Council for Research and Technological Development (CNPq) for the financial support provided.

TABLE OF CONTENTS

ACKNOWLEDGEMENTS	iv
LIST OF TABLES	vi
ABSTRACT	viii
CHAPTERS	
1 INTRODUCTION	1
Statement of the Problem	1
Project Objectives	4
2 CACAO PROCESSING	5
Growth and Distribution of Cacao	5
Harvest and Processing of Raw Cacao	6
Cacao Fermentation	7
Drying of Cacao	14
Cacao-Grounding and Chocolate Manufacturing	16
3 LITERATURE REVIEW	19
Drying Theories Used for Cacao and Foods	20
Drying Theories and Related Topics as Applied to Cacao Beans	24
4 MATHEMATICAL MODEL	29
Constitutive Equations	32
Mass and Energy Balance Equations	33
Mass Balance for Dry Solids	36
Balance Equation for Moisture	34
Balance Equation for Amino Acid	35

	Energy Balance Equation	18
	Initial and Boundary Conditions	48
3	MODEL SOLUTION	49
	Finite Difference Approach	49
	Stability Criteria	53
	Gauss-Seidel Algorithm	53
4	EXPERIMENTAL PROCEDURES	54
	Sample Preparation	56
	Drying Tests	57
	Sample Analysis and Moisture Content Determinations	61
	Product Physical Properties	62
	Mass Diffusivity	65
7	RESULTS AND DISCUSSION	68
	Product Physical Properties	69
	Geometric Characterization and Bulk Mass	70
	Relationships for Equilibrium Moisture Content and Latent Heat of Vaporization	73
	Program Testing and Parameter Analysis	77
	Effect of Shrinkage	83
	Drying Curves	88
	Moisture Diffusivity	91
	Model Validation	93
	Temperature Profile	100
	Effect of Ambient Air Relative Humidity	105
	Product Acidity	106
8	CONCLUSIONS	108
APPENDICES		
A	CONSTITUTIVE EQUATIONS	115
B	BALANCE EQUATIONS	117
C	BASIC MASS TRANSFER RELATIONSHIPS	127
D	EXPERIMENTAL AND SIMULATED RESULTS	130

2	FORTRAN PROGRAM FOR SIMULATING TRANSPORT PHENOMENA IN THE DRYING OF FULLY DEPOSED CACAOS BEANS	179
LIST OF REFERENCES		188
GEOGRAPHICAL SKETCH		208

LIST OF TABLES

Table	Page
1.1 Evolution of world maize bean production	2
1.2 Maize-bean-bean systems and Brazilian exports in 1994/1995	3
4.1 Conditions of the drying air used in the experimental tests	58
7.1 Values of parameters product and air temperatures used to generate the temperature profiles of Figure 7.1	76
7.2 Summary of maize-drying experiments	84

LIST OF FIGURES

Figure	Page
2.1. Center of origin and evolution of cacao and other species of the genus <i>Theobroma</i> 11	6
2.2. Major cacao-producing countries 7	7
2.3. Schematic representation of cacao fermentation, principal agents involved in the different stages and resulting metabolic products 10	10
2.4. Flowdiagram of cacao grading, production of butter and powder, and manufacturing of plain chocolate 16	16
4.1. Sections of cacao-leaflets 1. undecomposed showing compact crystalline 2. fermented showing open crystalline 30	30
5.1. Partial view of the node-network representation of the described solution domain 44	44
5.2. Node arrangement for a typical grid point in the interior of a three dimensional region 46	46
5.3. Simplified flow chart of the computer algorithm used to implement the drying model/ numerical solution 54	54
6.1. Schematic representation of the laboratory drier showing centrifugal fan, heater bank, control panel with temperature controller, plenum, temperature sensor and drying tray 58	58
6.2. Typical calibration chromatogram for the high pressure liquid chromatography 61	61

6.3	Definition of cross beam dimensions: length, width and thickness	62
7.1	Relative size changes of fermented cacao beans with moisture content	70
7.2	Calculated date of equilibrium moisture content for fermented cacao beans using Equation 7.4	72
7.3	Total vaporization heat of beaded moisture in fermented cacao beans for different temperatures	73
7.4	Total vaporization heat of beaded moisture in fermented cacao beans for the moisture content range of 0.01 to 0.30	74
7.5	Average temperature profiles from computations for 1, 1 and 3 dimensional domains	76
7.6	Comparison of average moisture profiles for different combinations of equally spaced node numbers in the direction of length, width and thickness	78
7.7	Node distributions along the principal directions used for non-uniform spatial grid	79
7.8	Comparison of average moisture and temperature profiles for different external node volumes used	80
7.9	Change in cacao bean volume with moisture content	81
7.10	Effect of shrinkage term internal on the output of the cacao-drying simulation model	83
7.11	Average moisture loss profiles for cacao beans dried in the air velocity of 2.5 m/s	87
7.12	Drying rate of fermented cacao beans computed for different drying temperatures	88
7.13	Effective moisture diffusivity of fermented cacao beans	90
7.14	Comparison between experimental and preliminary simulated results for cacao-dried at 70°C and 2.5 m/s	92

7.15	Comparison between experimental and preliminary simulated results for maize dried at 60 °C and 2.5 m/s	93
7.16	Moisture profiles for drying experiments at 2.5 m/s	94
7.17	Moisture profiles for drying experiments at 1.5 m/s	95
7.18	Moisture profiles for drying experiments at 1.5 m/s	95
7.19	Moisture profiles for drying experiments at 0.5 m/s	96
7.20	Moisture profiles for drying experiments at 0.5 m/s	96
7.21	Moisture profiles for drying experiments at 0.5 m/s	97
7.22	Moisture profiles for drying experiments at 0.5 m/s	97
7.23	Convective transfer coefficients for heat and moisture	99
7.24	Average temperature profiles for air velocity of 2.5 m/s	100
7.25	Average temperature profiles for air velocity of 0.5 m/s	100
7.26	Simulation of a drying test as average and variable ambient relative humidity and air velocity of 2.5 m/s	102
7.27	Acid concentration profiles for maize dried at 70 °C and 2.5 m/s	104
7.28	Acid concentration profiles for maize dried at 60 °C and 2.5 m/s	104
7.29	Acid concentration profiles for maize dried at 50 °C and 2.5 m/s	105
7.30	Acid concentration profiles for maize dried at 40 °C and 2.5 m/s	105
7.31	Acid concentration profiles for maize dried at 30 °C and 2.5 m/s	106

KEY TO SYMBOLS

a_w	water activity, dimensionless
A	surface area, m ²
B_x	element volume interface area perpendicular to the x direction
B_y	element volume interface area perpendicular to the y direction
B_z	element volume interface area perpendicular to the z direction
c_p	specific heat capacity, J/kg °C
C	mass concentration, kg/m ³
d	beam diameter, m
D	mass diffusivity, m ² /s
e	specific internal energy, J/kg
h_c	convective heat transfer coefficient, W/m ² °C
h_m	convective mass transfer coefficient, kg/m ² s
H_v	latent heat of vaporization, J/kg
\dot{I}	rate of mass production or consumption due to phase change, kg/m ² s
J	Chilton-Colburn j -factor
k	grounded heat transfer through soil area
K_g	grounded transfer coefficient

k	thermal conductivity, W/m °C
l	beam length, m
L_p	generalized photorecological coefficient
m	mass, kg
\mathbf{n}	surface-directed normal unit vector
Pr	Prandtl number
q	heat flow, W
R	ideal gas constant, m ³ Pa/kg °C
Re	Reynolds number
Sc	Schmidt number
t	time, s
T_f	temperature, °C
\mathbf{v}	velocity vector, m/s
V	volume, m ³
w	beam width, m
\mathbf{W}	dry beam momentum-content, deconvol
x	distance in the x direction, m
\mathbf{x}	position vector
y	distance in the y direction, m
Y	ion ionization ratio, deconvol
z	distance in the z direction, m

Greek symbols

ξ_i	retarded-derived normal unit vector
ρ	mass density or concentration, kg/m ³
ρ_s	density of heavy-duty material, kg/m ³

Superscripts

t	time
-----	------

Subscripts

α	scalar and
α	band conversion
i	index for the x direction
j	index for the y direction
k	index for the z direction
l	liquid phase
q	heat
α	state of equilibrium or flow state
s	solids
v	vapor phase
w	mass flow
α'	slipping net (bulk volume)

*Abstract of Dissertation Presented to the Graduate School
of the University of Florida in Partial Fulfillment of the
Requirements for the Degree of Doctor of Philosophy*

**MODELING TRANSPORT PHENOMENA IN THE DRYING PROCESS OF
FERMENTED-CACAO BEANS**

By

Erando Jairo Freire

December, 1995

Chairperson: Dr. Khe Yuen-Chao

Major Department: Agricultural and Biological Engineering

Cocoa is a tropical crop well known for its end product, the chocolate. Before reaching this point, the fresh seeds have to be cured in the farm. Curing involves fermentation and drying, which are essential processes to the development of the chocolate characteristic flavor and color, later, in the manufacturing stages.

The transfer mechanisms related to the drying of cocoa beans are little understood and studied. Most of the research carried-out up to now has focused on large scale drying trials and adaptation of driers used for other products. As a consequence, many farm processing systems have low efficiency and do not yield a competitive product. To achieve higher efficiencies in processing operations, there is need for developing simulation models to predict transport phenomena in the drying of cocoa that take as inputs the physical properties inherent to the product.

A mathematical model, based on the theories of heat and mass diffusion, was derived and used to simulate the drying of fully exposed cheese-brine. The model consisted of four partial differential equations to describe the transfer of solids due to shrinkage, energy, moisture and acetic acid produced during fermentation. This model was also used to determine a regression model for mass diffusivity from drying data as a function of product temperature and moisture. A computer program was implemented to solve the model equations numerically. The control volume approach was used to derive the difference equations which were solved by the explicit finite difference method.

Experimental tests were designed to determine moisture diffusivity in cheese and to validate the model in the temperature and airflow ranges normally used to dry the product. The drying air temperatures varied from 48 to 76 °C, while air velocities were in the range of 0.1 to 3.3 m/s.

Good predictions of average moisture content were obtained with the model. However, it was not possible to drive off perceptible quantities of water used by drying cheese at temperatures up to 62 °C. Therefore, in this respect, artificial drying may not contribute to improve the quality of cheese with high acetic acid concentrations.

CHAPTER I INTRODUCTION

Statement of the Problem

Cacao is a cash crop and the major source of revenue for many producing countries. This has contributed to the large production increases in world production during the past few decades. Global production of dry beans has doubled since 1960 (Table I.1) and reached the record of 2.4 million tons in 1992/93 (Presting, 1994). Area expansion and new plantings in some countries were the principal reasons, rather than increases in productivity and efficiency (Gersh, 1990). This factor and the low elasticity of the product demand have led to a depression in the international market prices. With the current situation the market is most competitive, particularly for those producers that had to modernize farming systems to cope with the need for higher drying capacities and quality standards.

Use of new technologies and services involved significant capital investments and contributed to the total production cost escalation. This is the case for some Asian and South American countries, as opposed to those in West Africa. African production systems are typically low-input, low-output and low-technology systems (Lant, 1990). Latin American countries have the highest total producing costs. The costs for processing

most cases on the same leaves the same tree) and are comparable to those of Asian countries (Edmonfield, 1994)

Table 1.1. Evolution of world cacao bean production (x 1000 metric tons)
(Source: International Cocoa Organization - ICCO, 1993)

Year	1960	1970	1980	1990
Production	1445	1466	1632	2207

Brazilian cacao, in particular, has other problems associated with quality. Chocolate manufacturers are strict on their requirements. They need cacao that can be processed into chocolate with natural flavor (Furnell, 1991). Some have claimed that Bolivian cacao has some undesirable flavors such as contamination by smoke and insect activity. The product originating countries in Europe impose strict standards on Bolivian cacao to the point of not importing any from Brazil. American manufacturers also impose some restrictions. The maximum amount of Bolivian cacao included in their blends is between 30 and 35% (Table 1.2). It is alleged that anything higher than that would alter their product flavor and reduce sales (Salerno, 1991).

There has been a great deal of research effort to apply engineering knowledge to drying of fermented cacao. Studies and improvement of existing drying facilities have been done in Brazil (McDonald and Pinner, 1981, 1992; McDonald et al., 1995; Cadez, 1991). Work to adapt drying equipment used for other grains and to develop new

depress the market has also been clear (Clark, 1973a, 1973b, Fawcett et al., 1984, Cusack, 1989).

Table 3.3. Major cocoa-bean consuming and breeding imports in 1991/1992 (Source: International Cocoa Organization - ICICO, 1993)

Country	Consumption		Breeding imports	
	Per capita (kg)	Total (t)	(t)	(%)
Belgium	5.114	44,000.00	0.00	0.00
Netherlands	4.921	34,600.00	0.00	0.00
Germany	3.279	277,000.00	4.13	1.70
England	3.114	332,400.00	7.87	4.20
France	2.795	235,400.00	0.00	0.00
Netherlands	2.488	34,200.00	9.92	27.40
United States	2.227	944,700.00	129.04	24.06
Canada	1.796	44,400.00	11.66	25.82
Italy	1.287	70,400.00	0.00	0.00
Japan	0.919	320,300.00	10.16	9.30

Despite these efforts, there is need to develop research in this area as a means of better understanding the process and obtaining more reliable information about drying of cocoa. The drying behaviour of a material depends on its physical properties, and very little attention has been paid to the accurate characterisation of cocoa beans with respect to their drying.

It is necessary to face the urgency of the situation and the scarce resources available for research. Field investigations are laborious, time consuming and expensive (Sangh et al., 1993). With precise engineering modeling, it may be possible to design efficient, cost-effective drying systems and sound procedures for processing raw cocoa. Therefore, there is great demand for using more rational approaches to the problem. This involves the use of tools such as mathematical modeling, simulation and optimization techniques. Computer simulation has proved to be useful in getting insight into the physics of transfer processes (Pinto, 1998). The availability of powerful and cheap microcomputers makes these approaches feasible. The final goal is to obtain a more competitive product in terms of both production costs and quality improvement.

Project Objectives

The global objective of this research project was to simulate the drying process of fermented cocoa beans under conditions of fully exposed beans or thin layer drying. The following were the major specific aims:

1. Develop a mathematical model to describe the simultaneous phenomena of mass and heat transfer involved in cocoa-drying.
2. Determine the effective mass diffusion coefficients for fermented cocoa beans.
3. Validate the simulation model under the conditions with which cocoa is normally dried.

CHAPTER 2 CACAO PROCESSING

The Swedish naturalist Carlus Linnaeus (1707-1778) named the species as *Theobroma cacao*. *Theobroma* is the Greek equivalent for "food of the gods" (De Zeeu, 1994). The current literature suggests the use of the word *cacao* to refer to the species and the crop itself, whereas the term *cocoa* should be used for the product (Wood and Lee, 1995), a product obtained in the grinding and manufacturing plants. This nomenclature, however, finds more common and frequent use in the commercial milieu and everyday life.

Origin and Distribution of Cacao

This species and several others of the same genus, which are of importance or of commercial importance, seem to have their origin in the Amazonian region, a center of diversity, where a great populational variation may be found (Wood and Lee, 1995). According to the most accepted theories, two major groups originated from the lower Amazon river basin through the process of natural selection (Smith, 1994). Figure 2.1 depicts the origin and migration of cacao to the major producing regions in the world.



Figure 2.4. Center of origin and evolution of cacao and other species of the genus *Theobroma*
(Source: Adapted from CIPLAC, 1982)

One group is known as *Croton cacao*. It is devoted in the international market to five three-tones. The reason for this lies in the fact that this type of cacao has a much stronger bouquet and distinctive flavor (Williams, 1985). The varieties that belong to this group are presently grown in small areas of some countries in Central America, Caribbean islands, Far East Asia and in some Pacific islands.

The crop itself is very susceptible to plant diseases and it is more exigent in terms of cultivation requirements. Its participation in the total world production is not very significant, however. It may comprise less than 10% of the whole volume traded yearly in the international market. The trend is for less cocoa to disappear, as predicted by some specialists (Powell, 1981).

The second group is usually known as Forastero cocoa or bulk cocoa in the commercial jargon. This kind of cocoa has a weaker chocolate flavor and makes up the bulk of the product marketed in the world (Wood and Lear, 1983). It is grown in some countries of the Americas, Africa and Asian continents, in the so-called cocoa belt (Cedeno, Undated). This region encompasses the equatorial belt, a stage around the globe within 70 degrees of latitude north and south of the equator line (Figure 1.2). Ivory Coast and Ghana are the leaders in the rank of producing countries, accounting for nearly half of the world's production. About 90% of the Brazilian production comes from the southern part of Bahia State (hence, the expression Bahia cocoa used as international trademark).

These two groups present some major differences in the characteristics of their seeds. Forastero-cocoa has cystolates of purple color due to the presence of anthocyanins. It also takes more time to be fully fermented. The Criollo cocoa, on the other hand, has seeds with white or light color anthers. Its fermentation requires a very short time, nearly half or less of that required by Forastero cocoa (Lopez, 1986). The time required for full development of chocolate flavor during cooking is also comparatively shorter.



Figure 3.2. Major cacao producing countries.
(Source: adapted from COTAC, 1989)

Crosses between specimens of these two subtypes produced a third type known as *Lobatale-cacao*. This is a very heteropassive group and its supply in the market is intermediate between the other two groups (Lobatale and *Potomero*, 1985).

Harvest and Processing of Raw Cacao

Harvest of cacao consists of removing ripe and partially ripe pods from the trees. The fruits are then gathered in convenient piles in the field or transported to the fermentation for the task of pod opening and extraction of the seeds. The frequency with

which are then are collected versus maturity from region to region (Jones and Jones, 1983) and with the season.

The time between harvest and seed maturation may also vary. Pod storage for periods of up to 32 days, with other related practices, are recommended in some producing areas for crop conditioning. This procedure helps to achieve better quality by diminishing subsequent mold formation during the curing process (Duman et al., 1989; Alonazy, 1994). Reduction of the bean total acidity enhances chocolate flavor in the seed product (Lima, 1970). Winkler Brown has been found in chocolate prepared from beans with pH values less than 4.5. The occurrence has been verified for samples with pH values above 5.8 (Paul et al., 1989). However, when the weather is very humid and hot, pod storage may not be feasible due to mold development and rapid product decay. Furthermore, conditioning does not always yield the expected outcomes (Dhan and Arula, 1990).

Raw cocoa has to be processed or cured before it can be marketed. Curing is usually done in the farms. The fresh seeds have a moisture content approximately 60% wet basis (Francis and Francis, 1989). In addition, the seed coat has an outer layer made of a mucilaginous and sticky pulp. These characteristics make handling of the fresh material a difficult operation. The raw product is quite unsuitable for long distance shipping and storage.

Curing involves two major practices: fermentation and subsequent drying. Both are equally important to the quality of the product (Lopez, 1994).

Cacao Fermentation

The term *fermentation* is commonly used to describe the physical and chemical changes, which occur in the preparation of the beans before drying. It is considered as a misleading expression by some specialists. Curing has been suggested to provide a more comprehensive picture of the process (Rangp, 1953; Fairyth and Quesnel, 1963; McDonald et al., 1961). This is to reflect physical and chemical complexities of the process, the variety of agents responsible for them, and the association with the drying process.

Microbial or true fermentation takes place in the process, but more important are the subsequent chain of biochemical changes inside the beans. Development of chocolate flavor potential in the product strongly depends on them (Lopez, 1986). Undesired ferment also develops no characteristic chocolate flavor whatsoever, if dried and roasted.

The simplified diagram shown in Figure 2.3 illustrates the chemical changes of cacao fermentation. It is based on data found in several reviews and technical papers published on the subject. It is important to stress, however, that the fermentation stages are not clear cut, there is considerable overlaps among them.

The pulp that surrounds the cacao seed may account for up to 40% of its weight, and nearly 90% of the pulp is water (Frost et al., 1990). It contains an average of about 14% of fermentable sugars. Sucrose is the predominant sugar and its concentration may achieve levels up to 60% of the total sugar content (Roberts, 1979). The pulp is split and,

pH value around 3.5, due to the presence of citric acid. The pulp makes up an adequate substrate for the growth of several categories of microorganisms.



Figure 2.5 Schematic representation of cheese fermentation, principal agents involved in the different stages and resulting metabolite products

Batch fermentation is the most common method used in Brazil. It consists of fermenting the product in wooden containers subdivided into two or more compartments. Each compartment has a volumetric capacity of 1-2 m³. The average output of one compartment varies between 800 and 900 kg of fermented cheese. This process may take from five to seven days (Freire et al., 1992).

The mass of casing in each compartment of the fermenter is turned over and mixed at least once every other day in the course of the process. Turning helps providing aeration (Juliano et al., 1998), and uniformity of the mass undergoing fermentation.

The physical characteristics of the pulp at the beginning of the process help to form a medium of low oxygen tension in the fermenter. The prevailing conditions and the rich substrate allow the proliferation and development of yeasts at first. This group of microorganisms metabolizes fermentable sugars into ethanol and carbon dioxide (Pérez and Galay, 1983). Higher levels of CO_2 , lower acidity and moderate temperature elevation favor the growth of lactic acid bacteria. Production of lactic acid takes place to a greater or lesser extent, depending on the maintenance of adequate conditions.

Simultaneously, the breakdown of the pulp cells, fibers, pectins and other components occurs, helping the drainage of the liquid pulp through the mass of beans. This promotes increasing aeration, which is further achieved by turning the product. Modification in the condition of the medium occurs continuously and induces changes in the type of population of microorganisms that predominate. Eventually acetic acid bacteria prevail over the yeasts and oxidize ethanol into acetic acid, which is further broken down into CO_2 and water. This sequence of reactions involving microorganisms progresses enough fast to raise the product temperature well above the ambient. The temperature of a batch under fermentation may achieve values up to 34 °C (Schwan, 1984).

Acetic acid is the major volatile and present in fully fermented Brazilian corn. Its concentration after six days of fermentation is about 1.3% (Lopes, 1983). Diffusion of

water used over the coagulum leads to acid death (Quarant, 1967). The consequences are the loss of internal compartmentation, prevention of buffer degradation by residues in the fermentation process, and disintegration of the surrounding pulp. Lack of cellular rigidity increases permeability among the cells. This allows better contact between enzymes and substrates (Lohman and Peterson, 1940), and triggers a chain of complex and extremely important biochemical reactions responsible for the formation of compounds generally known as precursors of chocolate flavor.

The beans experience a concomitant and steady change of color, due to enzymatic oxidation, which is responsible for the production of brown pigments. This effect has auxiliary importance in the comparison of chocolate flavor precursors. Moreover, use of color change to monitor and decide when the process ends is a very common practice. After a period of five to seven days, a sharp browning appears around the coagulum. It can be easily seen when the bean is cut open. Color is also used for assessing the quality of dry cacao through the so-called cut test. Despite its convenience in some circumstances, it has severe limitations for evaluating the potential of chocolate as a sample (Lopez and Molinari, 1981).

Overfermentation can cause harm to the product. Higher enzyme activities and lower acidity are the normal conditions at the end of the process. The medium temperature is still high, therefore, the growth of spore forming bacteria occurs (Schone, 1984). They may decrease the quality of the mass of cacao residues in the fermenting box over time. This group of microorganisms produces substances responsible for some odd flavors in the chocolate. Excessively long fermentations cause polychaetae

of the pulp and skin and development of objectionable flavors (Percyck and Quesnel, 1963). Molds and fungi, other than yeasts, may also grow and further spoil the product. They present the greatest problem during drying (Lopez, 1986).

Drying of Cocoa

Drying of the beans should start soon after completion of the fermentation process to avoid deterioration of the wet product. The initial moisture of fermented cocoa beans varies between 58 and 65% wet basis, depending on region, variety and season (Elsbeth and Carles, 1933; McDonald and Fraser, 1980). Drying must bring moisture down to 7 to 8% for safe storage (Caramazza et al., 1990). This results in the removal of large quantities of water, roughly equivalent to half of the freshly fermented bean weight. Fermentation makes drying easier: the pulp decay increases the permeability of the bean shell. Even so, cocoa drying is an energy intensive process.

One should not consider drying of cocoa as a matter of water reduction only. It requires extra care not normally required for other agricultural products. Progression of the oxidative reactions associated with the development of the characteristic chocolate brown color and reduction of bitterness and astringent flavor (McDonald et al., 1981). Drying in this context should be regarded as an integral part of the curing process since it contributes to the improvement of cocoa intrinsic quality.

Sun drying is the most common method used in many countries (McDonald et al., 1980). In Brazil, in particular, it is carried out on flat wooden platforms with shiffling made to protect the beans at night and during rains (Elsbeth and Carles, 1933). The drying

area of these plantations varies from 4 m² in small holdings, to 72 m² in large plantations (Finer et al., 1952). Natural drying is strongly dependent on weather conditions. Its drying rate may take from 7 to 30-days for completion. Weather permitting, it has some advantages. It is a slow process, therefore, it allows for a smooth condensation of the curing sections and their completion to the desired level. On the other hand, the product may be spoiled under bad weather conditions. Low output per unit area and need for regular clearing are also major drawbacks to its use (McDonald et al., 1961). Very often drying has to be finished with the aid of heated air. Artificial drying is especially essential in growing areas where the rainy season coincides with the mango harvest.

In artificial drying the product is subjected to a stream of hot air. Either natural or forced convection are used to force air through a static bed of leaves (McDonald and Finer, 1951). In both cases, indirect heating of the drying air is indispensable to avoid contamination of leaves with products of combustion (McDonald and Finer, 1952). Dried leaves have a better content up to 57% (Ribeiro, 1966), it is proved to effluence against Smoky Borer was a major constraint imposed on Brazilian coconut in the past (Berbert and Lopes, 1979). Sample modifications in the industrial drying facilities have considerably contributed to the solution of this problem (McDonald et al., 1960).

There is a consensus in the literature that the temperature of the product should not reach values much higher than 40 °C before the desired level of becoming is attained. Very high temperatures may accelerate the reactions involved in biochemical changes.

Cacao Grinding and Chocolate Manufacturing

After drying the product may be stored before marketing. Pure cocoa is usually done for very short periods of time, no more than three months. The dried beans are ready to be processed into liquor or chocolate. Figure 2.4 illustrates the basic operations carried out in the processes of grinding, production of cocoa butter, powder, and liquor or plain cocoa mass and manufacturing of plain chocolate. In some plants the whole beans are roasted just after cleaning, then they are cracked and winnowed.

Roasting is one of the most important steps of chocolate manufacturing since it is in this process that chocolate flavors are formed. During roasting, the beans are heated to temperatures between 100 and 120 °C for about 45 to 70 minutes (Wood and Lase, 1983).

Most of the terms used in the diagram are self-explanatory. The word *nit* refers to the pieces of nibs/beans obtained after a coarse grinding. The expression *liquor* is used to designate the mass of cocoa finely ground. The liquor has an average butter content close to 33% (Clark, 1973). The amount of butter in the powder varies according to its end use and manufacturer. High fat powders, containing 12 to 25% of butter, are used for cocoa based drinks, while low fat powders (3 to 13%) are used as food fillers (Wood and Lase, 1983).

Plain chocolate may be obtained from the liquor by addition of butter and sugar. Additional treatments of the mixture, such as conching and tempering, are required to enhance the chocolate flavor.

Conditioning is a practice that consists of subjecting the chocolate paste to a controlled thermal treatment and agitation combined with mechanical shearing. The main aim being improvement due to increase in consistency, elimination of some undesirable residues and controlled oxidation (Cook, 1992). Tempering consists of controlling the cooling the chocolate mass to avoid formation of better crystals.



Figure 2.4 Flowchart of cocoa grinding, production of butter, powder, sugar and plain chocolate

Alkalization is another method used to control insect acidity of some cases. This is a thermal process that consists of treating the silage or hay with an alkali solution. It can be used to produce coarse powder of a diversity of cases in the leaves made to suit the consumer's needs (de Zeeuw, 1934). This treatment was first devised as a tool to improve quality of those cases administered as waste in the market. However, the "Dutch process", as it is known, does not lead to improvement or strengthening of leaves. On the contrary, it has the same effect as insect acidity, that is, it tends to weaken the structural fibres of the untreated product (Clark, 1952).

Caseolene is the principal product derived from fermented cases. Yet many other countries use so many branches of the food, chemical, pharmaceutical and aerospace industries.

CHAPTER 1 LITERATURE REVIEW

Drying is an old activity (Hall, 1988). Man has been using it to preserve his primary food provisions since the prehistoric era by exposing them to the sun and wind (Karel, 1988). This practice has undergone considerable development over the years. Nowadays it is employed as a common means of preparing agricultural and animal products for storage and marketing. The process of drying is one of the most energy intensive operations (Stratella and Lopez-Garcia, 1987). However, it can be made simple and cheap compared to other forms of food preservation. Efficient equipment is available, as a result of effective process design, which can be used with success.

The drying operation consists of extracting moisture from the associated material by supplying energy to it. A conventional method, hot air, is commonly used to heat the product, and its energy causes the moisture driven off from the material. In fact, the term drying applies to the removal of volatile substances from a solid material through heating (Karel, 1988; Meena and Migondec, 1987).

Drying Theories Used for Gums and Foods

Moisture migration in hygroscopic materials may be described by many physical mechanisms as proposed in the literature (van Arkel, 1963; Rames and Chao, 1968;

Brennink and Kadis, 1968; Bruckner et al. 1992)

1. Liquid migration due to capillary action or gradients in capillary pressure.
2. Liquid diffusion due to moisture concentration gradients inside the material.
3. Diffusion of layers of liquid adsorbed on the pore walls due to gradients at these surfaces.
4. The evaporation-condensation mechanism in partially filled pores due to partial pressure gradients.
5. Vapor transfer due to gradients in total pressure occurs when the material surface temperature well above the boiling point.
6. Vapor flow due to density gradients in the medium known as thermal diffusion.
7. Liquid flow in porous materials due to gravitational and centrifugal forces.
8. Effusion flow or Knudsen diffusion when the pore diameter is of the order of the mean free paths of the vapor molecules.
9. Transport owing to osmotic pressure. This type of pressure is a function of the moisture gradient in the medium.

Drying simulation models may be classified according to their capability of coping with one or more of the mechanisms of moisture migration (Rames and Hayakawa, 1977)

They may occur either independently or simultaneously during drying, depending on the conditions and product.

Extensive reviews of the area, development and advances in the theoretical foundations of drying kinetics are presented in Hengstler (1982). They reveal most of the developments and investigation on the use of empirical, semi-empirical and theoretical models. Empirical models do not allow for any aspects of the basic principles of conservation to make predictions about the transfer of mass and energy (Pate, 1999). Their use, therefore, are restricted to the material and conditions for which they were developed (Fulford, 1969). Theoretical models are founded on the principle of conservation, mass and energy conservation. Basically, the approach to drying theory consists of establishing a set of partial differential equations of heat and mass transfer with phase change (Mitsynaka et al., 1988). They may be complemented with the concepts of interactive fluxes of the thermodynamics of irreversible processes (Furtos, et al., 1981).

The mathematical treatment of these models is considerably involved (Furtos and Haykawa, 1992), and especially difficult to validate (Litchfield and Olson, 1982). Besides, the mass transfer coefficients are not amenable to direct measurement in all cases. This is so because drying comprises highly complex interactions between heat and mass transfer. In addition, several simultaneous mechanisms by which moisture migrates within the material may be present (Fulford, 1969). In many instances, the transfer coefficients for the different mechanisms are lumped together or one may be considered as overruling the others. This is usually done for practical reasons, resulting in some

empirical models that are more tractable. Some-empirical models are used in situations where the present state of knowledge and the complexity of the process do not permit a formulation of the problem based solely on theoretical arguments.

Molecular transport, either in the form of liquid or vapor transport, may be used for describing moisture movement during drying. This is represented by Equation (1) for transfer under transient regime (Crank, 1975). Although this is not universally accepted, it seems to be the approach most used for simulating drying behavior of foods and grains.

$$\frac{\partial M}{\partial t} = \nabla \cdot (D \nabla M) \quad (1)$$

where M = moisture concentration

t = time

D = moisture diffusivity

Analytical solution of this partial differential equation with different types of boundary conditions may be expressed as terms of infinite series for bodies of regular geometries (Crank, 1975; Middleton and Davis, 1988). Usually the solution used in drying research is for prescribed or exposed boundary conditions and the assumption of a constant diffusion coefficient.

Diffusion appears to be the most agreed upon controlling mechanism (Henderson and Orm 1963; Peury, 1965; Pao and Duganases, 1980; Sun and Woods, 1994). Isothermal conditions under the product are assumed. When both vapor and liquid migration are present, the diffusion coefficient represents the combined effect of both mechanisms and may be considered as an effective coefficient.

Drying theories as applied to agricultural crops and foods consist of treating the process of heat and mass transfer as a two-component system. That may be a reasonable approach for some materials, where the drying mechanism involves exclusively heat transfer and moisture migration. In most practical situations water is the major constituent of moisture and the only concern. For example, the major function of grain drying is to remove excess water to control the growth of microorganisms.

With other products, however, volatile compounds should be considered. These substances usually play an important role in the organoleptic characterization of the product. Sometimes losses of desirable compounds are deleterious—whereas in other cases it is required to remove undesirable substances to levels acceptable for consumption, depending on the end use of the product.

Acetic acid produced during fermentation and curing of meats is one of the compounds that have to be reduced to desired levels. It seems that acetic acid degradation under the basic curing formulation is not representative of salting and Pickering (1983). Part of it is lost in this stage and in the drying process, as well as during the further stages of ultimate manufacturing.

Gray (1972) suggested the use of the multicomponent diffusion theory for dealing with this kind of situation. This procedure consists of deriving a separate continuity equation for each mass species in the system. When so, it leads to a set of coupled partial differential equations of the form

$$\frac{\partial C_i}{\partial t} = \sum_{j=1}^N D_{ij} \nabla^2 C_j \quad (A.2)$$

where C_i = concentration of species i
 t = time
 D_i = diffusivities and cross diffusivities.

Because of the correspondence between mass diffusion and heat transfer by conduction in solids, both processes may be treated similarly. Therefore, energy may be regarded as another species and included into the system of equations above by adding its mathematical treatment.

Drying Theories and Related Topics as Applied to Cassia Beans

Several reviews and selected papers on drying of cassia can be found in the literature. All the reviews give good account of the process and related topics, the many types of driers in use in different countries (McDonald et al., 1987; Wood and Laro, 1985), and in Brazil (Dantas and Sanches, 1994). The major engineering problems of equipment design, adaptation for cassia and improvement of thermal efficiency are also dealt with (Pillay, 1973b; Cunha, 1981). An important aspect of the subject is the relation between the engineering and biochemical basis of the process (McDonald et al., 1987).

Most of the research work carried out on cassia-drying was concerned with field drying experimentation. Several types of driers were tested with special regard to thermal performance, effect of different drying schemes on the product quality and operational costs. Lumped energy and mass balances were used to develop simple mathematical expressions to calculate coefficients of global efficiency for drying systems. Usually

these coefficients grouped together the efficiencies of fuel combustion, heat exchange and efficiency of the drying process itself.

McDonald et al. (1981, p. 19) proposed the use of the overall drying efficiency (Equation 3.3) to make comparisons among different kinds of drying systems. The definition of this coefficient is given as "the proportion of the energy liberated at the combustion stage which is actually used for the evaporation of moisture with the remaining proportion representing lost heat." Although care is recommended when employing this coefficient, the authors state that it can be useful for comparing different drying systems running under similar conditions. The latent heat of moisture evaporation is assumed constant and equal to that of boiling free water.

$$\eta = \frac{W E}{F C} \quad (3.3)$$

where: η = coefficient of overall efficiency (dimensionless)

W = amount of water evaporated in the process (kg)

E = latent heat of vaporization of water (J/kg)

F = mass of fuel used (kg)

C = combustion heat of the fuel (J/kg)

An exception to this type of approach was presented by Barro and McLean (1973). These researchers investigated the behavior of ovens during drying in packed beds at the maximum temperature recommended in the literature, approximately 63 °C. Regression procedures were used to find the relationship between the time to dry the product to a measure of 6-6N (log base) and as initial moisture content, surface area and bed depth (Equation 3.4). The model was further used as a means of determining

where: This approach may be considered an improvement over what had been done in the

$$\theta = \frac{(X_s - 0.3)}{\exp(-2.6482 + 0.0277U - 66.154R)} + 22 \quad (2-4)$$

where: θ = time required to dry the product to 4-6% dry basis (hours)

X_s = initial moisture content (decimal, dry basis)

U = air velocity (ft/min)

R = length of the static bed of cocoa-product)

Many important components of cocoa-drying are discussed in a review by

McDonald *et al.* (1980). This paper covers a broad area of field research on cocoa-drying and quality of the product. Theoretical aspects that pertain to cocoa itself are examined in purely descriptive terms. Some topics considered are the relation between heat and moisture transfer and water and evaporation, and the interface between this process and fermentation. Loss of water and during-drying seems to be a controversial matter. Some researchers believe that considerable amounts of this loss can be obtained off during drying, whereas others are skeptical about this possibility and state that these losses are derived entirely from the moisture of the beans. The rate of moisture removal is high enough to not allow for sufficient time for acid diffusion and evaporation.

Brune and McGee (1934) seem to be the first researchers to carry out a study on the fundamentals of the drying of cocoa. They investigated drying of fully exposed beans under controlled air conditions and gave a mathematical interpretation to the drying curves. The range of airflow rates and temperatures used were between 0.05 and 1.75 m/s and 17 to 55 °C, respectively. In this work, three distinct drying periods were

observed. Logarithms of the slopes of these portions of the moisture loss curves were empirically correlated to the drying air conditions such as temperature and surface rate (Equations 3-5, 3-6 and 3-7, respectively). The first period, the constant rate period, was given as a function of air velocity and temperature, whereas the last two depended on the drying air temperature only.

$$\ln\left(-\frac{dX}{dt}\right) = -2.48 + 0.0253T + 0.0186U \quad (3-5)$$

$$\frac{d^2(\ln X)}{dt^2} = 0.00565T + 0.114 \quad (3-6)$$

$$\frac{d^2(\ln X)}{dt^2} = 0.0031T + 0.0075 \quad (3-7)$$

where: X = product moisture content (g/moisture dry basis)

t = drying time (hours)

T = air temperature ($^{\circ}\text{C}$)

U = air velocity (m/min)

Analogy of Newton's law of cooling has also been used to describe the constant drying behavior of mass in this layer. An expression for this layer drying may be obtained by analogy to transient heat conduction of a lumped mass subjected to forced convection (Equation 3-8). The primary and important assumption is that the material itself offers negligible resistance to mass transport. The actual resistance to moisture transfer is distributed across the film enveloping the body (Sawyer and Pitts, 1972; Karel and Black, 1980; Insaparam and Devaux, 1990). It is sometimes called the exponential or logarithmic model in the drying literature (Jussabai et al., 1990).

$$\ln(R) = \frac{M - M_e}{M_e - M_0} = \exp(-kt) \quad (3-8)$$

where: $M(R)$ = moisture ratio

M = actual product moisture

M_e = equilibrium moisture content

M_0 = initial moisture content

k = drying constant of the material

t = drying time.

The equilibrium moisture content (M_e) may be defined as the amount of moisture present in the product when its internal vapor pressure equals that of the environment to which it is exposed. This parameter denotes the extent to which a material can be dried under a specified state of the drying air (Corpe, 1973; Steenlike and Kadis, 1980; Baudou et al., 1993).

The expression above resembles the analytical solution of Equation 3.1 for prescribed boundary conditions if the series is truncated after the first term. According to Dan and Woods (1994) Equation 3.8 has a strong theoretical foundation, since it represents the first term of the infinite series. If that was so, then the drying constant would represent the internal resistance to moisture transport. This contradicts the basic assumption behind Newton's law of cooling, which is the lack of internal resistance to moisture transfer.

Similar model was used for cases under different drying air temperatures (Casta, 1940). Two major drying periods were observed. The first was characterized by a constant drying rate that can be more appropriately described by means of analogies to the Newton's law of cooling. The second stage was characterized by a falling rate

behavior, suggesting a change in the type of resistance to moisture transfer. Despite the relatively high amount of free moisture in fermented cassia, only one surface rate of about 0.15 m/s (based on suggestions available in the cassia literature for drying under leach) conditions (Dadebo, 1987; Wood, 1971), was used to obtain the model. Introduction of extra parameters into the Newton's law improves curve fit for cassia as reported by Samson (1984). This is expected, since it is always possible to obtain better fit of a model to a set of experimental data by adding more regression constants to the model. (Jagan et al., 1994)

Although it has been possible to achieve good agreement between experimental and simulated data, these models do not consider some aspects inherent in cassia beans. Some peculiarities of cassia are the size of the beans and the large volume shrinkage that occurs during the drying process. Cassia beans are much larger than common grains. Typical length, width and thickness for freshly fermented beans are 24-35, 11-18 and 4-10 mm, respectively (Chen, 1973b, 1976). These characteristics vary considerably with variety, however. Radiation in bulk volume of cassia during drying may be as high as 30% of the initial volume (Chen et al., 1983). Shrinkage has considerable effect on the response of simultaneous heat and mass transfer models used for drying simulation of beans (Dadebo, 1987).

The literature reviewed confirms that very little is known about the drying behavior of cassia. The models used may fit specific experimental data well, but they can not be generalized. None of them takes into account the special characteristics of cassia beans.

CHAPTER 4 MATHEMATICAL MODEL

Mathematical modeling is a powerful tool for formulating engineering problems in terms of formal mathematical statements so that prediction of future events can be made possible. Nevertheless, a model is a compromise between the complexity of the physical phenomena and the capability of solving the problem, either analytically or numerically (Stanton, 1992).

A model for simulating transport phenomena in the drying of a material should be as complex as possible in order to give in-depth insight into the actual phenomena that take place during the process. The impossibility of measuring some parameters directly in some circumstances does not guarantee the kind of insight claimed in the literature. This is a characteristic of most models (van Brakel and Hoogen, 1974). The higher the number of model parameters, the worse the case.

Also, it is highly desirable to represent reality to the best of the experimental knowledge of the physical parameters available or to be measured. While the model should be realistic, it should be suitable for practical application and use. Besides it should be reliable to prevent mistakes at further stages of equipment design, developing drying schedules and choosing optimum drying conditions (Baldmann, 1993). The quality features of the product should not be put in jeopardy.

A reliable description of the drying behavior of a product depends greatly on the accuracy in modeling the internal and external transports of energy and moisture. Drying of fermented meats is fundamentally a process of simultaneous energy and mass transfer under transient conditions, as it is for many agricultural and food products. Therefore, a simulation model based on the principles of energy and mass conservation was derived. A distributed type of model was preferred because the iteration within the house could be portrayed as a function of location and time (Jayas et al., 1990).

The model consists of a set of three nonlinear partial differential equations, representing general energy and mass balances for the product. Transport of water and steam and air is included in the mass balances. The constitutive equations required for coupling with the internal transfer mechanisms, the initial and boundary conditions for external transfer and completeness of the whole model were also derived. General assumptions underlying the process of development of the model are presented and discussed.

Drying of some structure supply of energy usually by a convective medium, and driving off moisture. Moisture here may be considered as composed of water and the moisture and produced during fermentation. Therefore, a simulation model to be used in this case has to cope with more than one mass transfer component. The model has to be, however, based on some assumptions required by the nature of the product. Fermentation induces some physical changes inside the house. Collapsion of flesh parts are expected and towards approximating a continuous structure. Fermentation causes their separation and reveal the actual physical appearance of the intestine that is, a pair of uncollated or

fermented soybeans (Kook, 1972; Wood, 1973; Latham and Patterson, 1983). Figure 4.1 is a schematic drawing of beans cut open before and after fermentation.

Fermented beans exhibit some small and irregular cracks that run and influence in several directions, notably lengthwise, characterizing a highly complex internal geometry. Loss of cohesiveness makes a realistic mathematical treatment of the problem virtually infeasible. Consequently, there is need for working with effective parameters for mass and heat diffusion.

Constitutive Equations

Drying of agricultural products is a multicomponent transport process. The description of the flows involved in the process and their interactions may be based on the flux relations as derived in Appendix A. The theoretical concepts of irreversible thermodynamics were applied by Fortin and Obert (1961a,b) to develop a mathematical model capable of accounting for the major mechanisms of moisture transfer in the drying of corn kernels.

For a product where the transport of heat and two mass components (water and water vapor) take place, the following set of linear combinations may apply

$$\begin{aligned} J_q &= L_{qT} \nabla T + L_{qH} \nabla p_H + L_{qV} \nabla p_V \\ J_H &= L_{HT} \nabla T + L_{HH} \nabla p_H + L_{HV} \nabla p_V \\ J_V &= L_{VT} \nabla T + L_{VH} \nabla p_H + L_{VV} \nabla p_V \end{aligned} \quad (4.1)$$



Figure 4.1. Sections of cacao beans (not to scale)
 1. unfettered showing compact cotyledons (left)
 2. fettered showing open cotyledons (right)

The fluxes of heat, water and acids will be functions of the strength and vector driving forces that is, the gradients of temperature, water and the acids compound chemical potentials. In other words, the flux of energy is not only a function of the temperature gradient, but also of mass distribution. Likewise, mass transports depend on the differences of chemical potentials and on thermal diffusion.

Equations 4.1 form a set of constitutive equations. They describe the response behavior of a particular product in the course of a change process induced by one or more

driving potentials. Therefore, they allow for an understanding of the phenomena involved in such a process.

Unfortunately, it is difficult to measure gradients of chemical potentials experimentally (Jiles and Madsen, 1982). The equations mentioned above may be rewritten by expressing the driving forces in terms of gradients of temperature and concentrations of the chemical compounds involved in the process (Equation 4.2). Here the principles of thermodynamics of irreversible processes do not apply. The matrix of coefficients K is not symmetric. Its elements are not constant and may take positive or negative signs. Actually, they are function of temperature and concentrations. This approach is related to in the mass transfer literature as the generalized Fick's law (Taylor and Krishna, 1993), combined with the Fourier law of heat conduction

$$\begin{aligned} J_x &= -K_{xx} \nabla T - K_{xy} \nabla C_x - K_{yx} \nabla C_y \\ J_y &= -K_{yx} \nabla T - K_{yy} \nabla C_y - K_{xy} \nabla C_x \\ J_z &= -K_{zz} \nabla T - K_{zx} \nabla C_x - K_{xz} \nabla C_y \end{aligned} \quad (4.2)$$

In practice, the crosswise coefficients or influences are negligible and very often disregarded (Kory, 1972). Equations (4.2) may be simplified by assuming that the interference of water and concentrations on the other side was negligible or had no effect at all. This assumption may be founded on the fact that water used is present at low concentrations. In comparison with that of water, it is smaller by a factor of nearly 100 for wet gases.

The equations were further modified and uncoupled by allowing for the dependence of the mass and thermal diffusivities on the concentration of water and

temperature. It was assumed that the diffusivity of water and did not depend on its own concentration. Therefore, a set of equations analogous to those of Fourier for heat conduction and Fick for mass transfer was obtained as given below

$$\begin{aligned} \mathbf{J}_q &= -k \nabla T(\mathbf{x}, t) \\ \mathbf{J}_m &= -D_m \nabla C_m(\mathbf{x}, t) \\ \mathbf{J}_s &= -D_s \nabla C_s(\mathbf{x}, t) \end{aligned} \quad (4.1)$$

Mass and Energy Balance Equations

Mass and energy balance equations were derived from the fundamental principles of conservation and they form the core of the mathematical model. The approach used here for deriving the general mathematical model is similar to that found in the literature on transport phenomena for homogeneous and heterogeneous flows (Bird, 1963; Sieder, 1964; Slattery, 1967, 1981). It is usually called the macroscopic or integral formulation. It is preferred because it is more general compared to the differential procedure, since it applies to volumes of arbitrary shape and size. It consists of applying the basic conservation laws in integral form to a control volume to obtain the local intensive forms. Jump balances apply to variables that suffer discontinuities at phase change interfaces. A summary of the theoretical foundations and the derivation of the generalized equations are presented in Appendix B.

Mass Balance for the Dry Solids

Dry matter occupies the whole bean volume that shrinks during dehydration. If the assumption that the mass of water forms a continuous medium can be accepted, then no abrupt or sharp transition occurs with this component, even at the phase interface. Also no dry solid covers the external surface, which moves due to shrinkage. There is no source or sink of dry matter in the medium, hence, the principle of conservation of mass assures that the total amount of steady-dry solids in the whole volume remains constant. The concentration of this component changes due to shrinkage, though. Since this constituent is conserved, the equation for conservation of mass derived in Appendix B can be used for the present purpose with slight modifications to obtain the following equation:

$$\frac{\partial \rho_s}{\partial t} = -\nabla \cdot \mathbf{J}_s \quad (B.4)$$

Inside the bean there is a flux of dry matter given by the velocity of shrinkage and transport of dry material occurs in the opposite direction of the transfer of moisture (Ferguson et al., 1990):

Balance Equations for Moisture

Moisture exists in the wet product as both liquid and vapor. A first assumption to make here is that there is a sharp and well-delimited separating front within the bean. The liquid phase is confined by this surface interface. This phase

interface recedes at an arbitrary speed as drying proceeds. The speed of displacement is equal to the component of the velocity vector with respect to the unit vector normal to the interface.

The heat shell is considered as part of the volume and, therefore, presents no extra resistance to mass transfer. This is justifiable because it is relatively thin in comparison with the overall dimensions.

Molecular mass transport is assumed to occur in each phase (either liquid or vapor), but phase change from liquid to vapor occurs at the phase interface. At this surface instantaneous conditions of equilibrium are assumed to prevail. Therefore, this situation is analogous to transport phenomena for more than one species. The generalized balance equations for species and the jump conditions of flux at the singular interface are also derived in Appendix B. Therefore, the following expressions may be used for moisture

1. Liquid phase

$$\frac{\partial \rho_1}{\partial t} + \nabla \cdot (\rho_1 \mathbf{v}_1) = 0 \quad (4.2)$$

2. Vapor phase

$$\frac{\partial \rho_2}{\partial t} + \nabla \cdot (\rho_2 \mathbf{v}_2) = 0 \quad (4.3)$$

3. Flux at the phase interface

$$\rho_1 (\mathbf{v}_1 - \mathbf{v}_0) \cdot \mathbf{e}_0^2 = \rho_2 (\mathbf{v}_2 - \mathbf{v}_0) \cdot \mathbf{e}_0^2 \quad (4.4)$$

The conversion of liquid into vapor, which is the actual flow phenomenon at the jump interface may be considered as sink of liquid and source of vapor in the corresponding

phase (Sikury, 1972). This is an analogy to heterogeneous chemical reactions. Thus the phase interface flux conditions may be added to the phase balance equations by expressing them in terms of rates of mass production and consumption, as appropriate:

1. Liquid phase

$$\frac{\partial P_L}{\partial t} = -\nabla \cdot \mathbf{J}_L + I_L \quad (4.6)$$

2. Vapor phase

$$\frac{\partial P_V}{\partial t} = -\nabla \cdot \mathbf{J}_V + I_V \quad (4.7)$$

3. Both phases

$$\frac{\partial P_m}{\partial t} = -\nabla \cdot \mathbf{J}_m \quad (4.8)$$

Balance Equation for Ionic Acid

A reasoning similar to that used for molasses gives the following partial

differential equation

$$\frac{\partial P_A}{\partial t} = -\nabla \cdot \mathbf{J}_A \quad (4.9)$$

Energy Balance Equation

Heat conduction and mass diffusion are analogous phenomena. Consequently, expressions corresponding to Equations 4.3 and 4.5 apply to the substrate, and 4.7 to the phase interface. This analogy leads to the following mathematical expression

$$\frac{\partial T}{\partial t} = -\nabla \cdot \mathbf{J}_T \quad (4.10)$$

This modeling approach may be further simplified by assuming that moisture evaporation takes place at the external surface. That is, the evaporation front and external surface coincide and move with unitary displacement speed. For many fish specimens it is quite reasonable, at least during most of the drying process. Carcin has high initial moisture content and relatively low temperatures are used in drying to preserve its surface characteristics, mainly those related to flavor. Such simplification leads to a model where the energy and mass balance equations become coupled by their boundary conditions. This may be accomplished by including terms that account for the latent heat of vaporization in the expressions for the boundary conditions. The contribution due to the evaporation of water may be neglected, since it is present in very small concentrations. Equation 4-4 needs not be solved formally. The beam volume may be allowed to change with position in the numerical procedure.

By expressing concentrations in terms of mass ratio based on the weight of the bone-dry material (dry basis) and substituting the energy content for an expression in terms of temperature, the following set of mass and energy balance equations are obtained:

$$\begin{aligned}\frac{\partial W}{\partial t} &= \nabla \cdot (D_0 \nabla W) \\ \frac{\partial C_i}{\partial t} &= \nabla \cdot (D_i \nabla C_i) \\ \rho C_p \frac{\partial T}{\partial t} &= \nabla \cdot (k \nabla T)\end{aligned}\quad (4.12)$$

This is a set of nonlinear partial differential equations in the mass ratios of moisture (W), acetic acid (A) and temperature (T), where the thermal properties of the material and the diffusion coefficients vary with either temperature or moisture content or both. It is assumed that the muscle behavior inside the canner basket is isotropic.

Initial and Boundary Conditions

Three auxiliary conditions describe the physical situation at the onset of a change process and on the boundary of the domain of the partial differential equations. They are required to guarantee the uniqueness of the model solution (Furrow, 1982). The initial distribution of the potential variables: temperature, moisture content and acetic acid mass ratio, may be assumed to be uniform and constant throughout the bean volume. The initial conditions for the model are given by the following expressions:

$$1. \quad \text{Moisture} \quad W(x, 0) = W_0, \quad x \in V \quad (8.14)$$

$$2. \quad \text{Acetic acid} \quad A(x, 0) = A_0, \quad x \in V \quad (8.15)$$

$$3. \quad \text{Temperature} \quad T(x, 0) = T_0, \quad x \in V \quad (8.16)$$

The boundary conditions are given by the following relationships:

1. Moisture

$$-D_{eff} \rho_s \frac{\partial W}{\partial z} = h_d [T(x, t) - T(\infty, t)] \quad z = S \quad (4.17)$$

This is a nonhomogeneous boundary condition of the third kind. The drying air boundary ratio depends on case.

2. Acetic acid

$$A(x, t) = 0, \quad z = S \quad (4.18)$$

This is a homogeneous boundary condition of the first kind. Acetic acid concentration is assumed to be zero at the beam surface¹

3. Temperature

$$-k \frac{\partial T}{\partial z} = h_d [T(x, t) - T(\infty, t)] + h_{ac} [T(x, t) - T(\infty, t)] W_{ac} \quad z = S \quad (4.19)$$

This boundary condition is more complex, since it involves latent heat of vaporization. The drying air temperature is constant. Other conditions are the same as before.

Involvement of the set of constitutive equations (4.5) into the corresponding balance equations (4.17) results in a set of partial differential equations that together with the auxiliary conditions make up the mathematical model to be solved.

¹The use of this type of boundary condition for acetic acid is justifiable due to its higher volatility as compared to that of pure water. On evaporation, it diffuses quickly through the convective medium as it is not so sticky significant resistance in the air film that surrounds the product (Kerry, 1977).

CHAPTER 3 MODEL SOLUTION

Equations 4-13 and their initial and boundary conditions 4-14 to 4-18 are the basis for the mathematical model developed to simulate the drying of cacao. This is a set of nonlinear partial differential equations. They characterize propagation problems (Ames, 1977), with dissipation effects. This type of equations is usually associated with diffusion processes (Anderson et al., 1984), where the fluctuations of the solution (in m seconds) add to the marching procedure progresses with time. These equations are not amenable to analytical solution, therefore, a numerical procedure was used (opted). Among the many numerical schemes available, the explicit finite-difference technique was used.

Finite-Difference Approach

The basic idea underlying the formulation of finite difference methods is to represent the problem governing differential equations and their boundary conditions by discretized counterparts or approximate difference equations (Smith, 1978). As a consequence, approximations to the solution of the differential equations are searched for selected and well defined points, rather than everywhere in the domain. This leads to a set

of algebraic equations either linear or nonlinear, depending on the nature of the original differential equations.

Crucial beams have approximately an oval shape when fully wet, becoming flatter as saturation is lost. They were assumed to have the shape of their disks with average measured length, width and thickness. This simple geometry was adopted to reduce computational time because, if successful, this single beam model would be incorporated into a block bed drying model.

The following mass ratios between length (l), width (w) and thickness (depth = d) apply to crucial beams:

$$\begin{aligned} \frac{l}{w} &= 1.865 & \text{and} & & \frac{w}{d} &= 2.768 \\ \frac{d}{l} &= 0.361 & \text{and} & & \frac{l}{d} &= 2.634 \\ \frac{w}{l} &= 0.536 & \text{and} & & \frac{l}{w} &= 1.865 \end{aligned} \quad (8.4)$$

Typical mass values of these parameters are 2.439, 1.308 and 0.881 cm , respectively for length, width and thickness (Black, 1976).

The assumed continuous domain was then replaced by a three dimensional domain configuration, at first with unequal side spacing in the x , y and z directions. Discretization of the domain was carried out for only one eighth of the disk volume because of the symmetry of the problem. This resulted in boundary conditions of no heat

The solution of a partial differential equation-describing a physical process may be accomplished in different ways (Anderson et al., 1984)

1. Taylor's series expansion and truncation
2. polynomial fitting
3. semi-integral method
4. control volume method.

The last option was used here for the inherent advantages of this method of approximating the governing equations. It allows for direct use of the fundamental conservation principles of physics, giving better insight into the phenomenon behind the problem to be solved. Numerical schemes derived from these principles are said to have the conservative property, that is, they maintain the conservation statement locally in the neighborhood of each mesh point, and throughout the domain, including the boundary nodes, in the process of assembling the single node differential equations. Such schemes represent the problem governing equation accurately and are said to be consistent (Anderson et al., 1984). The Lax equivalence theorem guarantees that a consistent numerical scheme converges to the original partial differential equation if it is stable. Hence, the convergence problem reduces to that of finding the appropriate values of the increments in the independent variables to achieve stability (Aches, 1977).

Formulation of the difference equations was based on the three-dimensional, centered or computational molecule as depicted in Figure 5.1. In this fashion, the mass of each elemental volume of the spatial grid is considered as concentrated at the mass of the molecule. The control sphere in the figure is highlighted for illustrating purposes only

It is connected by imaginary conducting rods to six surrounding nodes. This computational molecule represents a typical interior node with its associated elemental volume and interface areas. The axes x , y and z of the coordinate system are identified with the index letters i , j and k , respectively. Distances between two adjacent nodes are Δx , Δy and Δz in the corresponding directions.

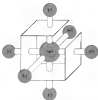


Figure 5.2 Node arrangement for a typical grid point in the interior of a three-dimensional region.

Transient energy flows from the neighbour towards the central node of the computational molecule are balanced as in Equation 5.2 (Kerfoot and Black, 1988)

$$\left[\text{change in the internal energy} \right]_{\text{of node } (i,j,k) \text{ during } \Delta t} = \sum_{n=1}^{N_{\text{cell}}} \dot{Q}_{n,i,j,k}$$

Using Fourier's law and an expression for the energy associated with the node (i,j,k) yield the following difference equation:

$$\begin{aligned} \rho c_p \frac{(T^{n+1} - T^n)_{i,j,k}}{\Delta t} \Delta V = & \\ k_{n+1/2} B_x \frac{(T_{i+1/2} - T_{i-1/2})^n}{\Delta x_1} + k_{n+1/2} B_y \frac{(T_{i+1/2} - T_{i-1/2})^n}{\Delta x_{n+1}} + & \\ k_{j+1/2} B_x \frac{(T_{i,j+1/2} - T_{i,j-1/2})^n}{\Delta y_1} + k_{j+1/2} B_y \frac{(T_{i,j+1/2} - T_{i,j-1/2})^n}{\Delta y_{j+1}} + & \\ k_{k+1/2} B_x \frac{(T_{i,j,k+1/2} - T_{i,j,k-1/2})^n}{\Delta z_1} + k_{k+1/2} B_y \frac{(T_{i,j,k+1/2} - T_{i,j,k-1/2})^n}{\Delta z_{n+1}} \end{aligned} \quad (5.3)$$

A method of testing the modulus thermal conductivity consists of averaging the property at two adjoining grid points (Faulkner, 1988). Therefore, the thermal conductivities, for example, $k_{i+1/2}$ and $k_{i-1/2}$ are evaluated as the average of the values of two adjoining nodes, that is, the nodes $(i-1/2)$ and $(i+1/2)$, respectively.

The terms on the right hand side of Equation 5.3 change if the nodes are located on the surfaces of symmetry and external faces of the disk. There is no heat flux across the planes of symmetry and those nodes on the external surfaces exchange energy with the drying medium through convection and vaporization of moisture. Nodes on the planes

of symmetry and so the external surfaces have characteristic dimensions that are different from those of the interior nodes. A subroutine was developed to calculate material dimensions, surface areas and volumes for the various types of nodes in the domain. Derivation of the various node equations is a repetitive task. Therefore, finite difference equations are presented for a few surface nodes, as examples.

Node (I, J, K) the outer node, has three surfaces of symmetry, which are equivalent in calculating surfaces and three conducting nodes. Therefore, this node is surrounded by three nodes with which it exchanges energy. Equation 3.3 can be modified as follows:

$$\begin{aligned}
 \rho c V_r \frac{(T^{n+1} - T^n)_{I,J,K}}{\Delta t} \Delta V_{I,J,K} &= 0 & + k_{x=1} B_x \frac{(T_{x=1/2} - T_{I,J,K})}{\Delta x_{x=1}} + \\
 0 &= 0 & + k_{y=1} B_y \frac{(T_{y=1/2} - T_{I,J,K})}{\Delta x_{y=1}} + \\
 0 &= 0 & + k_{z=1} B_z \frac{(T_{z=1/2} - T_{I,J,K})}{\Delta x_{z=1}} \quad (3.4)
 \end{aligned}$$

A node located on the internal surface, such as node (J, m, n), exchanges heat by convection and through phase change with the medium. The corresponding difference equation is of the form

$$\begin{aligned}
& \rho \omega_s \frac{(T^{n+1} - T^n)_{i,j,k}}{\Delta t} \Delta V = \\
& k_{n+1} B_s \frac{(T_{i,j,k} - T_{i,j,l})'}{\Delta x_{i,j}} + h_s B_s (T_a - T_{i,j})' + \\
& k_{n+1} B_s \frac{(T_{i,j,k} - T_{i,j,l})'}{\Delta y_{i,j}} + h_s B_s (T_a - T_{i,j})' + \\
& k_{n+1} B \frac{(T_{i,j,k} - T_{i,j,l})'}{\Delta x_{i,j}} + h_s B (T_a - T_{i,j})' = B'_{\text{th}} \quad (9-9)
\end{aligned}$$

where P'_{th} is the total heat loss owing to the amount of moisture vaporization accumulated with that particular node, and T_a is the temperature of drying air.

The left-hand side of these equations refer to the rate rate of accumulation of internal energy in the volume associated with the specific element. Since the specific heat capacity varies with temperature and moisture the numerical solution requires iteration to improve accuracy and, thus, to deal with the nonlinear nature of the differential equations. For most situations two to three iterations are sufficient to attain the accuracy desired (Sunderman et al., 1994). Another approach is to calculate the properties for the current time level (or that of the temperature and moisture at the last time level) (i.e., plus half the change in temperature and moisture during the last time step).

The difference equations for moisture transfer are quite the same, except for the boundary nodes and treatment term. By expressing the product moisture content as mass

rate with respect to the mass of dry solids and using Fick's law instead of Fourier's, the following expression can be written:

$$\begin{aligned} & \frac{(W^{n+1} - W^n)}{\Delta t} \Delta V = \\ & D_{n+1} S_1 \frac{(W_{1,1,1} - W_{1,1,2})}{\Delta x_1} + D_{n+1} S_2 \frac{(W_{2,1,1} - W_{2,1,2})}{\Delta x_{2,1}} + \\ & D_{n+1} S_3 \frac{(W_{3,1,1} - W_{3,1,2})}{\Delta x_3} + D_{n+1} S_4 \frac{(W_{4,1,1} - W_{4,1,2})}{\Delta x_{4,1}} + \\ & D_{n+1} S_5 \frac{(W_{5,1,1} - W_{5,1,2})}{\Delta x_5} + D_{n+1} S_6 \frac{(W_{6,1,1} - W_{6,1,2})}{\Delta x_{6,1}} \end{aligned} \quad (3-6)$$

The numerical solution of the equation requires no iteration. The procedure is approximate: the value of mass diffusivity between two adjacent nodes points of the same material used for thermal conductivity.

Nodes on the surfaces of symmetry are treated exactly in the same way as in the preceding case. There is no external surface exchange (neither through convection with the drying air). This process is analogous to heat transfer by convection without phase change. Therefore, the difference equation (3-7) can be applied. Conditions of equilibrium on the external boundaries are assumed to exist. This implies that the vapor pressure on the external surface equals that of the air in close contact with the product. In the expression below this situation is given in terms of humidity ratio (X) of the air in equilibrium with the moisture content of the surface volume elements. The driving force is the difference between this humidity ratio and that of the drying air. Conditions of

equilibrium can be obtained from curves of moisture isotherms determined for the product. The density of the bone-dry material (ρ_s) is constant

$$\begin{aligned} \frac{(W^{t+\Delta t} - W^t)_{i,j,k}}{\Delta t} \Delta V &= \\ D_{x,x} B_x \frac{(W_{i,j,k+1} - W_{i,j,k})'}{\Delta x_{i,j}} + \frac{h_{x,x} B_x (T_{x,i} - T_{x,j})'}{\rho_s} + \\ D_{x,y} B_y \frac{(W_{i,j,k+1} - W_{i,j,k})'}{\Delta x_{i,j}} + \frac{h_{x,y} B_y (T_{x,i} - T_{x,j})'}{\rho_s} + \\ D_{x,z} B_z \frac{(W_{i,j,k+1} - W_{i,j,k})'}{\Delta x_{i,j}} + \frac{h_{x,z} B_z (T_{x,i} - T_{x,j})'}{\rho_s} \end{aligned} \quad (8.7)$$

Equations for water and air developed with the same approach used for moisture. The boundary conditions on the external surfaces are simpler, however. Zero concentration was imposed at the elements on these surfaces. For the external boundary nodes

$$\begin{aligned} \frac{(A^{t+\Delta t} - A^t)_{i,j,k}}{\Delta t} \Delta V &= D_{x,x} B_x \frac{(A_{i,j,k+1} - A_{i,j,k})}{\Delta x_{i,j}} + \\ D_{x,y} B_y \frac{(A_{i,j,k+1} - A_{i,j,k})}{\Delta x_{i,j}} + D_{x,z} B_z \frac{(A_{i,j,k+1} - A_{i,j,k})}{\Delta x_{i,j}} \end{aligned} \quad (8.8)$$

For the other node types the finite difference equations match exactly the corresponding equations derived for moisture transfer.

Stability Criteria

The transport-difference equations for interior nodes, as represented by Equation 13, can be rearranged to yield expressions explicit in terms of temperature T as follows:

$$\begin{aligned} T_{i,j,k}^{n+1} = & \frac{k_{i,j,n}}{\rho C_p} \Delta t \frac{\partial_i}{\partial x_i \Delta F} T_{i,j,k}^n + \frac{k_{i,j,n}}{\rho C_p} \Delta t \frac{\partial_i}{\partial x_{i+1} \Delta F} T_{i+1,j,k}^n + \\ & \frac{k_{i,j,n}}{\rho C_p} \Delta t \frac{\partial_i}{\partial y_i \Delta F} T_{i,j+1,k}^n + \frac{k_{i,j,n}}{\rho C_p} \Delta t \frac{\partial_i}{\partial y_{i+1} \Delta F} T_{i,j+2,k}^n + \\ & \frac{k_{i,j,n}}{\rho C_p} \Delta t \frac{\partial_i}{\partial z_i \Delta F} T_{i,j,k+1}^n + \frac{k_{i,j,n}}{\rho C_p} \Delta t \frac{\partial_i}{\partial z_{i+1} \Delta F} T_{i,j,k+2}^n + \\ & \left[1 - \Delta t \left[\left(\frac{k_{i,j,n}}{\rho C_p} \frac{\partial_i}{\partial x_i \Delta F} + \frac{k_{i,j,n}}{\rho C_p} \frac{\partial_i}{\partial x_{i+1} \Delta F} \right) + \right. \right. \\ & \left. \left(\frac{k_{i,j,n}}{\rho C_p} \frac{\partial_i}{\partial y_i \Delta F} + \frac{k_{i,j,n}}{\rho C_p} \frac{\partial_i}{\partial y_{i+1} \Delta F} \right) + \right. \\ & \left. \left. \left(\frac{k_{i,j,n}}{\rho C_p} \frac{\partial_i}{\partial z_i \Delta F} + \frac{k_{i,j,n}}{\rho C_p} \frac{\partial_i}{\partial z_{i+1} \Delta F} \right) \right] \right] T_{i,j,k}^n \end{aligned} \quad (14a)$$

According to the maximum principle, the coefficients for temperature on the right-hand side of Equation 14 should be nonnegative and sum to one (Ames, 1977).

This fact allows for the calculation of the stability criterion at the value of the time increment to assure stability for the energy equations. Specifically, it has to be such that the coefficient associated with $T_{i,j,k}$ at time t in Equation 5.9 is equal or greater than zero. This same criterion has to be applied to all finite difference equations (involving, for

Computational Algorithm

A computer program was written in FORTRAN to implement the numerical solution of the model. A listing of the program is given in Appendix E. The flowchart of Figure 3.3 shows the major calculations used by the main program to carry out the numerical procedure. The main program, module CACAO (BURNING), consists of three nested loops for the three independent space variables inside a fourth loop for time. In addition, it is used to input process data and to output results from the computations.

Subroutine CRUD is used to calculate the geometric parameters for the spatial mesh used in the numerical solution of the model. It is called inside the time loop to assemble the initial space discretization and then to update the mesh characteristics to reflect physical changes due to moisture content. The subroutine CRUD generates nodes in the three dimensions that are not equally spaced, so as to have nodes with smaller volumes near the material boundaries (Figure 3.3).

Modules TEMPERATURE, MOISTURE and ACETIC ACID are called inside the time loops to compute temperature, moisture content and acetic acid concentration at each grid point and time step. The marching procedure starts at the most internal mesh

point, node (1,2,3) and proceeds outwardly until the most-external point is reached, node (5,4,4). The computations for each time increment are done using data from the previous time level.

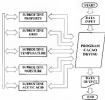


Figure 3.3. Simplified flow chart of the computer algorithm used to implement the drying model numerical solution.

The block PROPERTY, in the diagram, comprises a set of modules to compute product properties and drying air physical and psychrometric parameters. It also includes other auxiliary modules to compute average retentate time profiles for the dependent variables. In addition, four subroutines of the National Research Institute package (Peters et al., 1982) were also incorporated into the program to be used in the procedure

the measuring mass diffusivity. They were used to fit cubic splines to the drying data, compute slopes of drying curves, perform numerical interpolation and to search ordered tables of data.

The mass module and the submodules **CAD TEMPERATURE**, **MOISTURE**, **ACETIC ACID** and some modules of the **PROPERTY** block store data stored in external blocks of memory (Figure 3.7).

The program was tested and used to appraise the response behavior of the model relative to changes in some input parameters namely, domain dimensions, grid refinement and time increment, drainage time step, drying air relative humidity and velocity. A modified version of the original program was employed to determine mass diffusivity from the drying data. Then **CAD DRYING** was used to simulate the drying process of various forms by utilizing the proposed model.

CHAPTER 4 EXPERIMENTAL PROCEDURES

Due to the lack of availability of mango in Florida and the susceptibility to pack deterioration of the fermented mango, the research experimental work was carried out at the Brooklyn-Corcoran Research Center in Baltimore, Talca State, Brazil.

Sample Preparation

The product used in the experimental trials was mango obtained from ripe and partially ripe pods kept in the field for two to three days after removed from the trees. The fresh pods were taken to the fermentary and fermented regularly for six days in 1 m³ batches, following standard procedures and recommendations for handling and selection of the product during the process. After completion of fermentation, samples of approximately 12.5 kg were taken randomly from a single fermentation box and stored for no more than one week in a large freezer. This amount of mango was sufficient to carry out the set of four drying tests planned for five to six working days. Prior to cold storage, the samples from the fermenter were divided into four 3.5 kg samples and placed into plastic bags. The next samples were taken from the freezer the day before and left at ambient temperature (between 25 and 30 °C) overnight to defrost and equilibrate to room

temperature. This process required from 18 to 30 hours. Each set of tests consisted of four drying temperatures and one air velocity.

Drying Tests

Drying tests of fully hydrated maize heads were carried out to obtain moisture and weight loss curves to determine the effective diffusivities for these compounds and to validate the mathematical model. These tests were done in a laboratory drier depicted in the schematic diagram of Figure 6.1.

The test drier consisted of a centrifugal blower driven by a 0.375-kW and 2850 RPM motor that delivered ambient air to a bank of four electric resistance heaters with a combined rating of 7.5 kW. A control panel was used for controlling the system operation. The electric current to one of the heaters was controlled by a Foster Cambridge Clinequip (model F154L) controller. The drying air temperature could be maintained to within $\pm 0.5^{\circ}\text{C}$ of the set value. The test sample was held on the screen tray (0.3 m in diameter), rotated on a conical planetary distributor. The air velocity was measured with a Laidrich-KG vane anemometer. Temperature of the drying air well upstream of dry bulb and wet bulb temperatures were monitored by means of type K thermocouples (diameter about 0.34 mm) connected to a 12-point Foster Cambridge temperature recorder.



Figure 6.1 Schematic representation of the laboratory-dryer showing centrifugal fan (A), heater bank (B), control panel (C) with temperature controller (D), phosor (E), temperature sensor (F) and drying tray (G)

The temperature recorder was calibrated against an Omega Engineering precision calibration model CL 650 (precision $\pm 1^\circ\text{C}$, accuracy $\pm 0.5^\circ\text{C}$) at the beginning of each run-run. Then its readings were checked periodically with a Comark electronic thermometer with resolution and accuracy comparable to those of the calibration.

Air temperatures of 40, 50, 60, 70 and 80°C were used in the drying tests. The last value was used in the tests with the highest air velocities only. Temperatures above this range were not recommended for maize since higher temperatures interfere with enzymatic reactions that occur within the product during this process. The lower limit of this range

is close to the temperature values experienced by the product stored in the sun under the prevailing conditions at Dallas. Sun drying is also often used as a control for experiments designed to investigate effects of processing variables on the quality of cocoa and chocolate.

The values of airflow rate used to determine the effect of mass diffusivities were chosen based on data available in the literature for products of similar size (Miao and Easa, 1983). These data were the starting point for a set of preliminary tests to find the lowest limit of air velocity that did not interfere with the kinetics of cocoa drying. These tests showed that the process kinetics were not affected by velocities above 1.8 to 2.8 m/s.

The four air velocities used in the tests were about 0.1, 0.3, 1.0 and 2.3 m/s. The highest value was used to determine the reference mass diffusivities. The three lower values are within the airflow range used for cocoa. A summary of the test conditions are given in Table 4.1.

The drying curves were obtained by periodic weighing of a smaller sample, approximately 0.1 kg, kept in plastic bag placed in the drying tray of Figure 4.1. Weighing was done manually on a Mettler balance (model PL120) with capacity for up to 120 g, resolution of 0.01 g.

The concentrations of the most important acids found in fermented cocoa beans were maintained by taking samples of about 10 g from the drying tray at regular time intervals. These samples were processed, *in-situ*, for concentrations of citric, lactic and acetic acids.

Table 6.1. Conditions of the drying air used in the experimental tests

Velocity (m/s)	Temperature (°C)
0.1	40
	50
	60
	70
0.5	40
	50
	60
	70
1.0	40
	50
	60
	70
1.5	40
	50
	60
	70

Sample Analysis and Moisture Content Determinations

Asial concentrations were measured using High pressure liquid chromatography (HPLC). The system used (Silicon France S. A.) consisted of

1. Gilson pump (model 302)
2. Gilson pressure controller (model 302)
3. Beckman IR detector (model 98 50)
4. CG integrator/processor (model 300)
5. BAC-2-AD fermentation monitoring column (30x7 mm) for sugars, organic acids and alcohols

The following procedures were used for corn, beta, and sorghum

1. Extraction
 - i. grinding of approximately 6 g of biomass in home blender
 - ii. mixing with 50 g of distilled water
 - iii. homogenization for less than 2 minutes
 - iv. centrifugation for about 3 minutes at 5000 RPM
 - v. filtration in Glassman membrane with pore diameter of 0.25 µm
2. Asial quantifications
 - i. injection of 20 µl aliquot
 - ii. solvent used: H_2PO_4 0.005 M

- iii. Size of 5-5 cubes
- iv. Temperature of approximately 25 °C (ambient)
- v. Duration of approximately 15 minutes
- vi. Number of repetitions per sample: 2 or 3 depending on the repeatability of two consecutive outputs

The instrument was calibrated at the beginning of each use by external standardisation and checkability. A standard mixture containing 8.4% of water, lactose and citric acid was used. Figure 6.3 shows an example of the chromatograms obtained in the presence of calibration of the equipment.

Moisture contents of wet and dry samples were determined by drying the beans in a ventilated oven at a temperature of $105 \pm 1^\circ\text{C}$ for 24 hours.

Product Physical Properties

Solution of the drying model requires the availability of data for some parameters of the product which usually depend on its temperature and moisture content. The following properties were needed:

1. Geometrical characteristics: bean size (length, width and thickness), area and volume.
2. Thermal properties: specific heat capacity, thermal conductivity, latent heat of moisture evaporation and convective heat transfer coefficient.
3. Mass transfer properties: mass diffusivity, equilibrium moisture content and convective mass transfer coefficient.

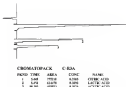


Figure 4.2. Typical calibration chromatograms for the high pressure liquid chromatography.

The length (l), width (w) and thickness (t) of the bones, as illustrated in Figure 4.3, were measured super-externally using a caliper. Drying tests were carried out to measure changes in mass with constant volume. Bones randomly marked, no less than ten, from wet samples of approximately 1 kg, were measured and weighed periodically during the drying process. Actual bone volume was measured with a pneumatic pycnometer constructed specially for bone-bone (Friede et al., 1987). For comparison purposes, surface area and volume were calculated from the length, width and thickness, assuming a finite slab shape. The relationships between these parameters and

moisture content were determined by means of polynomial regression, following the procedure described by Latif et al. (1991).



Figure 4.3 Definition of cassia bean dimensions (not to scale): length (l), width (w) and thickness (e)

The effect of temperature was not assessed, since it is normally not noticeable. Furthermore, the ranges of drying air temperatures used for cassia are not very high, a maximum of about 40°C above ambient.

The following empirical expressions were obtained from the literature for the specific heat and thermal conductivity of branched cassia beans (Sawyer, 1994):

$$c_p = 3696 + 16208^{\circ} - 15.808^{\circ^2} \quad (4.3)$$

$$k = 0.13 + 0.2864T = 7.61 \times 10^{-4} T \quad (6.2)$$

A mathematical expression for the latent heat of vaporization was derived from various vapour pressure equations, available for water, following the procedure used by Reichen et al. (1987). The methodology is based on the Clausius-Clapeyron equation and it takes into consideration the thermodynamics of the evaporation process that imposes some restrictions on the range of applicability of the vapour pressure equations selected as fit vapour data for a product. The heat involved in a pure vapour process should decrease with the increasing content of the material or its temperature.

Evaporation data available in the literature were almost exclusively determined for applications to storage problems. They were measured through moisture uptake rather than desorption methods. Furthermore, they are restricted to very narrow temperature ranges around the ambient temperature.

The expression of Equation 6.3 represents the Duj and Nielsen's modified Henderson equation for fermented cacao-bean as determined by Dujos (1994). It covers a broader temperature range and was used in this work.

$$\alpha_w = \exp\left(41.4 + 10^{-10} T^{10} \exp(-0.0001 T^{10})\right) \quad (6.3)$$

Convective heat transfer coefficients were calculated from the general expression determined by Patankar and Givoni (1965) for single periods of several shapes and orientations with respect to the fluid flow (Equation 4.6). The characteristic dimension used to calculate the Reynolds number (Re) is defined as the ratio of the total surface area

to the maximum length of the perimeter of the body projected area (perpendicular to the flow). Equation 6.4 is valid for Reynolds numbers in the range of 500 to 5000

$$j_d = \frac{h}{(\rho_{\text{air}} v_{\text{air}}^2)^{1/4}} \text{Pr}^{1/3} = 2.692 \text{Re}^{-1/4} \quad (6-1)$$

The empirical analogy of equality of the Chilton-Colburn j -factor for heat, mass and momentum transfer by convection (Bird et al., 1982) leads to the following expression for the convective mass transfer coefficient

$$j_m = \frac{h}{v_{\text{air}}} \text{Sc}^{1/3} = 5.67 \text{Re}^{-1/4} \quad (6-2)$$

Equation 6.2 is valid for gases and liquids with Sc and Pr numbers in the range of 0.6 to 2400 (Sherwood, 1967).

Mass Diffusivity

Mass diffusivity is an indispensable transfer property in mathematical modelling and simulation of drying processes. This parameter depends on the product composition and moisture content. No direct method can adequately cope with products of irregular shape. In this case, analysis of drying data is a technique that can be used to determine effective values for mass diffusivity.

The analytical solution of the partial differential equation that governs diffusion in a brick-shaped solid may be given by the product solution or Newman's rule (Fellner, 1982). The end result comes from the product of the individual infinite sine

solutions in the three directions of a rectangular coordinate system. Hence, the distribution of a general dependent variable in space and time can be described as

$$M(x, y, z, t) = M(x, t)M(y, t)M(z, t) \quad (6.4)$$

The individual solutions, may be given in terms of infinite series expansion (Mikulaev and Gavril 1984)

Average dimensionless concentration can be obtained by integrating the solution of Equation 6.6. For a rectangular parallelepiped of dimensions $2L_x, 2L_y, 2L_z$, constant initial distribution, prescribed boundary conditions and large enough times, the series solution simplifies to (Polivan, 1991)

$$M(t) = 1 + \frac{R}{\pi^2} \exp \left[\frac{D_0 \pi^2}{4(Q^2 + \pi^2 + D^2)} \right] \quad (6.7)$$

This expression was used to estimate effective mass diffusivities from the slopes of the plots of the experimental values of $\ln[M(t)]$ versus time. The slopes needed were evaluated by means of cubic spline approximation, numerical interpolation and differentiation (Press et al., 1992). With this procedure, it is possible to relate mass diffusivity to product moisture content and temperature. Similar relationships have been used for grains and food products (Tong and Leach, 1990)

$$D = \alpha \exp \left(\beta W + \gamma W^2 + \delta W^3 + \frac{\lambda}{T} \right) \quad (6.8)$$

where $\alpha, \beta, \gamma, \delta$ and λ are regression parameters

This mathematical model has several statistical properties that motivated its choice. It is not too complex as compared to others that are available and the regression parameters under the brackets have similar close-to-linear estimation behavior (Kutner et al., 1990). This allowed for use of linear regression with iterative log-logarithmic transformation without incurring significant errors. The same procedure may be applied to find a similar mathematical relationship for the diffusivity of acetic acid.

There is a small limitation to the above procedure. The assumption underlying Equation 4.7, that is, its validity only for large values of time, makes it not suitable for determination of mass diffusivity at the beginning of the drying process. If the above procedure were applied during the initial stage of drying, the resulting mass diffusivity would be lower than the actual value because Equation 4.7 does not reflect the time lag phenomenon at the beginning of the drying process. These values should not be used in the regression analysis to determine the parameters of Equation 4.4.

CHAPTER 7 RESULTS AND DISCUSSION

This chapter includes presentation and discussion of the results obtained during testing of the computer program developed to simulate the drying process of fermented corn, as well as its output behavior as function of various model parameters and drying conditions. The experimental results presented are data obtained for physical properties, moisture loss, mass diffusivity, outcomes from the model validation and product quality. Analysis was expressed and measured in terms of concentrations of the most important acids found in corn leaves, namely citric, lactic and acetic acids.

Product Physical Properties

The physical properties of the product and the latent heat of moisture vaporization play an important role in the solution of the drying model equations. Therefore, they have to be analyzed with respect to the accuracy with which they were measured. The following section presents the results of heat rate measurements, their changes with respect to moisture content and the total heat of vaporization at different temperatures and moisture contents.

Geometric Characteristics and Stem Mass

Linear regression was used to analyze the data obtained for the properties associated with stem form size, namely: length, width, thickness, volume and mass. The following regression equations were determined (independent expressed in millimeters):

1. Length,

$$l = 21.903 + 1.790l^* - 1.966l^{*2} + 1.610l^{*3} \quad (7.1)$$

standard deviation estimate: 0.362

multiple correlation coefficient: 0.9261

2. Width,

$$w = 1.071 + 1.074l^* - 1.875l^{*2} + 5.075l^{*3} \quad (7.2)$$

standard deviation estimate: 0.003

multiple correlation coefficient: 0.9996

3. Thickness,

$$d = 0.734 + 0.018l^* + 0.017l^{*2} - 1.671l^{*3} \quad (7.3)$$

standard deviation estimate: 0.161

multiple correlation coefficient: 0.9965

4. Volume (mm³)

$$V = 2072.672 + 322.143l^* - 161.936l^{*2} - 40.134l^{*3} \quad (7.4)$$

standard deviation estimate: 15.304

multiple correlation coefficient: 0.9917

5. Stem mass (g)

$$m = 1.878 + 0.026l^* \quad (7.5)$$

standard deviation estimate: 0.002

multiple correlation coefficient: 0.9994

These regression equations are valid for moisture contents within the range of 0.09 to 1.36 (dry basis). The lower values of the mean square error and multiple correlation coefficient associated with Equation 7.1 reflect a greater degree of variability of the beam length in relation to the other dimensions. This seems to be a characteristic of the natural wood, rather than measurement errors.

The plots shown in Figure 7.1 are the average dimensional values of these properties versus initial moisture content obtained at the experiments done for wood measurements. Nonlinear transformation was carried out by expressing the parameters in terms of the ratios of their actual values to the corresponding initial values. Due to the internal structure of the beam, the change in the size of the beam during drying is not the same in all directions.

Unformulated wood woods are flat and characterized by a compact and smooth surface. Upon formulation the corrugated cupules (Wood, 1972) tend to separate from each other as a consequence of the isotropic penetration and penetration of liquids resulted from the formulation process. Separation occurs sideways and in the direction of the thickness, but not in the direction of the largest dimension (length). This phenomenon tends to make the beam to become plump, as compared to the unfurnished flat woods, and to loosen the hull from the cupules after roasting. During drying the reverse takes place, that is, the cupules tend to go back to their initial position, that the occurrence of deformational size reduction. The initial portion size is not fully achieved. Reduction of the beam thickness with moisture loss was remarkably larger than size reductions in the other dimensions. Thickness decreased by approximately 20% of its

total value, as compared to nearly 13.1% and less than 3% for the beam width and length, respectively. Shrinkage caused by desorption of moisture itself was comparatively smaller. Most of the volume reduction observed was due to partial separation of particles of the solid polymer inside the beam area, rather than contraction of the solid material, owing to the hygroscopic properties of the material.

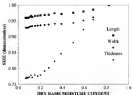


Figure 76. Relative size changes of extruded beam beams with moisture content.

Relationships for Equilibrium, Moisture Content and Latent Heat of Vaporization

The mathematical expression used to compute the latent heat of vaporization of bound moisture was derived from the relative humidity-equilibrium moisture content relationship by Chapin (1934) as in Equation 4-3 of Chapter 4.

$$x_{\text{w}} = 1 - \exp \left[A \exp^B \exp^{C/T} \right] \quad (1.6)$$

$$\begin{aligned} \text{where } A &= -6.414 \times 10^{-21} \\ B &= 10.43 \\ C &= 4.688 \times 10^3 \\ D &= -1.714 \end{aligned}$$

Predictions of equilibrium moisture content from this relationship are plotted against values of water activity in Figure 7.1, for temperatures in the range of 20 to 30 °C. Equilibrium moisture content of fermented sauer is somewhat lower than that of unfermented beans and other products when compared at the same conditions. The loss of compartmentalization of the internal structure of the seed during the fermentation process brings moisture and butter in close contact. Casein butter, being a hydrophobic substance, repels water when both are put together. This fact explains the relatively lower equilibrium moisture content and it is also the reason why fermented sauer has to be dried to a much lower moisture content, 7 to 8% (wet basis), before it can be stored and marketed. The curves of Figure 7.1 show that most of the equilibrium moisture is within 0 to 0.125 for values of water activity less than 0.6.

The total loss of moisture vaporization in the drying process comprises the loss of desorption (R_d) plus that required to evaporate water (R_w) in free state

$$R_{\text{tot}} = R_d + R_w \quad (1.7)$$

The first term in Equation 1.7, the desorption loss, depends on the product moisture content and temperature and should decrease with increasing moisture and temperature

The heat of vaporization of free water is a function of its temperature and may be computed by means of several expressions for saturation vapor pressure available. Usually these relationships lead to equations for the latent heat of vaporization that satisfy the condition that this property should also decrease with increasing temperature. The expression used in this study was the one determined by Wexler and Giauque (1971). Its predictions of saturation vapor pressure and those from several other relationships available agree very well for temperatures within the range of 0 to 100 °C (Wilhelm, 1970). Although it is relatively more complex, it is sometimes recommended because it is founded on more universal data.

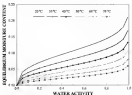


Figure 3.6. Calculated data of equilibrium moisture content for limonite using Equation 3.6.

By using the analytical procedure developed by Dolan *et al.* (1987), the following expression was derived:

$$R_{\text{eq}} = R \left(\frac{-\exp\left[\frac{\Delta T^{\text{eq}}}{R} \ln\left(\frac{p}{p^{\text{eq}}}\right)\right]}{1 - \exp\left[\frac{\Delta T^{\text{eq}}}{R} \ln\left(\frac{p}{p^{\text{eq}}}\right)\right]} \right) \left[\frac{\Delta T^{\text{eq}}}{R} \ln\left(\frac{p}{p^{\text{eq}}}\right) + \ln\left(\frac{p}{p^{\text{eq}}}\right) \ln\left(\frac{p}{p^{\text{eq}}}\right) \right] + R_0 \quad (7.4)$$

where A , B , C and D are the same as in Equation 7.7, and R_0 is the ideal gas constant.

Computed results obtained from this equation are plotted against product moisture content and temperature, respectively, in Figures 7.3 and 7.4. These curves have negative slopes indicating that the latent heat of moisture vaporization decreases with increasing temperature and moisture content.

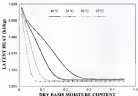


Figure 7.3 Total vaporization heat of heated moisture at different moisture basis for different temperatures

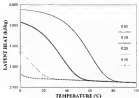


Figure 7.4 Total vaporization heat of bonded moisture in fermented cacao beans for the moisture content range of 0.05 to 0.30

It can be verified from these graphs that, for higher temperatures, the heat of desorption decreases with increasing moisture content and approaches that of pure water, under the same temperature, very quickly (Figure 7.3). Figure 7.4 shows that this property is significantly higher than that of water in the range of temperatures studied, for lower moisture contents. This indicates that the desorption heat of fermented cacao beans is important in drying simulations, since the product has to be dried to quite low moisture contents.

English, Testing, and Parameter Analysis

The computer program was used to test some parameters under restricted conditions. Parameters investigated were associated with the numerical technique used, that is, the explicit finite difference method. Number of domain dimensions, node number, node spacing and the time step required to generate a stable and accurate solution comprised the set of parameters studied.

Initially, the dimension number was analyzed varying it a reduction in the time required to run the computer program. These tests were carried out with the subprogram written to solve for the energy equation. Values of parameters and conditions used in these runs are given in Table 7.1. These values were taken from the literature, either for steam or for other products with similar geometry and used under conditions that are somewhat alike. The results obtained showed that the reduction of the number of dimensions could lead to quite different solution profiles. Therefore, the possibility of reducing the dimension number for the problem was discarded. Curves for change of the mean temperature with time are shown in Figure 7.5 for wet product. Since all flow controlling parameters were held constant throughout the remainder of the testing process, the different rates of temperature increases are due to differences in the total surface area of the slab. A flame brick shaped slab has greater exposed surface for heat exchange with the convective medium. The results from the numerical and analytical solutions compared very well, confirming the accuracy of the finite difference solution.

Table 7.1. Values of parameters, product and air temperatures used to generate the temperature profiles of Figure 7.1.

Specific heat ($\text{kJ/kg}^\circ\text{C}$)	3500
Thermal conductivity ($\text{W/m}^\circ\text{C}$)	0.4
Convective heat transfer coefficient ($\text{W/m}^2^\circ\text{C}$)	50
Base length (m)	2.8×10^{-2}
Base width (m)	1.8×10^{-2}
Base thickness (m)	0.8×10^{-2}
Product mass density (kg/m^3)	1500
Product temperature ($^\circ\text{C}$)	25
Air temperature ($^\circ\text{C}$)	50

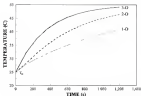


Figure 7.5. Average temperature profiles from computations for 1, 2 and 3 dimensional domains.

Trial runs to determine the stability conditions of the finite-difference scheme were done with the subroutines developed to solve for the product moisture content and temperature. At first, the subroutines were tested separately and later they were coupled. These tests were conducted for constant moisture diffusivity coefficient and thermal properties. The values of moisture diffusivity and drying air temperature used were $4.5 \times 10^{-7} \text{ m}^2/\text{s}$ and 70°C , respectively. Both values are relatively high. This choice was made no purpose to have increases in short run times and to obtain stable time-step values. For a given intranodal space configuration, the higher the diffusivity the lower the time step required to achieve stability. A time step of 0.25 s was needed to obtain stability, when the mass beam was represented by 12 nodal points in each of the three perpendicular directions.

Results of average moisture content integrated for some node number combinations are shown in Figure 7-6 as a function of time. Node number combinations are expressed in terms of nodal point numbers, sequentially, in the length (x), width (y) and thickness (z) directions. Uniform spacing was used in these computational networks. The same curve pattern was obtained for the nodal nodal temperature profiles, except that the product temperature increases during the drying process.

Networks with unequally spaced nodes were investigated in association with node number combinations. Four mesh size was used near the slab external surfaces, where the dependent variable experience steeper gradients. In this way, results obtained with smaller numbers of nodes could be comparable to those from finer grids. The node number combination of 10101 used with this type of network produced average moisture

profiles that agreed well with those for larger number of nodes in networks with equal internodal spaces. A schematic representation of the node distribution used is depicted in Figure 7. It is shown for one direction only for the sake of simplicity.

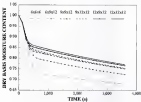


Figure 16. Comparison of average moisture profiles for different coordinates of equally spaced node numbers.

The element volume interfaces were positioned so as to generate 10, 15, 20 and 25-percent node types. Coarsest node interfaces produced the 10-percent node type. Positioning of the interfaces closer to the most external nodes, at points 18, 15 and 12% from these nodes generated the corresponding type of mesh. These percentages also correspond to the size of the volumes associated with the external nodes, relative to the

distance between them and their immediate internal neighbors. Hence, the terminology

10-, 15-, 20 and 30-percent internal nodes

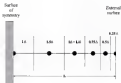


Figure 7.5 Node distribution along the direction axis for one uniform spatial grid.

The average moisture and temperature profiles presented in Figure 7.8 are for different types of external nodes, as described above. External nodes of the 30-percent type yielded poorer results when compared with nodes associated with smaller values, while 10-percent nodes eventually reduced variability in the computations, as a consequence of shrinkage. This type of node required a much shorter time step (0.1 s) to achieve stability. Results from computations done for 15-percent and 20-percent nodes were comparable to those obtained for 10-percent nodes. The maximum discrepancy

verified for moisture computed with the mesh used, a refined grid with 25-percent external nodes, and the grid with 12x12x12 equally spaced nodes was about 0.02 and average difference less than 0.004.

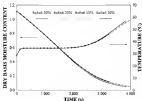


Figure T-8. Comparison of average moisture and temperature profiles for different internal node volume sizes

Effect of Shrinkage

Cane leaves undergo considerable weight loss and volume reduction in the course of the drying process as shown in Figure T-9. The total volumetric change, when wet leaves are dried to a moisture content of about 0.20 (dry basis), is approximately half of

their initial volume. Below this moisture content, volume change is negligible. Loss of weight to obtain dry mass is about the same order of magnitude.

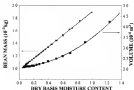


Figure 7.6. Change in mass/bone volume and mass with moisture content

To investigate the effect of this parameter on the predicted data, the bone volume was adjusted according to its dependence on moisture. Linear regression was used to fit cubic polynomials to the experimental data obtained for the bone geometric dimensions. Computer runs were carried out to find out the optimum time interval between volume measurements. Problem properties, except those directly related to the problem itself and drying conditions were maintained invariant throughout the simulation tests to single out

the effect of shrinkage on the computed results. The purpose was to reduce computer time as much as possible without compromising the quality of the results.

Plots for several shrinkage time steps are presented in Figure 7.16 for comparison. As it can be seen from that figure, no allowance for volume contraction, in the simulation of mass drying, can produce reasonable discrepancies in the predicted results for both product temperature and moisture. On the other hand, there is no need to use a shrinkage time interval of the same order of the time increment required by the numerical procedure. For practical purposes, shrinkage time steps up to 300 s may be used for cases A. A shrinkage time step of 120 s was adopted for this work. Predictions obtained by using this time interval were not much different from those obtained for the time interval of one second.

For mass drying simulations, the time interval chosen is very small because the actual drying rates are much lower as compared to those of Figure 7.16. The chosen drying time interval at a temperature of approximately 70 °C took about 13.5 hours to lower the product moisture content from its initial value down to 0.05.

Corrections for shrinkage was done by regular adjustments of the volume element after each shrinkage time step. The dimensions of the disk were corrected according to the product average moisture content. Changes for moisture contents below 0.20 (dry basis) were assumed negligible. A shrinking disk also results in faster moisture and heat transfer.

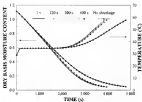


Figure 7.18. Effect of drainage time interval on the output of the vacuum drying simulation model

Drying Curves

A summary of the drying conditions is given in Table 7.2. The average drying air temperature varied from 40 to about 71 °C, except for tests 07 and 08 which were conducted at 18 °C for reasons to be discussed later. The figures presented in Table 7.2 for ambient air temperature and relative humidity are also average values averaged over the duration of each test. The complete set of data of moisture loss during the drying experiments is included in Appendix D.

Table 2.1. Summary of mass drying experiments

Trial no.	Ambient air		Drying air		Moisture content		Test (Densimetric Flow)
	Temp (°C)	RH (%)	Temp (°C)	Velocity (m/s)	Initial (%)	Final (%)	
1	27.8	82.8	78.8	2.58	1.1566	0.0764	15.9
2	29.2	76.1	68.3	2.58	1.1009	0.0760	16.5
3	28.4	80.2	68.8	2.58	1.0883	0.0743	27.9
4	27.2	78.4	48.2	2.56	1.1708	0.0817	40.8
5	28.6	87.8	71.2	2.58	1.1263	0.0816	15.8
6	29.2	77.9	48.6	2.56	1.1544	0.0748	29.2
7	28.8	68.1	48.1	2.56	1.0317	0.0799	28.3
8	28.8	71.4	48.2	2.58	1.1708	0.0833	45.8
9	29.2	79.3	76.7	2.57	1.2086	0.0834	9.5
10	28.3	78.6	79.8	2.58	1.0838	0.0838	14.9
11	26.2	73.6	78.2	1.85	1.2864	0.0815	15.2
12	28.4	69.3	68.6	0.83	1.2547	0.0827	15.6
13	26.8	73.4	58.2	0.85	1.1211	0.0808	26.2
14	29.2	78.4	48.4	1.83	1.2440	0.0802	30.8
15	25.8	85.6	58.6	1.81	1.0786	0.0803	28.6
16	25.3	78.8	48.8	0.87	1.1277	0.0816	40.3
17	27.2	76.7	78.6	1.83	1.0877	0.0810	19.8
18	27.2	72.7	68.7	1.87	1.0513	0.0791	16.6
19	26.3	79.1	70.8	1.01	1.0764	0.0815	16.8
20	25.8	82.1	48.0	0.85	1.0711	0.0818	40.8

Continued

Table 1.2 *Continued*

Time (s)	Ambient air		Drying air		Moisture content		Total Diameter (mm)
	Temp. (°C)	RH (%)	Temp. (°C)	Velocity (m/s)	Initial (g/kg)	Final (g/kg)	
21	28.4	74.7	28.0	0.32	1.0015	0.9943	12.0
22	28.4	78.9	28.1	0.48	1.0347	0.9945	28.5
23	28.4	81.9	28.8	0.67	1.0712	0.9948	48.0
24	25.9	75.8	28.0	0.50	1.1409	0.9950	17.5
25	28.1	74.7	28.1	0.33	1.1872	0.9951	14.8
26	25.8	79.3	28.2	0.48	1.3258	0.9949	28.0
27	23.4	73.7	28.1	0.33	1.5218	0.1378	38.5
28	28.4	78.2	28.0	0.33	1.3781	0.9954	28.0
29	24.6	83.2	28.9	0.69	1.1598	0.9785	33.0
30	28.3	78.2	27.9	0.88	1.1988	0.9951	17.5
31	25.3	84.1	28.1	0.33	1.3212	0.9940	33.0
32	26.6	78.2	28.2	0.60	1.5450	0.9925	17.8
33	24.3	82.3	28.1	0.69	1.3262	0.1317	48.0
34	25.2	78.8	28.1	0.32	1.3388	0.9954	27.2
35	25.4	77.2	28.0	0.69	1.2006	0.1040	17.5
36	25.4	78.3	28.6	0.33	1.3580	0.9792	46.8

Actual ambient temperatures and relative humidities changed periodically. The former varied within the range of 23 to 33 °C, while the relative humidities varied from 68 to 86%, during the time of execution of the drying experiments. Conditions of higher temperatures and lower relative humidities of the ambient air were frequent.

Durations of the drying were dependent on the ambient air conditions, drying temperature, air velocity and product initial and final moisture contents. Initial dry basis moisture content of the samples varied within the range of 1.08 to 1.40. The tests were ended when the final moisture content was in the 0.09-0.19 range. The minimum duration observed was about 15 hours for the highest temperature and air velocity used, about 70 °C and 2.58 m/s, respectively. The maximum duration was about 48 hours for the drying temperature of 48 °C and air velocity of 0.08 m/s.

Experimental results of moisture loss for four preliminary drying tests are plotted in Figure 7.11 for different temperatures. The moisture data were standardized with respect to the corresponding initial values owing to some variation in the initial moisture content of the samples. A short delay, which may be related to the initial time to heat up the superficial moisture, was observed particularly in those tests carried out at lower temperatures. All curves exhibit a high rate of moisture loss in the initial stages of the drying process. For the highest rate of moisture loss shown, observed for the drying temperature of 70 °C, the sample moisture content was reduced by nearly 50% in an elapsed time of about half an hour. This shows that the amount of moisture loosely bonded to the solids is very significant in filamentous cases like these. This can be verified by examining the initial portions of the curves for elapsed times up to two hours.

Drying rates were computed from the slopes of the drying curves by fitting cubic splines to the experimental data. The slopes of the drying curves of Figure 7.11 are shown in Figure 7.12. The rates of moisture loss varied markedly with the drying temperature. Drying was dropped sharply as the moisture content of the product reached

approximately 0.75. From this point onwards, decreases in the rate of drying were relatively lower.

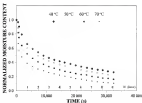


Figure 7.11 Average moisture loss profiles for mean beets dried in the air velocity of 2.5 m/s

Further analysis of Figure 7.12 shows that periods of constant drying rates seem to have occurred. This was more apparent in the tests conducted at lower temperatures. The constant rate period seems to be short, however, as compared to the duration of the test. It may correspond to evaporation of free water from the external skin of the beets. Thus the drying rate seems to be controlled by 'beet shell itself'. From this stage onwards, although the beet shell was apparently dried out, moisture in liquid form could be

usually observed in the interior of the beans, filling the spaces of the cotyledons, until later stages of the process. Internal liquid movement could be detected at moisture contents as low as 0.3 to 0.6. This could be easily observed by agitating partially dried beans (skin dried beans) or by cutting them lengthwise. Before this moisture stage, moisture transfer by diffusion within the solid matrix seemed to start to play an important role in the process as the major rate controlling mechanism. The drying rate became considerably lower from this point to the end of the process.

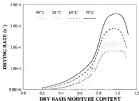


Figure 7.12. Drying rate of fermented water beans computed for different drying air temperatures at 2.5-m/s velocity.

Constant drying rate periods were much larger in these experiments than combined use of low drying air temperature and velocity. The duration of this drying stage depends on the drying air conditions such as temperature and relative humidity and velocity. Determination of precise critical moisture content for fermented corn beans could not be determined under the circumstances of the present work, since the relative humidity of ambient air was not controlled. The solution of the mathematical model allowed the variable boundary conditions, however.

Moisture Diffusivity

Moisture diffusivities were estimated from the slopes of the drying curves for the highest value of air velocity (2.3 m/s) at different air temperatures, and corrected by means of the trial-and-error procedure, as explained in the section about mass diffusivity of Chapter 6. The integral expression of Equation 3.3 was discretized by means of linear regression analysis. The determination coefficient (R^2) obtained for the regression equation was 0.984.

$$D = 29.42 \times 10^{-9} \exp \left(-3.8728^{\circ} + 16.1228^{\circ} - 9.1138^{\circ} - \frac{43456}{T} \right) \quad (3.9)$$

Predictions of moisture diffusivities made with the foregoing expression are shown in Figure 2.13. Plotted diffusivities are effective values computed for bean average moisture content and temperature, since local values for these variables could not be measured. The values of moisture diffusivity estimated varied within the approximate

range of 10^{-10} to 10^{-9} m/s, which is comparable to the diffusivities of some gases, with a possible exception for the lower bound of the range. Commercial wax is fitted to a final moisture content (between 7 to 45%, wet basis) much lower than that of other grains.

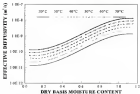


Figure 7.13. Effective moisture diffusivity of laminated waxed leaves

Model Validation

The purpose of model validation is to assess the ability of a model to simulate actual processes it was designed to represent. The criterion usually used as validation standards those of this study consists of measuring the goodness of agreement between predicted results and data collected experimentally.

The preliminary simulations carried out with the moisture diffusivity model similar to Equation 7.8, determined using the whole range of water moisture content, led to rather poorer predictions. This fact can be appreciated from the plots shown in Figure 7.14. In general, the results, experimental and simulated, differed from each other regardless extent in the initial stages of the drying process and tended to a better agreement towards the end of the tests. At the very beginning, for lower heat transfer limit, the drying model got treated over-predominant, and, then, the opposite was observed. The discrepancies achieved values up to 8-15 g/kg fresh moisture content. The same sort of response pattern from the drying model was verified for lower drying air temperatures and velocities. Figure 7.15 is an example for drying temperature of 40 °C and the same surface.

The probable explanation, why the outcome from the simulation runs failed to agree with the experimental data, seems to be associated with the scope of validity of the mathematical expressions used to estimate moisture diffusivities from the slope of the experimental drying curves. As already mentioned, the equation inferred to above is valid for larger values of time. Another cause, which likely contributed to the source of disagreement, is the fact that the equation used can describe moisture transfer under isothermal conditions only. This situation occurs during the initial drying period of some foods, when the evaporation rate is high enough to maintain the product temperature constant. This time interval, for the conditions of high airflow used in the experiments designed to determine moisture diffusivity, was shown to be very short in the simulations: less than half an hour, when compared with the total drying time. Besides, this portion of the

drying curve fell below the range of validity of the solution of the mass transfer equation, as discussed previously.

Despite the weaknesses of the slope method, its estimates were much closer to the experimental data than those obtained by use of diffusivity models determined for other products. In some cases, the results from these attempts did not resemble the expected curves at all. The closeness between the results from the slope procedure and the experimental data was very reflective, as a starting point, in the process of fitting out a better approximation and eventually the best solution as provided by method and

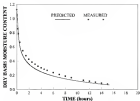


Figure 7.14 Comparison between experimental and preliminary simulated results for curves dried at 70 °C and 2.5 m/s

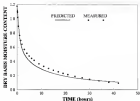


Figure 7.15. Comparison between experimental and preliminary simulated results for maize dried at 40 °C and 2.5 m/s

Simulation of maize-basis drying using the moisture-diffusivity model of Equation 7-9 produces the results shown in Figures 7.16 through 7.23. These graphs are plots of product-average moisture content versus time for maize samples dried at temperatures in the range of 40 to 70 °C. These average temperature profiles were also computed, but not used for comparison since no experimental temperature data were collected. The reason for this was the difficulties inherent in temperature measurement in small batches that experience significant shrinkage during drying.

Comparison between measured and actual drying data showed that good agreement was achieved. In general, the average differences between simulated and

experimental moisture contents were 0.02 (thermal-dry basis). Greater discrepancies were observed at the initial stages of the drying process, for moisture above 0.05, for some experiments carried out at higher air velocities (0.50, 1.00 and 2.50 m/s). It took less than one hour to reach 0.05 moisture in these tests. For experiments carried out at the lowest air velocity, 0.10 m/s, noticeable differences between predicted and measured values were found up to a moisture content of approximately 0.05. This was more apparent for the lowest drying temperature (40 °C), shown in Figures 7.21 and 7.22.

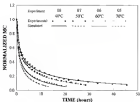


Figure 7.16: Moisture profiles for drying experiments at 2.5 m/s

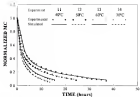


Figure 7-17. Moisture profiles for drying experiments at 1 Grain

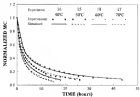


Figure 7-18. Moisture profiles for drying experiments at 1.6 Grain

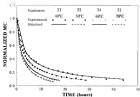


Figure 7.19: Moisture profiles for drying experiments at 0.5 m/s.

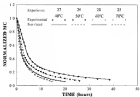


Figure 7.20: Moisture profiles for drying experiments at 0.5 m/s.

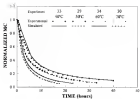


Figure 7.21. Moisture profile for drying experiments at 3.1 m/s

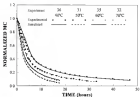


Figure 7.22. Moisture profile for drying experiments at 3.1 m/s

The probable reason for higher deviations between predicted and experimental results at lower air velocities is the equations used for calculating the convective heat and mass transfer coefficients. The lowest air velocity corresponded to a Reynolds number of about 58.0 that was well below the recommended range of the equation used. These deviations occurred at the initial stage of the drying process, when the results were not greatly controlled by the external resistance to heat and moisture transfer, rather than the internal parameters, the heat and mass diffusion rates, which play a more important role towards the end of the process.

Air velocity acts directly on the external resistance to heat and mass transfer. The convective transfer coefficients increase with increasing airflow. As mentioned above, the Reynolds number calculated for the lowest airflow rate was below the range of 100 to 2000. Reynolds number for the air velocity of 1.1 m/s was right below this range, approximately 486, and for 2.3 m/s was about 2000. The heat and the mass transfer coefficients varied within the ranges of 1 to 48 $\text{W/m}^2\text{ }^\circ\text{C}$ and 0.007 to 0.003 $\text{kg/m}^2\text{ s}$, respectively. Figure 7.23 shows the variation of the heat and mass transfer coefficients with air velocity of a typical slice size of 25x1x1 mm.

Temperature Profiles

Computed average product temperature profiles, for some of the experiments, are presented in Figures 7.24 and 7.25. These profiles also show that the beta samples experienced a short warming up period at the very beginning of the drying process. Then a period of nearly constant temperature followed. The length of this period depended on

the drying air temperature and velocity. Shorter periods of low temperature were associated with drying conditions of high air temperatures and velocities, and vice-versa.

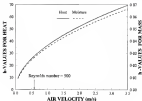


Figure T.23. Convective transfer coefficients (h values) for heat ($\text{W/m}^2\text{ }^\circ\text{C}$) and mass ($\text{kg/m}^2\text{ s}$)

Although sample temperatures were not measured in the drying bins for comparison purposes, the cooling effect, resultant from evaporation of free moisture, could be noted at the beginning of each run. The exhaust air from the bins, after passing through the drying tray, remained at relatively lower temperatures than the incoming air, for a length of time that varied with the drying. This effect was observed while liquid moisture could be viewed on the monolayers surface of the porous beans.

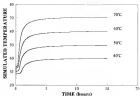


Figure 7.24. Average temperature profiles for air velocity of 2.5 m/s

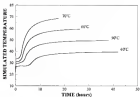


Figure 7.25. Average temperature profiles for air velocity of 5.5 m/s

After the simulated product temperature started rising it approached the drying air temperature quite fast for higher air velocities. This is plausible due to the high value of the convective heat transfer coefficient. For lower air flows the phenomenon took longer, as expected.

Effect of Airflow on Relative Humidity

Relative humidity affects the external potential that drives off moisture from the product in contact with the air. The product-equilibrium moisture content is a function of both air temperature and relative humidity. The former could be controlled and was maintained constant during the drying tests. The relative humidity of the drying air varied with that of the ambient.

In order to have an appraisal of the effect of this variable on the output of the drying model, some simulations were carried out at constant, equal to the average calculated for the drying test, and variable relative humidity. In this case the values monitored at the course of the corresponding experiment were used as input to the computer program. Comparison was made by superimposing the simulated results shown in Figure 7.24. The maximum deviation in moisture content, verified for this case was 0.003 (decimal dry basis). The curves obtained for temperatures presented more noticeable deviations. The maximum difference that was observed for the temperature profile was about 1.6 °C. Both occurred at the initial phase of the process, possibly in the constant drying rate period.

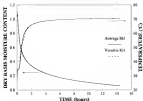


Figure 7.24. Simulations of drying test at average and variable ambient relative humidity (RH) and air velocity of 2.5 m/s

Product Stability

Acid in fermented maize results from the presence of several organic acids both volatile and non-volatile. Acetic acid is the most important volatile acid; it is formed during the fermentation process. Lactic acid and citric acids may be considered as the most important non-volatile acids. The former is produced in the course of the fermentation process, whereas citric acid occurs naturally in the pulp of fresh maize. This acid is partially used up during fermentation. Both types of acids are important for their role in

determining certain aspects of the flavor of cacao and products. However, lactic and acetic acids probably play the most important roles concerning the acidic taste in chocolate. Higher residual concentrations of these compounds in the dried beans usually lead to a sour end product, while the presence of acids in smaller quantities may contribute to the lipophilic flavor characteristics of the chocolate obtained from some types of cacao. By being a volatile constituent, acetic acid may be lost in several stages of the primary and final processing of cacao. These places include fermentation itself, drying, roasting and other heat treatments of the granulating process.

The results obtained in the experiments on drying of cacao, under thin-layer conditions, are shown in Figure T 27 through T 38. In these graphs, acid contents, expressed as mass of acid per unit mass of dry solids, are plotted against time for the drying experiments at 2.5 m/s and temperatures in the range of 60 to 70 °C. The data points presented were actually averages of three readings.

There was an detectable decrease in acetic acid concentration in the course of the drying units. There were some small fluctuations among the readings from the chromatographs. Acetic acid seemed to have a behavior similar to those of the other acids used for comparison, namely lactic and citric acids, which are sometimes referred to as food acids. The acid concentrations were about 0.01–0.03 and less than 0.05 for acetic, lactic and citric acids, respectively. These concentrations are comparable to some data available for Italian cacao in the literature (Lopez, 1991). The same pattern was observed for air velocities of 0.1, 0.5 and 1.0 m/s. The concentrations of acetic acid achieved the highest values, followed by those of lactic and citric acid (Appendix B).

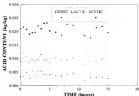


Figure 7.17. Acid concentration profiles for vacuum-dried at 70 °C and 2.5 m/s

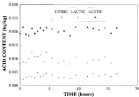


Figure 7.18. Acid concentration profiles for vacuum-dried at 60 °C and 2.5 m/s

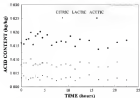


Figure 7.29 Acid concentrations profiles for oven-dried at 30 °C and 2.5 m/s

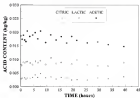


Figure 7.30 Acid concentrations profiles for oven-dried at 40 °C and 2.5 m/s

Two drying tests were carried out at 60 °C to further explore the possibility of any success in removing water-soluble by increasing the drying air temperature. Acetic acid concentrations remained nearly constant throughout the drying process as illustrated by Figure 7.11. Higher temperatures were not used due to limitations of the equipment used.

The acetic acid concentration in the 60 °C test of Figure 7.11 was somewhat lower than those of the previous experiments. This was due to the difference in the amount of liquid in the remaining fresh-cocoa pulp. Higher quantity of liquid/pulp tends to limit removal by obstruction of the interstitial spaces in the fermentation box. As a consequence, the fermented product may exhibit higher concentrations of lactic and acetic acids. The converse is results in lower removal and a less acidic fermented product.

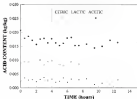


Figure 7.10 Acid concentration profiles for cocoa dried at 60 °C and 3.5 min

The results obtained in this work may appear to be in conflict with some findings reported in the same literature. There have been reports that sun drying (Erenne et al., 1949) and slower deep bed drying at 40-45 °C (Dun and Aris, 1953) removed acetic acid during the drying process. However, the drying conditions of this project are quite different from what have been done in the past, even though the range of temperatures may be similar.

Sun drying is a very slow process allowing time for the decomposition and migration of acetic acid while the product remains wet. The low temperature artificial drying that resulted in some loss of acetic acid were carried out in thick beds, 0.1 to 0.25 m deep. In thick bed drying, the product experiences conditions completely different from those found in its counterpart, thin layer drying or drying under fully exposed conditions. In thick bed drying, not all the beans are subjected to the same conditions of the inlet air, during all the process duration. In thin layer drying, the beans lose moisture at a much higher rate than the average drying rate of thick bed under the same conditions of air temperature and air velocity.

Roasting of commercial beans, in thin layers at air temperatures of 150 °C for about 30 minutes was effective in reducing the acetic acid content of the samples by as much as 22% of its initial content (Jung and Okamoto, 1991). Even higher reductions in acidity, up to 49%, have been reported in the literature surveyed by these authors. Consequently, it appears that removal of acetic acid from fermented beans is a physical process highly sensitive to terms of energy requirements. It appears that temperature is the critical factor in water removal rather than exposure time.

It may be inferred from Kemp and Dineen's work on bean roasting that the segment of insufficient data for acetic acid is significant since the extent of the loss to their extent is somewhat small. The strength with which acetic acid molecules are bonded to the cacao bean, solid matrix seems to be much higher than that of water. These bonds may be broken only under temperatures used in bean roasting. However, if the drying is done at very high temperatures the dried cacao would suffer some major and unpleasant consequences related to the progression of the flavor precursor forming chemical reactions. Demonstration of the equilibrium relationship between vapor pressure of acetic acid and its concentration in the beans at different moisture contents and temperatures may elucidate this problem.

CHAPTER 8 CONCLUSIONS

Based on the experimental and drying simulation results obtained during the execution of this work the following conclusions may be drawn from this study:

1. Cheese undergoes considerable shrinkage during the drying process. Change in size, expressed by changes in the dimensions of the brine, depends on cheese. Accommodation of the residual crystallites during drying accounts for most of the size changes, rather than shrinkage caused by the hygroscopic behavior of the product itself.
2. The wet heat of moisture evaporation is an important property in the study of cheese drying, owing to the fact that cheese brine is dried to fairly low moisture content, in the range of 7 to 8% (wet basis) for sale storage.
3. A mathematical model was developed to relate moisture diffusivity of brine-soaked cheese brine to changes in product average moisture content and temperature during drying.
4. The drying model developed to simulate the drying process of fully exposed brine-soaked cheese brine proved to be effective, since it could generate good predictions of average moisture changes during the process.

5. Water release reduction has significant effect on the results predicted with the simulation model for moisture loss. Models that do not account for the effect of this parameter may not be suitable for use with formulated steaks.
6. Although acetic acid is a volatile compound, it is not possible to remove perceptible quantities in the drying process carried out under recommended conditions of temperature (no higher than 70 °C). This compound, which is absorbed by the bones in the fermentation stage, has a similar behavior to those of citric and lactic acids, which are considered as fixed acids. Therefore, artificial drying does not contribute to improve product quality by reducing acidity.

It is claimed in the literature that the fermentation process of cases reduces the barrier imposed by the bone shell to moisture loss during drying. This particular component seems to have an important role in controlling the rate of moisture loss in the drying process, after the skin shed stage is attained. Therefore, it is recommended that future research works should concentrate efforts to measure moisture diffusivities for the bone shell and complicate, individually.

APPENDIX A CONSTITUTIVE EQUATIONS

In an ideal scenario, the transport phenomena that take place in hypocoagulant and porous media may be considered as isolated or independent events, that is, as noninteracting phenomena. Therefore, it can be said that the rate of flow of a component is a function of the gradient of the corresponding driving force or field potential variable only. This statement may be written in functional form as

$$J = J(X) \quad (\text{A.1})$$

The expression above may be expanded about the condition of equilibrium ($X=0$) using Taylor series to yield

$$J = J(X=0) + \frac{dJ(X)}{dX} \Delta X + \frac{1}{2!} \frac{d^2J(X)}{dX^2} (\Delta X)^2 + \dots \quad (\text{A.2})$$

Equation A.2 may be simplified for conditions of local equilibrium or microscopic reversibility. This implies that the rate of a fixed movement is small compared to overall fluctuations (Fokker et al., 1944). Therefore, for slow processes and small departures from equilibrium, the higher-order terms of the series above may be dropped off. This leads to a simple linear relationship between a flow and its driving force of the form

$$J = L X \quad (\text{A.3})$$

Every day experience has shown that this type of relationship is valid for a large class of observable phenomena and for wide ranges of experimental conditions (Mitschke and Gierke, 1982). Instances of its expression may be given by Fourier and Fick's laws of heat and mass transfer, respectively. Equations of this kind are empirical and generalized evidence (Jelencova, 1979). They are also considered as examples of a theory (Stauder, 1982). The coefficient L may be interpreted as generalized conductance or mobility (Katchalsky and Curran, 1967).

For multicomponent systems with intensive forces and fluxes, the relationships between causes and effects may be given by a set of mathematical equations as follows

$$J_i = J_i(X_j) \quad (4.4)$$

or

$$X_i = X_i(J_j) \quad (4.5)$$

for i and $j=1, 2,$

Reasoning similar to the one employed for independent flows or single component systems may be followed through for multicomponent systems. By using the same assumptions, a set of linear relationships, called phenomenological equations, may be derived (Wilensky et al., 1974). Employing the summation-convention, these relationships may be expressed as in Equation A.6

$$J_i = L_{ij} X_j \quad (A.6)$$

Coefficients with the same indices (α, β) are straight or direct coefficients that relate conjugated forces and generalized forces. That is, these coefficients associate forces to their mass-driving forces. While those with differing indices ($\alpha \neq \beta$), the cross coefficients, couple interactive nonconjugated forces and forces. They actually describe cross effects, due to they account for interfering influences of forces that act directly upon other forces. These coefficients may have important contributions to the total flow or not. Equation A.6 shows that any flow is given in terms of a linear combination of the interacting forces.

Mathematical expressions for the driving forces, as functions of physically measurable variables, may be derived from the entropy production function. It is required to perform some manipulations and to account for the underlying assumptions of a subject to. This equation may be further modified to yield the dissipation function. Both may be obtained from the combination of the first and second principles of thermodynamics for an open system or control volume. They can also be interpreted in terms of products of forces (variations of thermodynamic functions) and flows (quantities to be transferred). If flows and forces are properly chosen from the entropy production (Equation A.7) or dissipation function (Equation A.8) the matrix of coefficients L , is symmetric

$$\sigma = -J_s \nabla(T) - \sum_{i=1}^N \left(\frac{J_i}{T} \right) \nabla A_i \quad (\text{A.7})$$

$$\Psi = -J_s \nabla(T) - \sum_{i=1}^N J_i \nabla A_i \quad (\text{A.8})$$

Furthermore, the choice of the thermodynamic components on the ground of the Gibbs Phase Rule can guarantee the independence of forces (Poland et al., 1981). These expressions are bilinear of generalized forces and their conjugated forces. And they establish the basis for expanding for forces and forces as mathematical series.

APPENDIX B BALANCE EQUATIONS

Mathematical Description of a Flow Field

Transport phenomena taking place in multicomponent material media can be described by means of balance equations for extensive quantities. The intensive properties that characterize the local state of the components appear as drive equations. These quantities depend on position and time. Therefore, an arbitrary function or property q of the flow may be represented as

$$q = q(x, y, z, t) \quad (\text{B.1})$$

The position functions x , y and z depend on time t only. The total differential of q at a point can be obtained as follows:

$$dq = \frac{\partial q}{\partial x} dx + \frac{\partial q}{\partial y} dy + \frac{\partial q}{\partial z} dz + \frac{\partial q}{\partial t} dt \quad (\text{B.2})$$

Application of the chain rule of differentiation for composite functions yields the following expression (Kaplan, 1966; Lang, 1964)

$$\frac{d}{dt}(q) = \frac{\partial q}{\partial x} \frac{dx}{dt} + \frac{\partial q}{\partial y} \frac{dy}{dt} + \frac{\partial q}{\partial z} \frac{dz}{dt} + \frac{\partial q}{\partial t} \quad (\text{B.3})$$

This total time derivative has different meanings depending on the frame of reference (Whitcomb et al., 1993). For a fluid flow the positional variables do not change with respect to time, but the total and the partial time derivatives are equal:

$$\frac{d}{dt}(\varphi) = \frac{\partial \varphi}{\partial t} \quad (1.4)$$

If the reference frame is attached to the material particle and moves or is convected with the flow then the partial derivatives of the functions of position represent the velocity of the material particle with respect to a second and fixed frame. The total derivative is also called substantial derivative (Bird et al., 1986). Yet material or convective derivative (Aris, 1962):

$$\begin{aligned} \frac{d}{dt}(\varphi) &= \frac{\partial \varphi}{\partial x} v_x + \frac{\partial \varphi}{\partial y} v_y + \frac{\partial \varphi}{\partial x} v_x + \frac{\partial \varphi}{\partial t} \\ \text{or} \\ \frac{d}{dt}(\varphi) &= \mathbf{v} \cdot \nabla \varphi + \frac{\partial \varphi}{\partial t} \end{aligned} \quad (1.5)$$

Generalized Balance Equation for Homogeneous Control Volume

A material particle moving throughout a flow field may be represented by a small volume element (dV) as portrayed in Figure 1.1. The particle has an initial position \mathbf{x}_0 and then it is displaced and takes on a new configuration or position \mathbf{x} at time t . Therefore, the actual-particle position is a function of its (initial) location and time.

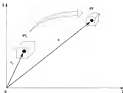


Figure B.6. Schematic representation of dilation in a flow field

The element volume may be distorted. Yet, it may undergo expansion or shrinkage along its path, while its integrity is preserved since the flow is continuous. The flow field as represented can be described by a point transformation (Aron, 1962):

Considering the following relations for the element volume:

1. Position vector
 \mathbf{x}_0 at time $t = 0$
 at time t

$$\mathbf{x} = \mathbf{x}(\mathbf{x}_0, t) \quad (\text{B-4})$$
2. Material particle (element volume)
 dV_0 at time $t = 0$
 dV at time t

$$dV_1 = dx_1 dy_1 + dx_2 \quad \text{and} \quad dV = dx_1 dy + dx_2 \quad (B.7)$$

3. Velocity vector
 \mathbf{v}_1 at time $t = 0$
 at time t

$$\mathbf{v} = \mathbf{v}(\mathbf{r}, t) \quad (B.8)$$

4. Gradient operator

$$\nabla = \frac{\partial}{\partial x} \mathbf{i} + \frac{\partial}{\partial y} \mathbf{j} + \frac{\partial}{\partial z} \mathbf{k} \quad (B.9)$$

5. Jacobian

$$J = \frac{\partial (x, y, z)}{\partial (x_1, x_2, x_3)} = \frac{dV}{dV_1} \quad (B.10)$$

6. Divergence

$$\operatorname{div} \mathbf{v} = \frac{1}{J} \frac{\partial J}{\partial t} \quad (B.11)$$

The control volume depicted in Figure B.2 illustrates a heterogeneous material body. The total volume of material (V_1), which includes regions 1 and 2, is confined by the external surface (S). The body experiences changes in shape and size such that its surrounding surface moves with velocity \mathbf{v} either inward, due to shrinkage, or outward, due to expansion, or yet with the bulk of fluid. The symbol \mathbf{n} is the outward normal unit vector to the body surface.

The front, represented by surface 2, also moves, moving or advancing, with an arbitrary velocity \mathbf{u} . This surface represents a singular interface (Saffery, 1961). At this surface jump conditions or discontinuities may arise (Taylor and Krishna, 1993). An

arbitrary variable may or may not suffer discontinuity across this interface. Phase change of a component of the medium is a typical example of discontinuity. In this case a variable under observation takes different limiting values on either of its sides. The outward normal unit vector to Σ is represented by \mathbf{n} .

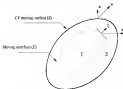


Figure 8.1. Schematic representation of a control volume showing an interface of discontinuity - phase change

A homogeneous region may be visualized by ignoring the presence of a jump interface as Figure 8.2, that is, by considering the total volume of the region bounded by surface (D). Any intensive quantity can be represented by a continuous field function $f(\mathbf{x}, t)$. The mass density or concentration of the material $\rho(\mathbf{x})$ also varies with position and time. The total amount (M) of this quantity contained in the volume domain is obtained by

integrating this function over $V(t)$. It represents the corresponding extensive property and it is a function of time only as in Equation B.12

$$F(t) = \iiint_{V(t)} \rho f(\mathbf{x}, t) dV \quad (\text{B.12})$$

Balance equations are expressed in terms of time rates of change. Thus, the total or material time derivative of the expression above has to be derived from

$$\frac{d}{dt} [F(t)] = \frac{d}{dt} \iiint_{V(t)} \rho f dV \quad (\text{B.13})$$

Since the domain of Equation B.12 depends on time, the differentiation above (Equation B.13) can not be worked out without performing transformation of coordinates (Kupka, 1994). Thus, by changing coordinates, Equation B.12 becomes

$$F(t) = \iiint_{V_t} \rho f(\mathbf{x}, t) \left(\frac{dV}{dV_t} \right) dV_t \quad (\text{B.14})$$

On substitution for the new expression for $F(t)$, use of the Leibnitz's rule of integration and carrying out the required manipulations Equation B.13 is obtained (Kupka, 1994). This expression of equations is known as the transition to the Reynolds transport theorem (Aris, 1962),

$$\frac{d}{dt} [F(t)] = \iiint_{V(t)} \left[\frac{\partial}{\partial t} (\rho f) + \nabla \cdot (\rho f \mathbf{v}) \right] dV \quad (\text{B.15})$$

Applying the divergence theorem to the integrand on the left hand side of Equation B.16 yields the following

$$\frac{d}{dt} \left(\int_{\Omega} \rho(\mathbf{r}) d\mathbf{r} \right) = \int_{\Omega} \frac{\partial \rho(\mathbf{r})}{\partial t} d\mathbf{r} + \int_{\partial\Omega} \rho(\mathbf{r}) \mathbf{v}_n \cdot \mathbf{n} d\mathbf{r} \quad (\text{B.16})$$

Equation B.16 renders prompt physical meaning. It may be inferred from this expression that the rate of change of the integral of an arbitrary field variable within a moving control volume is equal to the integral of the local rate of change added by the net flow across the volume surface. Flow through the system boundary may occur by advection or molecular diffusion. Generation or depletion of matter may also occur within the volume, but this is not considered here.

Generalized Balance Equation for Heterogeneous Control Volume

A heterogeneous system may consist of two or more phases. The volume of Figure B.2 satisfies this condition such that the following may apply:

1. Total volume

$$V(t) = V_L(t) + V_G(t) \quad (\text{B.17})$$

2. Phase interface constraint

$$\hat{V}_L + \hat{V}_G = 0 \quad (\text{B.18})$$

In accordance with Equations B.17, the integration of the time-varying extensive quantity F over the whole volume (Equation B.16) may be split into two integrals over each of the subvolumes (Long, 1999) to yield

$$F(t) = \iiint_{V(t)} (\rho g^i) dV + \iint_{S(t)} (\rho g^i) dV = \sum_{i=1}^N \left[\iiint_{V_i(t)} (\rho g^i) dV \right] \quad (9.19)$$

The same applies to the time derivatives

$$\frac{d}{dt} [F^i(t)] = \underbrace{\frac{d}{dt} \left[\iiint_{V_i(t)} (\rho g^i) dV \right]}_{\text{I}} + \underbrace{\frac{d}{dt} \left[\iint_{S_i(t)} (\rho g^i) dV \right]}_{\text{II}} \quad (9.20)$$

The time derivatives may be carried out by applying the Reynolds transport theorem to the terms I and II in the above expression:

1. Volume I: (see Figure 9.1)

$$\frac{d}{dt} \iiint_{V_i(t)} (\rho g^i) dV = \iiint_{V_i(t)} \frac{\partial (\rho g^i)}{\partial t} dV + \iint_{S_i(t)} (\rho g^i) (\mathbf{n} \cdot \mathbf{U}_i) dA \quad (9.21)$$

2. Volume II:

$$\frac{d}{dt} \iint_{S_i(t)} (\rho g^i) dV = \iint_{S_i(t)} \frac{\partial (\rho g^i)}{\partial t} dV + \iint_{S_i(t)} (\rho g^i) (\mathbf{n}_s \cdot \mathbf{U}_s) dA + \iint_{S_i(t)} (\rho g^i) (\mathbf{n}_f \cdot \mathbf{U}_f) dA \quad (9.22)$$

$(\rho g^i)_s$ and $(\rho g^i)_f$ are limiting values associated with any point that approaches another point on the singular surface from V_s and V_f , respectively

Addition of the integrals for volumes I and II results in the expression

$$\frac{d}{dt} \iint_{V_i(t)} (\rho g^i) dV = \iint_{V_i(t)} \frac{\partial (\rho g^i)}{\partial t} dV + \iint_{S_i(t)} (\rho g^i) (\mathbf{n}_s \cdot \mathbf{U}_s) dA + \iint_{S_i(t)} \left[\sum_{j=1}^N (\rho g^j) (\mathbf{n}_f \cdot \mathbf{U}_f) \right] dA \quad (9.23)$$

Interpretation of this total differential is similar to that for homogeneous system. The first term on the right hand side of Equation 9.23 accounts for the transfer rates across the phase change or jump interface (II)

From Equation 8.20 the following interpretations may apply to any arbitrary variable

1. "Jump" operator

$$\sum_{i=1}^N [\alpha(\mathbf{X}, \xi)]_j = \alpha_1(\mathbf{X}_1, \xi_1) + \alpha_2(\mathbf{X}_2, \xi_2) + \dots \quad (8.34)$$

2. "Jump" form of the divergence theorem.

$$\iiint_V \nabla \cdot \mathbf{X} \, dV = \iint_S \mathbf{X} \cdot \mathbf{n} \, dA + \iint_V \left[\sum_{i=1}^N (\mathbf{X}, \xi) \right] \, dA \quad (8.35)$$

Conservation of Mass

The law of conservation of mass for a substance occupying an arbitrary volume can be stated as

$$\left(\begin{array}{c} \text{rate of} \\ \text{accumulation} \\ \text{within the CV} \end{array} \right) = \left(\begin{array}{c} \text{net rate of} \\ \text{transport} \\ \text{across S} \end{array} \right) + \left(\begin{array}{c} \text{net rate of} \\ \text{generation/depletion} \\ \text{within the CV} \end{array} \right) \quad (8.36)$$

Assuming that there is no generation or depletion of mass, then the rate of accumulation is given by Equation 8.27. This conservation equation is expressed in terms of the material velocity relative to that of the external surface velocity (Bird et al., 1986; Sunden, 1984). Applying Equation 8.33 with $f = 1$

$$\frac{d}{dt} \iiint_{V(t)} \rho \, dV = \iiint_{V(t)} \frac{\partial \rho}{\partial t} \, dV + \iint_{S(t)} \rho (\mathbf{v}_s \cdot \mathbf{n}) \, dA + \iint_{V(t)} \left[\sum_{i=1}^N \rho (\mathbf{u}, \xi) \right] \, dA \quad (8.37)$$

Use of the divergence theorem of Equation 8.24 for $\mathbf{X} = \rho \mathbf{u}$ to transform the second term on the left of the foregoing expression leads to

$$\iint_{\Omega} \nabla \cdot \mathbf{J}(\mathbf{w}) d\mathbf{r} = \iint_{\Omega} \mathbf{J}(\mathbf{w}) \cdot \mathbf{n} d\mathbf{r} + \iint_{\Omega} \left[\sum_{i=1}^I \mathbf{J}(\mathbf{w}, \mathbf{e}_i) \right] d\mathbf{r} \quad (8.28)$$

Combining Equations 27, 28 and 29, the following expression is obtained

$$\iint_{\Omega} \left[\frac{\partial \rho}{\partial t} + \nabla \cdot \mathbf{J}(\mathbf{w}) \right] d\mathbf{r} = \iint_{\Omega} \left[\sum_{i=1}^I \rho(\mathbf{r} - \mathbf{r}_i) \dot{\mathbf{r}} \right] d\mathbf{r} \quad (8.29)$$

The integrands of the expression above must vanish everywhere. For each phase the local differential form of the equation of continuity is obtained

$$\frac{\partial \rho}{\partial t} + \nabla \cdot \mathbf{J}(\mathbf{w}) = 0 \quad (8.30)$$

At the phase interface the following flux jump-conditions apply

$$\sum_{i=1}^I \rho(\mathbf{r} - \mathbf{r}_i) \dot{\mathbf{r}} = 0 \quad (8.31)$$

Similar steps may be followed for individual constituents of a mixture. Thus for $j = 1, 2, \dots, N$ and $\mathbf{r} = \mathbf{r}_j$, the following may be obtained, for each phase

$$\frac{\partial \rho_j}{\partial t} + \nabla \cdot (\rho_j \mathbf{u}_j) = 0 \quad (8.32)$$

and for the phase interface the flux relationship is given by

$$\sum_{j=1}^N \rho_j (\mathbf{r}_j - \mathbf{r}_i) \dot{\mathbf{r}} = 0 \quad (8.33)$$

APPENDIX C BASIC MASS TRANSFER RELATIONSHIPS

Concentration Relationships

Binary System

System identification (G)

Total volume of the system (V)

Number of species in the mixture (n)

Total mass in the system

$$M = m_1 + m_2 + m_3 + \dots \quad \text{EC-1}$$

Mass density

$$\rho = M/V \quad \text{EC-2}$$

Concentration of species

$$\rho_i = m_i/V \quad \text{EC-3}$$

$$\rho = \rho_1 + \rho_2 + \rho_3 + \dots \quad \text{EC-4}$$

Mass fraction of species

$$w_i = \rho_i/\rho \quad \text{EC-5}$$

$$w_1 + w_2 + w_3 + \dots = 1 \quad \text{EC-6}$$

Mass ratio of species

$$R_i = \frac{m_i}{1 - m_1} = \frac{R_i - m_1 R_i}{R_i} \quad (\text{C-10})$$

Cons. Basis

Component 1 - ascorbic acid (ν_1)

Component 2 - moisture (wt. water)

Component 3 - dry basis mass (ν_3 , dry solids)

Total mass of wet basis

$$m = m_1 + m_2 + m_3 \quad (\text{C-11})$$

Mass concentration

Ascorbic acid

$$C_1 = m_1/V \quad (\text{C-12})$$

Moisture

$$C_2 = m_2/V \quad (\text{C-13})$$

Dry basis material

$$C_3 = m_3/V \quad (\text{C-14})$$

Dry mass density

$$\rho = C_1 + C_2 + C_3 \quad (\text{C-15})$$

Mass fraction (wt. wet basis)

Ascorbic acid

$$d_1 = m_1/m \quad (\text{C-16})$$

Moisture

$$d_2 = m_2/m \quad (\text{C-17})$$

Solids

$$S_{\text{sol}} = m_{\text{sol}}/m \quad (\text{C.15})$$

$$A_{\text{sol}} + W_{\text{sol}} + S_{\text{sol}} = 1 \quad (\text{C.16})$$

Mass ratio (oil, dry basis)

Ascoric acid

$$A_{\text{sa}} = m_{\text{sa}}/m_{\text{a}} \quad (\text{C.17})$$

Monoarom

$$W_{\text{sa}} = m_{\text{sa}}/m_{\text{p}} \quad (\text{C.18})$$

Dry solids

$$S_{\text{sa}} = m_{\text{sa}}/m_{\text{d}} = 1 \quad (\text{C.19})$$

$$A_{\text{sa}} + W_{\text{sa}} + S_{\text{sa}} \geq 1 \quad (\text{C.20})$$

Relationships between concentration and mass fraction

Ascoric acid

$$C_{\text{sa}} = \frac{m_{\text{sa}}}{F} = \frac{m_{\text{sa}}/m}{F/m} = \frac{A_{\text{sa}}}{1/\rho} = \rho A_{\text{sa}} \quad (\text{C.21})$$

Monoarom

$$C_{\text{p}} = \frac{m_{\text{p}}}{F} = \frac{m_{\text{p}}/m}{F/m} = \frac{W_{\text{sa}}}{1/\rho} = \rho W_{\text{sa}} \quad (\text{C.22})$$

Solids

$$C_{\text{d}} = \frac{m_{\text{d}}}{F} = \frac{m_{\text{d}}/m}{F/m} = \frac{S_{\text{sa}}}{1/\rho} = \rho S_{\text{sa}} \quad (\text{C.23})$$

Relationships between concentration and mass ratio

Acetic acid

$$C_a = \frac{m_a}{F} = \frac{m_a/m_b}{F/m_b} = \frac{A_a}{1/\rho_a} = \rho_a A_a \quad (C.14)$$

Methanol

$$C_m = \frac{m_m}{F} = \frac{m_m/m_b}{F/m_b} = \frac{B_m}{1/\rho_m} = \rho_m B_m \quad (C.15)$$

Solids

$$C_s = \frac{m_s}{F} = \frac{m_s/m_b}{F/m_b} = \frac{1}{1/\rho_s} = \rho_s \quad (C.16)$$

Relationships between mass fractions and mass ratio

Acetic acid

$$A_a = \frac{m_a}{m} = \frac{m_a}{m_b + m_m + m_s} = \frac{m_a/m_b}{m_b/m_b + m_m/m_b + 1} = \frac{A_a}{A_a + B_a + 1} \quad (C.17)$$

$$A_a = \frac{m_a}{m_b} = \frac{m_a}{m - m_s - m_m} = \frac{m_a/m}{1 - m_s/m - m_m/m} = \frac{A_a}{1 - A_a - B_a} \quad (C.18)$$

Methanol

$$B_m = \frac{m_m}{m} = \frac{m_m}{m_b + m_m + m_s} = \frac{m_m/m_b}{m_b/m_b + m_m/m_b + 1} = \frac{B_m}{A_a + B_a + 1} \quad (C.19)$$

$$B_m = \frac{m_m}{m_b} = \frac{m_m}{m - m_s - m_a} = \frac{m_m/m}{1 - m_s/m - m_a/m} = \frac{B_m}{1 - A_a - B_a} \quad (C.20)$$

Dry solids

$$DA_s = \frac{m_s}{m} = \frac{m_s}{m_b + m_m + m_s} = \frac{1}{m_b/m_b + m_m/m_b + 1} = \frac{1}{A_a + B_a + 1} \quad (C.21)$$

$$DA_s = \frac{m_s}{m_b} = \frac{m_s}{m - m_s - m_m} = \frac{m_s/m}{1 - m_s/m - m_m/m} = \frac{1}{1 - A_a - B_a} \quad (C.22)$$

Flow Relationships

Arbitrary System

Directed enclosed surface (ΔA)

Velocity of species i

$$\mathbf{U}_i = \frac{\Delta \mathbf{a}_i}{\Delta t} \quad (C.33)$$

Mass flow of species i

$$\dot{m}_i = \frac{\Delta m_i}{\Delta t} \quad (C.34)$$

Flux in terms of mass concentration

$$\mathbf{u}_i = \frac{\dot{m}_i}{\Delta A} = \frac{\dot{m}_i}{\Delta A} \frac{\Delta \mathbf{a}}{\Delta \mathbf{a}} = \frac{\Delta m_i}{\Delta A \Delta t} \frac{\Delta \mathbf{a}}{\Delta t} = \frac{\Delta m_i}{\Delta t} \mathbf{U}_i = C_i \mathbf{U}_i \quad (C.35)$$

Flux in terms of mass fraction

$$\mathbf{u}_i = (\rho \mathbf{U}) \mathbf{U}_i \quad (C.36)$$

Flux in terms of mass ratio

$$\mathbf{U}_i = \rho_{i,0} \mathbf{U}_i \quad (C.37)$$

Flux's law in terms of mass concentration

$$\mathbf{J}_i = -D(\nabla C_i) \quad (C.38)$$

Flux's law in terms of mass fraction

$$\mathbf{J}_i = -\rho D(\nabla w_i) \quad (C.39)$$

Flux's law in terms of mass ratio

$$\mathbf{J}_i = -\rho_{i,0} D(\nabla \chi_i) \quad (C.40)$$

Cauchy stress

Ped's law in terms of mass rates

For the solid

$$\mathbf{J}_s = -\rho_s D_2(\nabla \zeta_s) \quad (C.41)$$

for the gas

$$\mathbf{J}_g = -\rho_g D_2(\nabla \zeta_g) \quad (C.42)$$

Flux of dry solids

$$\mathbf{N}_s = \rho_s \mathbf{U}_s \quad (C.43)$$

APPENDIX D
EXPERIMENTAL AND SIMULATION RESULTS

Table B.3. Results of drying test (B).

Time (hour)	Dry basis moisture content		Dry basis acid composition (%)		
	Measured	Simulated	Crucic acid	Lactic acid	Acetic acid
0.00	0.1566	0.1566	0.0058	0.0102	0.0143
0.25	0.0752				
0.50	0.0784	0.0709	0.0034	0.0091	0.0034
0.80	0.0429	0.0429	0.0034	0.0077	0.0044
1.00	0.0398	0.0314	0.0033	0.0098	0.0039
2.00	0.0340	0.0079	0.0034	0.0083	0.0041
2.50	0.0306	0.0402	0.0032	0.0047	0.0023
3.00	0.0084	0.0038	0.0034	0.0027	0.0034
3.80	0.0786	0.0714	0.0038	0.0099	0.0038
4.00	0.0383	0.0435	0.0043	0.0069	0.0042
4.50	0.0369	0.0313	0.0033	0.0090	0.0053
5.00	0.0089	0.0044	0.0033	0.0087	0.0033
6.00	0.0730	0.0082	0.0030	0.0039	0.0044
7.00	0.0419	0.0344	0.0038	0.0083	0.0093
8.00	0.0317	0.0372	0.0030	0.0033	0.0049
9.50	0.0346	0.0014	0.0034	0.0042	0.0077
10.00	0.0033	0.0093	0.0037	0.0026	0.0030
12.00		0.0046	0.0033	0.0071	0.0033
13.00	0.0304	0.0014	0.0039	0.0099	0.0049

Air velocity: 2.88 m/s

Moist-drying air temperature: 70.4 °C

Moist ambient temperature: 37.8 °C

Moist ambient relative humidity: 82.6%

Table 6A.2. Results of drying run 62.

Time (min)	Dry basis moisture content		Dry basis acid concentrations		
	Measured	Simulated	Chloric acid	Lactic acid	Acetic acid
0.00	0.1058	0.1058	0.0025	0.0060	0.0474
0.17	0.0855	0.0317			
0.25	0.0141				
0.30	0.0028	0.0140	0.0023	0.0013	0.0049
1.00	0.0049	0.0130	0.0014	0.0000	0.0038
1.50	0.4005	0.4014	0.0015	0.0004	0.0033
2.00	0.4479	0.4379	0.0029	0.0071	0.0438
2.30	0.4045	0.3918	0.0023	0.0004	0.0070
3.00	0.2748	0.0133	0.0034	0.0004	0.0074
3.60	0.3495	0.3395	0.0034	0.0003	0.0043
4.00	0.3257	0.0044	0.0013	0.0000	0.0047
4.30	0.3058	0.0029	0.0023	0.0002	0.0038
4.80	0.3090	0.0471	0.0030	0.0000	0.0047
6.00	0.2400	0.2345	0.0034	0.0001	0.0051
7.00	0.2138	0.0446	0.0030	0.0004	0.0051
8.30	0.0058	0.0140	0.0013	0.0003	0.0437
9.00	0.0134	0.0176	0.0023	0.0071	0.0430
11.00	0.0390	0.0300	0.0030	0.0017	0.0447
12.00	0.0250	0.0190	0.0030	0.0010	0.0444
13.30	0.0115	0.0090	0.0034	0.0003	0.0433
14.30	0.0080	0.0000	0.0034	0.0003	0.0434
15.30	0.0071		0.0034	0.0000	0.0447
16.50	0.0017		0.0047	0.0004	0.0446
18.30	0.0040				

Air velocity: 2.55 m/s

Moist drying air temperature: 60.5 °C

Moist ambient temperature: 20.2 °C

Moist ambient relative humidity: 76.7%

Table 8.3. Results of drying test-03

Time (hour)	Dry basis moisture content		Dry basis acid concentrations		
	Measured	Simulated	Chloric acid	Lactic acid	Acetic acid
0.00	0.0060	0.0060	0.0070	0.0150	0.0017
0.15	0.0020	0.0020			
0.25	0.0009				
0.50	0.0052	0.0054	0.0026	0.0088	0.0021
1.00	0.0014	0.0175	0.0025	0.0054	0.0011
1.50	0.0040	0.0094	0.0046	0.0050	0.00150
2.00	0.0016	0.0060	0.0060	0.0050	0.0012
2.50	0.0022	0.0079	0.0018	0.0049	0.00180
3.00	0.0020	0.0110	0.0049	0.0045	0.00150
3.50	0.0022	0.0052	0.0037	0.0040	0.00115
4.00	0.0070	0.0022	0.0020	0.0072	0.0018
4.50	0.0064	0.0018	0.0020	0.0060	0.0010
5.00	0.0073	0.0029	0.0025	0.0070	0.0010
6.00	0.0053	0.0094	0.0044	0.0050	0.0014
7.00	0.0083	0.0069	0.0025	0.0040	0.0010
8.00	0.0043	0.0092	0.0066	0.0090	0.0010
9.00	0.0024	0.0102	0.0029	0.0096	0.0010
10.00	0.0044	0.0029	0.0020	0.0079	0.0014
11.00	0.0033	0.0092	0.0020	0.0070	0.0010
12.00	0.0022	0.0070	0.0020	0.0070	0.0012
14.00	0.0030	0.0061	0.0020	0.0070	0.0012
15.00	0.0084	0.0081	0.0004	0.0060	0.0010
16.00	0.0087	0.0096	0.0004	0.0070	0.0009
20.00	0.0072	0.0123	0.0003	0.0070	0.0010
22.00	0.0052	0.0070	0.0003	0.0046	0.0010

Air velocity: 2.00 m/s

Mass drying air temperature: 30-4 °C

Mass wet-bulb temperature: 21-4 °C

Mass wet-bulb relative humidity: 59-7%

Table G-4. Results of drying run 64

Time (min)	Dry basis moisture content		Dry basis acid concentrations		
	Measured	Simulated	Citric acid	Lactic acid	Acetic acid
0:00	0.1758	0.1758	0.0011	0.0091	0.0012
0:17	0.0608	0.0608			
0:23	0.0478				
0:30	0.0027	0.0179	0.0036	0.0002	0.0034
1:00	0.7143	0.7143	0.0013	0.0009	0.0130
1:50	0.0008	0.0008	0.0013	0.0008	0.0004
2:00	0.3482	0.3427	0.0015	0.0008	0.0137
3:00	0.3144	0.3089	0.0015	0.0007	0.0136
4:00	0.4028	0.4076	0.0012	0.0004	0.0140
5:00	0.4071	0.4079	0.0012	0.0011	0.0141
6:00	0.1791	0.1798	0.0013	0.0019	0.0135
7:00	0.1386	0.1398	0.0029	0.0096	0.0132
8:00	0.3143	0.3108	0.0018	0.0003	0.0136
11:00	0.2727	0.2782	0.0002	0.0009	0.0118
13:00	0.2673	0.2464	0.0015	0.0005	0.0124
15:00	0.2502	0.2513	0.0026	0.0006	0.0118
17:00	0.0184	0.0153	0.0000	0.0002	0.0137
19:00	0.1982	0.1972	0.0002	0.0006	0.0121
21:00	0.1799	0.1876	0.0002	0.0006	0.0131
24:00	0.1550	0.1604	0.0002	0.0004	0.0132
27:00	0.1602	0.1501	0.0002	0.0009	0.0125
30:00	0.1090	0.1001	0.0003	0.0007	0.0116
34:00	0.1232	0.1281	0.0002	0.0007	0.0121
38:00	0.1809	0.1771	0.0002	0.0003	0.0125
42:00	0.0817	0.1071			

Air velocity: 2.94 m/s

Mass drying air temperature: 40.2 °C

Mass ambient temperature: 27.1 °C

Mass ambient relative humidity: 79.4%

Table B.3 Results of drying test-35

Time (hour)	Dry basis moisture content		Dry basis acid-concentrations		
	Measured	Sampled	Crucic acid	Lactic acid	Acetic acid
0.00	0.1253	0.1253	0.0033	0.0009	0.0233
0.17	0.0334	0.0330			
0.33	0.7835				
0.50	0.9634	0.9634	0.0033	0.0121	0.0217
1.00	0.3402	0.3411	0.0030	0.0107	0.0207
1.30	0.6637	0.6646	0.0077	0.0096	0.0190
2.00	0.7846	0.7877	0.0074	0.0093	0.0195
2.30	0.5331	0.5339	0.0038	0.0090	0.0193
3.00	0.2946	0.2946	0.0033	0.0096	0.0201
3.30	0.2637	0.2600	0.0037	0.0113	0.0211
4.00	0.2413	0.2432	0.0043	0.0094	0.0230
4.30	0.2166	0.2201	0.0043	0.0094	0.0232
5.00	0.1967	0.2008	0.0043	0.0094	0.0233
6.00	0.1670	0.1692	0.0038	0.0100	0.0190
7.00	0.1304	0.1443	0.0037	0.0096	0.0136
8.00	0.1273	0.1340	0.0043	0.0094	0.0207
9.00	0.1070	0.1074	0.0043	0.0103	0.0204
11.00	0.0936	0.0936	0.0038	0.0076	0.0135
12.00	0.0674	0.0717	0.0031	0.0073	0.0176
13.00	0.0635	0.0631	0.0031	0.0099	0.0216

Air velocity: 2.59 m/s

Inlet drying air temperature: 71.2 °C

Inlet medium temperature: 25.0 °C

Inlet ambient relative humidity: 67.8%

Table 6a Results of drying test 6a

Time (days)	Dry basis moisture content		Dry basis ash concentrations		
	Measured	Standard	Clonal ash	Leaflet ash	Stem ash
0.00	0.2885	0.2885	0.0056	0.0081	0.0452
0.17	0.2854	0.2817			
0.33	0.2804				
0.50	0.2825	0.2818	0.0022	0.0087	0.0214
1.00	0.2817	0.2896	0.0030	0.0083	0.0430
1.50	0.4914	0.5707	0.0014	0.0099	0.0433
2.00	0.4328	0.4498	0.0022	0.0021	0.0277
3.00	0.3921	0.4040	0.0028	0.0084	0.0183
3.50	0.3860	0.3876	0.0049	0.0047	0.0201
3.90	0.3294	0.3378	0.0023	0.0073	0.0273
4.00	0.3090	0.3030	0.0036	0.0088	0.0204
4.30	0.2907	0.2900	0.0023	0.0023	0.0219
5.00	0.2894	0.2834	0.0040	0.0081	0.0208
6.00	0.2873	0.2840	0.0029	0.0083	0.0198
7.50	0.2812	0.1996	0.0028	0.0090	0.0202
8.00	0.1917	0.1793	0.0026	0.0088	0.0134
9.00	0.1744	0.1820	0.0028	0.0086	0.0217
11.50	0.1490	0.1342	0.0023	0.0083	0.0216
12.00	0.1360	0.1220	0.0044	0.0091	0.0212
13.00	0.1297	0.1128	0.0034	0.0094	0.0208
14.00	0.1280	0.1034	0.0041	0.0183	0.0212
15.00	0.1080	0.0827	0.0023	0.0083	0.0198
16.00	0.0983	0.0804	0.0043	0.0087	0.0214
18.00	0.0887	0.0772			
20.00	0.0744	0.0648			

Air velocity: 2 M/s

Main drying air temperature: 60.0 °C

Main ambient temperature: 29.3 °C

Main ambient relative humidity: 73.9%

Table B.2. Results of drying test 10.

Time (hour)	Dry basis moisture content		Dry basis acid concentrations		
	Measured	Simulated	Glucic acid	Lactic acid	Acetic acid
0.00	0.8317	0.8317	0.0034	0.0086	0.0121
0.21	0.8297	0.8344			
0.23	0.8414				
0.30	0.7714	0.7779	0.0041	0.0087	0.0137
1.00	0.6779	0.6779	0.0034	0.0086	0.0173
1.30	0.5544	0.5412	0.0036	0.0087	0.0173
2.00	0.4607	0.4607	0.0037	0.0081	0.0179
2.30	0.4347	0.4314	0.0035	0.0078	0.0155
3.00	0.4034	0.4073	0.0037	0.0081	0.0186
3.30	0.4020	0.3941	0.0035	0.0079	0.0183
4.00	0.3854	0.3713	0.0035	0.0087	0.0093
4.30	0.3615	0.3513	0.0041	0.0087	0.0188
5.30	0.3291	0.3178	0.0027	0.0085	0.0186
6.30	0.3073	0.2901	0.0030	0.0088	0.0133
7.00	0.2791	0.2647	0.0023	0.0073	0.0143
8.30	0.2580	0.2470	0.0029	0.0088	0.0158
9.30	0.2430	0.2368	0.0034	0.0083	0.0164
10.30	0.2340	0.2143	0.0036	0.0079	0.0139
11.30	0.2163	0.2008	0.0023	0.0063	0.0145
12.30	0.1964	0.1863	0.0023	0.0078	0.0174
14.30	0.1778	0.1670	0.0044	0.0086	0.0178
16.30	0.1580	0.1493	0.0037	0.0073	0.0138
18.30	0.1390	0.1344	0.0025	0.0074	0.0142
20.30	0.1200	0.1217	0.0012	0.0085	0.0173
22.30	0.1080	0.1088	0.0023	0.0093	0.0171
24.30	0.1043	0.1024			
26.30	0.0934	0.0877			
28.30	0.0760	0.0713			

Air velocity: 2.00 m/s

Moist drying air temperature: 40 °C

Moist exhaust temperature: 210 °C

Moist exhaust relative humidity: 64.1%

Table B.8 Results of drying test (8)

Time (hour)	Dry basis moisture content		Dry basis acid concentrations		
	Measured	Standard	Cryst acid	Lactic acid	Acetic acid
0.00	1.0204	1.0204	0.0076	0.0001	0.0117
0.17	1.0050	1.0050			
0.33	1.0279				
0.50	0.9900	0.9904	0.0071	0.0078	0.0176
1.00	0.7839	0.7898	0.0026	0.0090	0.0139
1.50	0.6950	0.6777	0.0032	0.0087	0.0171
2.00	0.5916	0.5766	0.0028	0.0090	0.0166
2.50	0.5076	0.5071	0.0032	0.0092	0.0200
3.00	0.4997	0.4907	0.0071	0.0084	0.0154
4.00	0.4450	0.4241	0.0034	0.0081	0.0188
5.00	0.4134	0.3846	0.0043	0.0083	0.0188
6.00	0.3839	0.3612	0.0034	0.0080	0.0179
7.00	0.3040	0.3078	0.0048	0.0093	0.0200
9.00	0.2131	0.2073	0.0023	0.0081	0.0162
11.00	0.2960	0.2761	0.0036	0.0080	0.0190
13.00	0.2408	0.2404	0.0028	0.0081	0.0173
15.00	0.2246	0.2246	0.0034	0.0080	0.0184
17.00	0.2002	0.2009	0.0032	0.0080	0.0160
19.00	0.1828	0.1813	0.0029	0.0081	0.0186
21.00	0.1680	0.1701	0.0026	0.0080	0.0171
23.00	0.1640	0.1539	0.0024	0.0081	0.0160
25.00	0.1374	0.1401	0.0032	0.0073	0.0164
27.00	0.1142	0.1062	0.0039	0.0077	0.0150
29.00	0.1042	0.0998	0.0036	0.0080	0.0140
45.00	0.0873	0.0879	0.0023	0.0081	0.0134

Air velocity: 0.94 m/s

Main drying air temperature: 40.2 °C

Main ambient temperature: 28.0 °C

Main ambient relative humidity: 71.4%

Table 10-9 Results of drying test 20

Time (min)	Dry basis moisture content		Dry basis acid concentrations		
	Measured	Standard	Citric acid	Lactic acid	Acetic acid
0:00	0.2256	0.2256	0.0082	0.0091	0.0222
0:25	0.0000				
0:50	0.4437	0.7541	0.0053	0.0046	0.0119
1:00	0.4582	0.7225	0.0042	0.0113	0.0225
1:50	0.4132	0.4136	0.0038	0.0097	0.0219
2:00	0.7640	0.3593	0.0023	0.0139	0.0232
2:50	0.3138	0.2991	0.0023	0.0135	0.0219
3:00	0.2753	0.2542	0.0026	0.0094	0.0204
3:50	0.2407	0.2267	0.0029	0.0092	0.0190
4:00	0.2134	0.2082	0.0023	0.0047	0.0168
4:50	0.1970	0.1777	0.0044	0.0047	0.0156
5:00	0.1762	0.1548	0.0046	0.0093	0.0170
5:50	0.1582	0.1423	0.0037	0.0074	0.0161
6:00	0.1402	0.1279	0.0042	0.0088	0.0146
6:50	0.1292	0.1134	0.0042	0.0069	0.0146
7:00	0.1113	0.1042	0.0028	0.0076	0.0171
7:50	0.0981	0.0943	0.0026	0.0086	0.0159
8:00	0.0879	0.0768	0.0018	0.0094	0.0161
9:50	0.0424	0.0432	0.0043	0.0076	0.0146

Air velocity: 2.87 m/s

Mean drying air temperature: 70.3 °C

Mean substrate temperature: 27.3 °C

Mean ambient relative humidity: 71.8%

Table B.16. Results of drying run 18

Time (min)	Dry basis moisture content		Dry basis acid concentrations		
	Measured	Simulated	Chloric acid	Lactic acid	Acetic acid
0.00	0.8976	0.8976	0.8815	0.8895	0.5284
0.17	0.8880	0.8816			
0.35	0.7345				
0.53	0.6145	0.7448	0.8834	0.8854	0.6170
1.00	0.4700	0.4926	0.8829	0.8854	0.6162
1.30	0.3947	0.4913	0.8840	0.8854	0.6071
2.00	0.3148	0.3777	0.8855	0.8855	0.6077
2.30	0.2814	0.2859	0.8851	0.8700	0.6078
3.00	0.2549	0.2722	0.8837	0.8682	0.6079
3.30	0.2383	0.2314	0.8827	0.8694	0.6083
4.00	0.1952	0.1997	0.8852	0.8698	0.6078
4.30	0.1748	0.1748	0.8850	0.8671	0.6082
5.00	0.1547	0.1554	0.8854	0.8584	0.6075
5.30	0.1402	0.1407	0.8854	0.8581	0.6081
6.00	0.1245	0.1258	0.8850	0.8595	0.6080
6.30	0.1213	0.1138	0.8852	0.8595	0.6082
7.00	0.1080	0.0928	0.8814	0.8587	0.6052
7.30	0.0958	0.0922	0.8850	0.8585	0.6078
8.00	0.0792	0.0779	0.8853	0.8554	0.6088
8.30	0.0624	0.0640	0.8872	0.8578	0.6044
10.00	0.0400		0.8817	0.8572	0.6050

Air velocity: 1.54 m/s

Mean drying air temperature: 79.6 °C

Mean substrate temperature: 78.3 °C

Mean substrate relative humidity: 76.5%

Table B.11. Results of drying test (L)

Time (hour)	Dry basis moisture content (%)		Dry basis solid concentrations		
	Measured	Assumed	Crystalline solid	Liquid solid	Aerated solid
0.00	1.2904	1.2904	0.0011	0.0001	0.0070
0.15	1.0006				
0.30	0.6489	1.0076	0.0011	0.0004	0.0071
1.00	0.6075	0.7196	0.0044	0.0056	0.0064
1.30	0.7668	0.7079	0.0041	0.0111	0.0068
2.00	0.4357	0.7108	0.0015	0.0000	0.0091
2.30	0.4104	0.4448	0.0025	0.0001	0.0087
3.00	0.4000	0.3958	0.0036	0.0041	0.0094
3.30	0.3871	0.3166	0.0046	0.0130	0.0213
4.00	0.1540	0.3300	0.0015	0.0004	0.0094
4.30	0.3048	0.2400	0.0025	0.0001	0.0201
5.00	0.3778	0.2410	0.0041	0.0004	0.0094
5.30	0.2460	0.2409	0.0014	0.0015	0.0071
6.00	0.2114	0.2007	0.0044	0.0017	0.0068
7.30	0.1784	0.1159	0.0022	0.0000	0.0064
8.00	0.0474	0.0319	0.0016	0.0004	0.0074
9.30	0.1989	0.0317	0.0021	0.0078	0.0067
10.00	0.0058	0.0007	0.0014	0.0075	0.0070
11.00	0.0019	0.0014	0.0011	0.0060	0.0070
12.50	0.0050	0.0076	0.0011	0.0070	0.0062

Air velocity: 1.05 m/s

Mass-drying air temperature: 79.3 °C

Mass-refractor temperature: 38.7 °C

Mass-refractor relative humidity: 73.0%

Table B.12. Results of drying test 12.

Time (hour)	Dry basis moisture content		Dry basis ash concentrations		
	Measured	Simulated	Crust ash	Leach ash	Ambit ash
0.00	1.2347	1.2347	0.8812	0.2681	0.0001
0.05	1.2346				
0.10	0.9718	1.8000	0.8828	0.2691	0.0161
1.00	0.7616	0.7500	0.8839	0.2687	0.0179
1.10	0.6443	0.7172	0.8843	0.2691	0.0191
2.00	0.5034	0.5343	0.8849	0.2681	0.0181
2.10	0.5096	0.4916	0.8847	0.2691	0.0166
3.00	0.4413	0.4441	0.8842	0.2697	0.0160
3.10	0.4308	0.4079	0.8844	0.2690	0.0177
4.00	0.3832	0.3717	0.8847	0.2682	0.0141
4.10	0.3837	0.3448	0.8838	0.2676	0.0181
5.00	0.3041	0.3008	0.8857	0.2695	0.0190
6.00	0.1558	0.2641	0.8844	0.2677	0.0183
7.00	0.2193	0.2341	0.8847	0.2675	0.0163
8.00	0.2008	0.2088	0.8841	0.2681	0.0161
9.00	0.1848	0.1873	0.8832	0.2672	0.0143
10.00	0.1460	0.1334	0.8841	0.2682	0.0161
11.00	0.1280	0.1198	0.8849	0.2687	0.0138
12.00	0.1132	0.1077	0.8843	0.2687	0.0132
13.00	0.1048	0.1176	0.8848	0.2675	0.0143
14.00	0.0920	0.1008	0.8841	0.2676	0.0141

Air velocity: 6.07 m/s

Mean drying air temperature: 60.4 °C

Mean ambient temperature: 27.4 °C

Mean ambient relative humidity: 69.7%

Table B.15. Results of drying test D.

Time (min)	Dry mass moisture content		Dry mass wet nanoparticles		
	Measured	Simulated	Clay wet	Laric wet	Ambic wet
0:00	1.1343	1.1343	0.0007	0.0000	0.0002
0:25	1.0608				
0:30	0.9621	0.9666	0.0010	0.0004	0.0012
1:00	0.7943	0.7943	0.0011	0.0001	0.0014
1:30	0.7024	0.7143	0.0010	0.0001	0.0020
2:00	0.5944	0.5827	0.0017	0.0000	0.0012
2:30	0.5114	0.5217	0.0011	0.0004	0.0011
3:00	0.4218	0.4888	0.0025	0.0003	0.0008
3:30	0.4421	0.4218	0.0014	0.0003	0.0003
4:00	0.4118	0.4238	0.0027	0.0005	0.0013
4:30	0.4007	0.3974	0.0029	0.0008	0.0004
5:00	0.3717	0.3752	0.0021	0.0004	0.0011
5:30	0.3152	0.3258	0.0013	0.0007	0.0048
6:30	0.3287	0.3271	0.0021	0.0006	0.0019
7:30	0.2914	0.2960	0.0028	0.0008	0.0080
8:30	0.2823	0.2782	0.0025	0.0009	0.0046
9:30	0.2668	0.2403	0.0018	0.0006	0.0013
11:30	0.2208	0.2168	0.0028	0.0011	0.0072
12:30	0.2111	0.2017	0.0017	0.0008	0.0052
14:30	0.1868	0.1774	0.0028	0.0004	0.0011
16:30	0.1800	0.1704	0.0013	0.0002	0.0002
18:30	0.1407	0.1407	0.0014	0.0005	0.0142
20:30	0.1241	0.1263	0.0008	0.0001	0.0013
22:30	0.1121	0.1143	0.0017	0.0009	0.0048
24:30	0.0901	0.1091	0.0008	0.0001	0.0018

Air velocity: 0.00 m/s

Mass drying air temperature: 50.3 °C

Mass ambient temperature: 26.8 °C

Mass ambient relative humidity: 73.4%

Table B.14. Results of drying run 14

Time (min)	Dry basis moisture content		Dry basis acid concentrations		
	Monosol	Semisol	Citric acid	Lactic acid	Acetic acid
0.00	0.3440	0.3440	0.0017	0.0017	0.0018
0.10	0.3540				
0.20	0.3436	0.3445	0.0014	0.0015	0.0015
1.00	0.0215	0.0466	0.0015	0.0016	0.0011
1.30	0.0167	0.0187	0.0014	0.0010	0.0010
2.00	0.0117	0.0124	0.0012	0.0015	0.0011
2.30	0.0119	0.0119	0.0011	0.0010	0.0010
3.00	0.0110	0.0116	0.0010	0.0016	0.0010
4.00	0.0105	0.0117	0.0010	0.0011	0.0010
5.00	0.0093	0.0110	0.0014	0.0017	0.0011
6.00	0.0110	0.0102	0.0012	0.0010	0.0012
7.00	0.0110	0.0098	0.0011	0.0010	0.0010
8.00	0.0098	0.0110	0.0012	0.0011	0.0012
9.00	0.0110	0.0110	0.0011	0.0011	0.0014
12.00	0.0110	0.0098	0.0012	0.0010	0.0015
14.00	0.0095	0.0096	0.0014	0.0011	0.0011
16.00	0.0114	0.0110	0.0012	0.0010	0.0010
18.30	0.0111	0.0116	0.0016	0.0011	0.0015
20.30	0.0097	0.0097	0.0017	0.0016	0.0016
22.30	0.0098	0.0096	0.0017	0.0016	0.0011
25.00	0.0115	0.0117	0.0014	0.0016	0.0010
27.00	0.0116	0.0115			
29.00	0.0110	0.0107			
31.00	0.0114	0.0110			
33.00	0.0110	0.0110			
35.00	0.0093	0.0110			
37.00	0.0097	0.0097			

Air velocity: 1.00 m/s

Mean drying air temperature: 40.4 °C

Mean cabinet temperature: 27.3 °C

Mean cabinet relative humidity: 74.4%

Table B.15 Results of drying run 15

Time (min)	Dry basis moisture content		Dry basis acid concentrations		
	Measured	Standard	Citric acid	Lactic acid	Acetic acid
0.00	0.8956	1.0956	0.0025	0.0047	0.0042
0.50	0.9339	0.9337	0.0017	0.0044	0.0078
1.00	0.9775	0.9767	0.0025	0.0033	0.0046
1.50	0.9333	0.9442	0.0025	0.0037	0.0043
2.00	0.9766	0.9732	0.0034	0.0036	0.0033
2.50	0.9333	0.9317	0.0033	0.0061	0.0036
3.00	0.9896	0.9811	0.0039	0.0033	0.0038
3.50	0.9366	0.9476	0.0036	0.0111	0.0036
4.00	0.9279	0.9376	0.0033	0.0039	0.0037
4.50	0.9881	0.9731	0.0026	0.0056	0.0033
5.00	0.9430	0.9368	0.0037	0.0045	0.0031
5.50	0.9879	0.9694	0.0043	0.0082	0.0033
6.00	0.9790	0.9815	0.0079	0.0059	0.0036
6.50	0.9340	0.9395	0.0036	0.0075	0.0031
10.00	0.9314	0.9407	0.0039	0.0066	0.0031
11.00	0.9739	0.9789	0.0043	0.0099	0.0031
12.00	0.9856	0.9680	0.0037	0.0062	0.0033
14.00	0.9379	0.9836	0.0039	0.0066	0.0046
16.00	0.9831	0.9828	0.0031	0.0091	0.0029
18.00	0.9738	0.9456	0.0027	0.0069	0.0033
20.00	0.9792	0.9319	0.0031	0.0092	0.0036
22.00	0.9723	0.9186	0.0029	0.0066	0.0041
24.00	0.9907	0.9879	0.0031	0.0075	0.0029
26.00	0.9865	0.9908	0.0027	0.0072	0.0026

Air velocity: 1.01 m/s

Mean-drying air temperature: 50.0 °C

Mean surface air temperature: 25.0 °C

Mean surface relative humidity: 83.4%

Table B.36 Results of drying test 15

Time (hour)	Dry basis moisture content		Dry basis solid concentrations		
	Measured	Simulated	Core solid	Layer solid	Surface solid
0.00	1.1277	1.1277	0.0066	0.0077	0.0238
0.50	1.0040	1.0283	0.0023	0.0054	0.0242
1.00	0.8795	0.9227	0.0041	0.0060	0.0275
1.50	0.7967	0.8364	0.0036	0.0061	0.0278
2.00	0.7019	0.7509	0.0048	0.0071	0.0237
2.50	0.6024	0.6383	0.0069	0.0073	0.0261
3.00	0.5012	0.5366	0.0096	0.0081	0.0221
3.50	0.5068	0.5402	0.0096	0.0084	0.0247
4.00	0.4924	0.4812	0.0099	0.0080	0.0242
4.50	0.4912	0.4771	0.0081	0.0080	0.0232
4.90	0.4774	0.4828	0.0082	0.0087	0.0276
7.50	0.3882	0.3743	0.0060	0.0086	0.0243
8.50	0.3646	0.3681	0.0069	0.0089	0.0268
9.00	0.3689	0.3794	0.0083	0.0090	0.0282
11.00	0.3189	0.2947	0.0073	0.0082	0.0278
13.00	0.2972	0.2683	0.0073	0.0090	0.0276
15.00	0.2912	0.2436	0.0099	0.0080	0.0238
17.00	0.2782	0.2230	0.0047	0.0074	0.0261
19.00	0.2711	0.2613	0.0062	0.0077	0.0272
21.00	0.1922	0.1989	0.0069	0.0081	0.0246
23.00	0.1788	0.1760	0.0073	0.0091	0.0272
25.00	0.1921	0.1877	0.0077	0.0088	0.0291
27.00	0.1930	0.1973	0.0062	0.0089	0.0242
31.00	0.1347	0.1399	0.0061	0.0079	0.0246
37.00	0.1096	0.1208	0.0062	0.0094	0.0241
42.00	0.0875	0.1015	0.0073	0.0081	0.0227

Air velocity: 0.97 m/s

Mean drying air temperature: 40.0 °C

Mean ambient temperature: 21.3 °C

Mean ambient relative humidity: 76.0%

Table B.17. Results of drying test 17

Time (h:min)	Dry mass spectrum moisture		Dry mass wet composition		
	Measured	Simulated	Carb acid	Lactic acid	Acetic acid
0:00	0.0877	0.0877	0.0044	0.0103	0.0179
0:30	0.0905	0.0946	0.0026	0.0090	0.0170
1:00	0.0207	0.0227	0.0009	0.0191	0.0150
1:30	0.0026	0.0073	0.0003	0.0173	0.0173
2:00	0.0049	0.0054	0.0000	0.0177	0.0179
2:30	0.0003	0.0000	0.0000	0.0090	0.0140
3:00	0.0004	0.0000	0.0004	0.0004	0.0142
3:30	0.0000	0.0000	0.0000	0.0000	0.0170
4:00	0.0073	0.0000	0.0007	0.0090	0.0104
4:30	0.0004	0.0000	0.0000	0.0113	0.0102
5:00	0.0003	0.0000	0.0000	0.0104	0.0100
6:00	0.0003	0.0173	0.0073	0.0077	0.0173
7:00	0.0044	0.0000	0.0000	0.0100	0.0143
8:00	0.0000	0.0000	0.0043	0.0003	0.0100
9:00	0.0003	0.0000	0.0000	0.0094	0.0170
10:00	0.0000	0.0143	0.0043	0.0004	0.0173
11:00	0.0000	0.0046	0.0043	0.0003	0.0104
12:00	0.0000	0.0000	0.0000	0.0073	0.0170
13:00	0.0004	0.0000	0.0026	0.0070	0.0102
14:00	0.0000	0.0000	0.0000	0.0004	0.0173
15:00	0.0000	0.0000	0.0000	0.0000	0.0142

Air velocity: 1.00 m/s

Mass drying air temperature: 30.0 °C

Mass substrate temperature: 27.0 °C

Mass substrate relative humidity: 75.7%

Table B-18. Results of drying test 18

Time (hours)	Dry basis moisture content		Dry basis acid concentrations		
	Measured	Simulated	Carb. acid	Lactic acid	Acetic acid
0.00	0.0513	0.0513	0.0034	0.0003	0.0003
0.50	0.0769	0.0769	0.0037	0.0004	0.0003
1.00	0.0719	0.0687	0.0039	0.0003	0.0173
1.50	0.3487	0.3487	0.0036	0.0006	0.0132
2.00	0.3726	0.4463	0.0021	0.0108	0.0133
2.50	0.4094	0.4676	0.0021	0.0090	0.0138
3.00	0.4193	0.4483	0.0036	0.0093	0.0132
3.50	0.3847	0.3754	0.0036	0.0073	0.0164
4.00	0.3503	0.3483	0.0040	0.0104	0.0133
4.50	0.2564	0.2560	0.0032	0.0090	0.0160
5.00	0.3083	0.3029	0.0040	0.0096	0.0174
6.00	0.2514	0.2664	0.0033	0.0108	0.0432
7.00	0.2308	0.2383	0.0048	0.0106	0.0416
8.00	0.2187	0.2433	0.0039	0.0132	0.0450
9.00	0.1943	0.1983	0.0043	0.0093	0.0456
10.00	0.1736	0.1736	0.0039	0.0093	0.0463
11.00	0.1582	0.1583	0.0037	0.0090	0.0449
12.00	0.1447	0.1426	0.0037	0.0093	0.0470
13.00	0.1228	0.1264	0.0039	0.0096	0.0449
14.00	0.1136	0.1194	0.0033	0.0093	0.0433
15.00	0.1186	0.1083	0.0037	0.0118	0.0473
16.00	0.0932	0.1013	0.0037	0.0133	0.0443
17.00	0.0963	0.0934			
18.00	0.0760	0.0679			

Air velocity: 1.00 m/s

Mean drying air temperature: 50 $^{\circ}$ CMean ambient temperature: 23.5 $^{\circ}$ C

Mean ambient relative humidity: 73.7%

Table B-25. Results of drying test 19

Time (h:min)	Dry basis moisture content		Dry basis acid concentrations		
	Measured	Simulated	Formic acid	Lactic acid	Acetic acid
0:00	0.0964	0.0964	0.0077	0.0090	0.0081
0:30	0.0981	0.0814	0.0079	0.0088	0.0080
1:00	0.0545	0.0796	0.0058	0.0088	0.0115
1:30	0.0679	0.0787	0.0040	0.0090	0.0179
2:00	0.0771	0.0687	0.0044	0.0085	0.0178
2:30	0.0581	0.0683	0.0049	0.0089	0.0179
3:00	0.0837	0.0619	0.0043	0.0088	0.0164
3:30	0.0899	0.0554	0.0077	0.0073	0.0165
4:00	0.0141	0.0576	0.0025	0.0085	0.0183
4:30	0.0360	0.0766	0.0049	0.0081	0.0207
5:00	0.0689	0.0977	0.0040	0.0088	0.0179
5:30	0.0583	0.0578	0.0054	0.0080	0.0196
6:00	0.0174	0.0883	0.0003	0.0073	0.0179
7:00	0.0877	0.0789	0.0079	0.0080	0.0169
8:00	0.0629	0.0543	0.0077	0.0080	0.0163
9:00	0.0488	0.0328	0.0043	0.0076	0.0154
10:00	0.0151	0.0168	0.0039	0.0079	0.0160
11:00	0.0178	0.0054	0.0038	0.0083	0.0158
12:00	0.0073	0.0060	0.0024	0.0079	0.0170
13:00	0.0071	0.0093	0.0039	0.0079	0.0170
14:00	0.0003	0.0060	0.0040	0.0088	0.0178

Air velocity: 1.00 m/s

Moist-drying air temperature: 70.0 °C

Mass substrate temperature: 26.1 °C

Mass substrate relative humidity: 71.1%

Table B.26 Results of drying test 29

Time (hour)	Dry basis moisture content		Dry basis acid concentrations		
	Measured	Simulated	Chloric acid	Leucic acid	Acetic acid
0.00	0.0751	0.0751	0.0004	0.0006	0.0494
0.10	0.0709	0.0730	0.0006	0.0005	0.0494
1.00	0.0736	0.0676	0.0007	0.0079	0.0423
1.50	0.0733	0.0634	0.0048	0.0005	0.0470
2.00	0.0763	0.0714	0.0017	0.0001	0.0451
3.00	0.0871	0.0990	0.0038	0.0000	0.0454
3.80	0.0900	0.0944	0.0079	0.0004	0.0402
5.20	0.0885	0.0888	0.0045	0.0009	0.0429
6.00	0.0707	0.0808	0.0032	0.0004	0.0474
8.50	0.0310	0.0361	0.0046	0.0005	0.0403
9.20	0.0479	0.0437	0.0045	0.0076	0.0477
9.50	0.0395	0.0408	0.0033	0.0004	0.0474
9.80	0.0447	0.0441	0.0034	0.0006	0.0477
9.90	0.0337	0.0345	0.0032	0.0005	0.0409
10.00	0.0609	0.0605	0.0039	0.0005	0.0447
12.00	0.0783	0.0767	0.0045	0.0031	0.0436
14.50	0.0790	0.0718	0.0039	0.0003	0.0433
16.30	0.0794	0.0713	0.0035	0.0001	0.0476
18.30	0.0307	0.0317	0.0030	0.0002	0.0430
20.50	0.0606	0.0579	0.0046	0.0073	0.0433
22.50	0.0619	0.0646	0.0079	0.0002	0.0427
24.30	0.0711	0.0724	0.0041	0.0004	0.0433
26.50	0.0401	0.0429	0.0048	0.0000	0.0436
28.50	0.0507	0.0502	0.0033	0.0000	0.0443
30.30	0.0500	0.0457	0.0025	0.0005	0.0476
34.30	0.0555	0.0508	0.0000	0.0001	0.0447
40.50	0.0638	0.0558	0.0007	0.0005	0.0402

Air velocity: 0.07 m/s

Mean drying air temperature: 40.0 °C

Mean cabinet temperature: 25.9 °C

Mean cabinet relative humidity: 83.3%

Table B.21 Results of drying test 21

Time (hour)	Dry bulk moisture content		Dry basis ash concentrations		
	Measured	Sampled	Clay ash	Lignite ash	Acid ash
0.00	0.0023	0.0023	0.0058	0.0062	0.0063
0.50	0.0067	0.0064	0.0070	0.0064	0.0063
1.00	0.0073	0.0070	0.0071	0.0067	0.0058
1.50	0.0702	0.0064	0.0073	0.0073	0.0041
2.00	0.0078	0.0064	0.0068	0.0063	0.0035
2.50	0.0103	0.0064	0.0060	0.0060	0.0030
3.00	0.0087	0.0071	0.0064	0.0064	0.0043
3.50	0.0044	0.0060	0.0063	0.0076	0.0048
4.00	0.0064	0.0064	0.0063	0.0064	0.0038
4.50	0.0086	0.0064	0.0060	0.0071	0.0017
5.00	0.0778	0.0068	0.0074	0.0061	0.0031
6.00	0.0043	0.0063	0.0064	0.0045	0.0040
7.00	0.0081	0.0061	0.0064	0.0066	0.0010
8.00	0.0760	0.0077	0.0060	0.0073	0.0035
9.00	0.0060	0.0059	0.0061	0.0063	0.0013
10.00	0.0044	0.0056	0.0063	0.0067	0.0028
11.00	0.0111	0.0058	0.0063	0.0067	0.0097
12.00	0.0048	0.0048	0.0063	0.0067	0.0017
13.00	0.0060	0.0073	0.0061	0.0061	0.0035
14.00	0.0058	0.0074	0.0063	0.0070	0.0019
15.00	0.0063	0.0067	0.0068	0.0068	0.0067

Air velocity: 0.50 m/s

Moist-drying air temperature: 70.0 °C

Moist ambient temperature: 26.4 °C

Moist ambient relative humidity: 70.7%

Table B-23. Results of drying test 22.

Time (hours)	Dry basis moisture content		Dry basis acid concentrations		
	Measured	Calculated	Carb. acid	Lactic acid	Acetic acid
0.00	0.0507	0.0507	0.0000	0.0000	0.0119
0.50	0.0478	0.0463	0.0000	0.0000	0.0128
1.00	0.0425	0.0409	0.0000	0.0001	0.0142
1.50	0.0380	0.0369	0.0000	0.0001	0.0167
2.00	0.0413	0.0393	0.0000	0.0001	0.0127
2.50	0.0326	0.0309	0.0000	0.0000	0.0111
3.00	0.0400	0.0383	0.0000	0.0000	0.0127
3.50	0.0380	0.0364	0.0000	0.0000	0.0119
4.00	0.0363	0.0353	0.0000	0.0000	0.0121
4.50	0.0368	0.0358	0.0000	0.0004	0.0108
5.00	0.0360	0.0349	0.0000	0.0001	0.0123
5.50	0.0309	0.0288	0.0000	0.0000	0.0134
6.00	0.0312	0.0290	0.0000	0.0000	0.0134
7.50	0.0208	0.0188	0.0000	0.0000	0.0118
8.00	0.0190	0.0170	0.0000	0.0000	0.0109
9.00	0.0163	0.0147	0.0000	0.0000	0.0113
10.50	0.0144	0.0129	0.0000	0.0000	0.0106
11.50	0.0193	0.0180	0.0000	0.0000	0.0127
13.50	0.0209	0.0193	0.0000	0.0000	0.0095
14.00	0.0190	0.0183	0.0000	0.0000	0.0090
14.50	0.0199	0.0182	0.0000	0.0000	0.0099
16.50	0.0158	0.0143	0.0000	0.0000	0.0090
20.00	0.0108	0.0097	0.0000	0.0000	0.0095
23.50	0.0130	0.0125	0.0000	0.0000	0.0099
24.50	0.0193	0.0179	0.0000	0.0000	0.0119
26.50	0.0129	0.0090	0.0000	0.0000	0.0091
28.00	0.0063	0.0007			

Air velocity: 0-10 m/s

Moist-drying air temperature: 50.0 °C

Moist-reheat temperature: 30.4 °C

Moist-mixing relative humidity: 70-95%

Table B.23 Results of drying test 23

Time (hour)	Dry basis moisture content		Dry basis acid concentrations		
	Measured	Calculated	Citric acid	Lactic acid	Acetic acid
0:00	0.0902	0.0902	0.0003	0.0009	0.0170
0:30	0.0902	0.0902	0.0003	0.0009	0.0167
1:00	0.0909	0.0909	0.0003	0.0009	0.0164
1:30	0.1164	0.1043	0.0003	0.0009	0.0166
2:00	0.1008	0.1008	0.0009	0.0003	0.0158
2:30	0.0976	0.0994	0.0003	0.0003	0.0171
3:00	0.0909	0.1046	0.0003	0.0009	0.0159
3:30	0.0943	0.1091	0.0003	0.0004	0.0019
4:00	0.1003	0.1104	0.0009	0.0009	0.0103
5:00	0.0938	0.1099	0.0009	0.0003	0.0143
6:00	0.1442	0.1071	0.0003	0.0009	0.0128
7:00	0.1178	0.1068	0.0003	0.0009	0.0116
8:00	0.1068	0.1068	0.0009	0.0009	0.0178
9:00	0.1184	0.1033	0.0003	0.0009	0.0123
11:00	0.1178	0.1146	0.0003	0.0009	0.0113
13:00	0.1034	0.1098	0.0003	0.0003	0.0107
16:00	0.1001	0.1001	0.0003	0.0004	0.0119
17:00	0.1483	0.1033	0.0009	0.0003	0.0123
19:00	0.1008	0.1094	0.0009	0.0003	0.0109
21:00	0.1118	0.1037	0.0009	0.0009	0.0133
23:00	0.1047	0.1098	0.0012	0.0009	0.0137
25:00	0.1094	0.1094	0.0013	0.0009	0.0111
29:00	0.1013	0.1003	0.0009	0.0009	0.0107
31:00	0.0411	0.1007	0.0003	0.0003	0.0114
33:00	0.1103	0.1096	0.0013	0.0009	0.0104
44:00	0.0990	0.1003	0.0009	0.0003	0.0114

Air velocity: 0.47 m/s

Mass-drying air temperature: 34.6 °C

Mass-substrate temperature: 28.4 °C

Mass-substrate relative humidity: 81.9%

Table B.24 Results of drying test 24

Drying time (h)	Dry basis moisture content		Dry basis solid concentrations		
	Measured	Simulated	Cryst. solid	Lactul. solid	Anhyd. solid
0.00	1.1409	1.1409	0.0033	0.0044	0.0046
0.50	0.9940	0.9940	0.0030	0.0039	0.0039
1.00	0.8587	0.8733	0.0031	0.0043	0.0038
1.50	0.8469	0.8738	0.0033	0.0040	0.0036
2.00	0.9035	0.9083	0.0033	0.0040	0.0041
2.50	0.9970	0.9970	0.0044	0.0049	0.0036
3.00	0.9994	0.9936	0.0044	0.0039	0.0039
3.50	0.9245	0.9060	0.0048	0.0030	0.0036
4.00	0.9646	0.9641	0.0033	0.0031	0.0040
4.50	0.9680	0.9688	0.0037	0.0034	0.0033
5.00	0.9381	0.9372	0.0043	0.0030	0.0039
5.50	0.9736	0.9687	0.0035	0.0031	0.0030
6.00	0.9382	0.9348	0.0027	0.0036	0.0031
7.00	0.9430	0.9440	0.0044	0.0033	0.0043
8.00	0.9211	0.9084	0.0040	0.0031	0.0040
9.00	0.9881	0.9866	0.0044	0.0044	0.0034
10.00	0.9739	0.9779	0.0033	0.0049	0.0039
11.00	0.9983	0.9877	0.0044	0.0048	0.0033
12.00	0.9733	0.9735	0.0033	0.0047	0.0039
13.00	0.9739	0.9730	0.0033	0.0046	0.0038
14.00	0.9775	0.9738	0.0044	0.0040	0.0044
15.00	0.9734	0.9738	0.0037	0.0037	0.0030
16.00	0.9939	0.9948	0.0043	0.0031	0.0038
17.00	0.9939	0.9948			

Air velocity: 0.50 m/s

Inflow drying air temperature: 60.0 °C

Inflow outdoor temperature: 25.0 °C

Inflow outdoor relative humidity: 70.0%

Table B.25. Results of drying test 25

Time (hour)	Dry basis moisture content		Dry basis acid concentrations		
	Measured	Sampled	Citric acid	Lactic acid	Acetic acid
0.00	0.1922	0.1922	0.0042	0.0050	0.0229
0.50	0.1943	0.1947	0.0048	0.0062	0.0231
1.00	0.1938	0.1921	0.0048	0.0058	0.0211
1.50	0.1987	0.1929	0.0040	0.0079	0.0208
2.00	0.1908	0.1914	0.0038	0.0058	0.0179
2.50	0.1982	0.1919	0.0048	0.0079	0.0186
3.00	0.1962	0.1927	0.0054	0.0068	0.0115
3.50	0.1915	0.1938	0.0052	0.0077	0.0204
4.00	0.1927	0.1938	0.0047	0.0067	0.0197
4.50	0.1950	0.1938	0.0040	0.0060	0.0179
5.00	0.1779	0.1948	0.0048	0.0068	0.0179
5.50	0.1942	0.1929	0.0047	0.0064	0.0150
6.00	0.1919	0.1905	0.0042	0.0068	0.0179
6.50	0.1760	0.1921	0.0040	0.0068	0.0160
7.00	0.1952	0.1948	0.0057	0.0062	0.0160
7.50	0.1930	0.1947	0.0047	0.0068	0.0189
8.00	0.1945	0.1997	0.0050	0.0068	0.0175
11.00	0.1124	0.1930	0.0038	0.0068	0.0177
12.00	0.0997	0.0958	0.0040	0.0052	0.0162
13.00	0.0772	0.0829	0.0062	0.0075	0.0094
14.00	0.0663	0.0727	0.0038	0.0031	0.0037

Air velocity: 8-15 m/s

Main drying air temperature: 78 °C

Main ambient temperature: 26.5 °C

Main ambient relative humidity: 74.7%

Table B.26: Results of drying test 26.

Time (hour)	Dry base moisture content		Dry base wet representations		
	Measured	Simulated	Clay wet	Lime wet	Acid wet
0.00	0.3054	0.3054	0.0000	0.0000	0.0000
0.20	0.2790	0.1790	0.0000	0.0000	0.0000
1.00	0.0670	0.0670	0.0000	0.0000	0.0000
1.50	0.0400	0.0400	0.0000	0.0000	0.0000
2.00	0.0164	0.0164	0.0000	0.0000	0.0000
2.20	0.0004	0.0004	0.0000	0.0000	0.0000
3.00	0.0000	0.0000	0.0000	0.0000	0.0000
3.50	0.0000	0.0000	0.0000	0.0000	0.0000
4.00	0.0000	0.0000	0.0000	0.0000	0.0000
4.50	0.0000	0.0000	0.0000	0.0000	0.0000
5.00	0.0000	0.0000	0.0000	0.0000	0.0000
6.00	0.0000	0.0000	0.0000	0.0000	0.0000
7.00	0.0000	0.0000	0.0000	0.0000	0.0000
8.00	0.0000	0.0000	0.0000	0.0000	0.0000
9.00	0.0000	0.0000	0.0000	0.0000	0.0000
10.00	0.0000	0.0000	0.0000	0.0000	0.0000
11.00	0.0000	0.0000	0.0000	0.0000	0.0000
12.00	0.0000	0.0000	0.0000	0.0000	0.0000
13.00	0.0000	0.0000	0.0000	0.0000	0.0000
14.00	0.0000	0.0000	0.0000	0.0000	0.0000
15.00	0.0000	0.0000	0.0000	0.0000	0.0000
16.00	0.0000	0.0000	0.0000	0.0000	0.0000
17.00	0.0000	0.0000	0.0000	0.0000	0.0000
18.00	0.0000	0.0000	0.0000	0.0000	0.0000
19.00	0.0000	0.0000	0.0000	0.0000	0.0000
20.00	0.0000	0.0000	0.0000	0.0000	0.0000
21.00	0.0000	0.0000	0.0000	0.0000	0.0000
22.00	0.0000	0.0000	0.0000	0.0000	0.0000
23.00	0.0000	0.0000	0.0000	0.0000	0.0000
24.00	0.0000	0.0000	0.0000	0.0000	0.0000
25.00	0.0000	0.0000	0.0000	0.0000	0.0000

Air velocity: 0.40 m/s

Inlet drying air temperature: 50 °C

Inlet ambient temperature: 25 °C

Inlet air flow relative humidity: 70.7%

Table B.25. Results of drying test 17

Time (hours)	Dry basis moisture content		Dry basis acid concentrations		
	Measured	Simulated	Chloric acid	Lactic acid	Acetic acid
0.00	0.3118	0.3118	0.0066	0.0068	0.0033
0.30	0.3063	0.3063	0.0066	0.0066	0.0030
1.00	0.1963	0.1769	0.0066	0.0071	0.0076
1.30	0.3148	0.0000	0.0066	0.0063	0.0076
2.00	0.0000	0.0118	0.0063	0.0066	0.0013
2.30	0.0000	0.0000	0.0067	0.0063	0.0018
3.00	0.0000	0.0000	0.0066	0.0061	0.0007
3.30	0.0000	0.0000	0.0068	0.0067	0.0000
4.00	0.0000	0.0000	0.0070	0.0068	0.0016
5.00	0.0076	0.0076	0.0066	0.0071	0.0076
6.00	0.0076	0.0076	0.0063	0.0071	0.0013
7.30	0.0000	0.0000	0.0066	0.0076	0.0000
8.00	0.0000	0.0000	0.0068	0.0068	0.0070
9.00	0.0000	0.0000	0.0067	0.0063	0.0076
10.00	0.0067	0.0000	0.0063	0.0067	0.0016
11.30	0.0000	0.0000	0.0067	0.0068	0.0013
12.00	0.0000	0.0000	0.0068	0.0066	0.0016
13.00	0.0000	0.0000	0.0066	0.0062	0.0016
14.00	0.0000	0.0000	0.0068	0.0063	0.0016
15.00	0.0000	0.0000	0.0068	0.0066	0.0016
16.00	0.0000	0.0000	0.0067	0.0066	0.0016
17.00	0.0000	0.0000	0.0068	0.0066	0.0016
18.00	0.0000	0.0000	0.0068	0.0066	0.0016
19.00	0.0000	0.0000	0.0068	0.0066	0.0016
20.00	0.0000	0.0000	0.0068	0.0066	0.0016
21.00	0.0000	0.0000	0.0068	0.0066	0.0016
22.00	0.0000	0.0000	0.0068	0.0066	0.0016
23.00	0.0000	0.0000	0.0068	0.0066	0.0016
24.00	0.0000	0.0000	0.0068	0.0066	0.0016

Air velocity: 0.33 m/s

Moist-drying air temperature: 40.0 °C

Moist ambient temperature: 26.0 °C

Moist ambient relative humidity: 73.7%

Table B-25. Results of drying test 28

Time (hours)	Dry basis moisture content		Dry basis solid concentrations		
	Measured	Sampled	Calc. sol.	Lactul. sol.	Acetic sol.
0:00	0.3761	0.3761	0.0047	0.0071	0.0196
0:30	0.3704	0.3699	0.0074	0.0047	0.0171
1:00	0.0261	0.0479	0.0079	0.0071	0.0456
1:30	0.0725	0.0566	0.0039	0.0071	0.0453
2:00	0.1564	0.0789	0.0048	0.0067	0.0447
2:30	0.4044	0.1877	0.0049	0.0091	0.0421
3:00	0.5477	0.5581	0.0044	0.0064	0.0477
3:30	0.6003	0.6764	0.0036	0.0070	0.0446
4:00	0.6077	0.6380	0.0079	0.0069	0.0477
4:30	0.4891	0.3800	0.0073	0.0064	0.0438
5:00	0.3264	0.5669	0.0043	0.0063	0.0428
5:30	0.1583	0.0414	0.0037	0.0039	0.0432
6:00	0.1774	0.7183	0.0046	0.0091	0.0437
7:00	0.2951	0.2804	0.0040	0.0066	0.0421
8:00	0.2689	0.5491	0.0034	0.0064	0.0483
9:00	0.2784	0.7736	0.0026	0.0090	0.0480
10:00	0.2909	0.2802	0.0044	0.0054	0.0483
11:00	0.1938	0.1810	0.0031	0.0052	0.0532
12:00	0.1682	0.1643	0.0038	0.0049	0.0483
13:00	0.1508	0.1499	0.0038	0.0058	0.0437
14:00	0.1290	0.1370	0.0027	0.0033	0.0470
15:00	0.1153	0.1258	0.0033	0.0048	0.0536
16:00	0.1876	0.1033	0.0045	0.0077	0.0506
18:00	0.1800	0.0943			
20:00	0.0864	0.0809			

Air velocity: 0.91 m/s

Mass drying air temperature: 60.0 °C

Mass ambient temperature: 26.5 °C

Mass ambient relative humidity: 79.7%

Table B-28. Results of drying test 29.

Time (hour)	Dry basis moisture content		Dry basis acid concentrations		
	Measured	Simulated	Citric acid	Lactic acid	Acetic acid
0.00	0.1548	0.1548	0.0073	0.0003	0.0114
0.50	0.1116	0.0479	0.0052	0.0064	0.0183
1.00	0.0445	0.0505	0.0046	0.0071	0.0127
1.50	0.0488	0.0537	0.0036	0.0067	0.0133
2.00	0.0788	0.0533	0.0068	0.0068	0.0167
2.50	0.0935	0.0526	0.0034	0.0063	0.0086
3.00	0.0818	0.0488	0.0036	0.0068	0.0136
3.50	0.0566	0.0623	0.0038	0.0080	0.0086
4.00	0.0700	0.0543	0.0038	0.0078	0.0094
4.50	0.0894	0.0723	0.0033	0.0083	0.0133
5.00	0.0827	0.0649	0.0037	0.0080	0.0083
5.50	0.0799	0.0598	0.0073	0.0082	0.0098
6.00	0.0441	0.0793	0.0044	0.0079	0.0133
6.50	0.0608	0.0649	0.0035	0.0076	0.0086
7.00	0.0784	0.0582	0.0042	0.0084	0.0073
7.50	0.0588	0.0984	0.0079	0.0074	0.0092
10.00	0.0714	0.0782	0.0025	0.0074	0.0084
11.00	0.0678	0.0564	0.0043	0.0073	0.0083
12.00	0.0473	0.0549	0.0044	0.0084	0.0079
14.00	0.0126	0.0203	0.0020	0.0041	0.0049
16.00	0.0905	0.0837	0.0025	0.0077	0.0086
18.00	0.0443	0.0628	0.0043	0.0078	0.0098
20.00	0.0489	0.0404	0.0040	0.0081	0.0088
22.00	0.0282	0.0362	0.0033	0.0041	0.0064
23.00	0.0708	0.0289	0.0030	0.0080	0.0087
25.00	0.0137	0.0133			
26.00	0.0804	0.0079			
27.00	0.0065	0.0058			

Air velocity: 0.89 m/s

Mean drying air temperature: 49.0 °C

Mean ambient temperature: 24.9 °C

Mean ambient relative humidity: 85.2%

Table B.20 Results of drying test 30

Time (hours)	Dry basis moisture content		Dry basis solid concentrations		
	Measured	Calculated	Clay and	Loam sand	Sieve and
0.00	0.1900	0.1900	0.0000	0.0004	0.0000
0.50	0.1783	0.0954	0.0000	0.0000	0.0000
1.00	0.0969	0.0767	0.0000	0.0000	0.0000
1.50	0.0664	0.0734	0.0000	0.0000	0.0000
2.00	0.0550	0.0609	0.0000	0.0000	0.0000
2.50	0.0567	0.0557	0.0000	0.0000	0.0000
3.00	0.0761	0.0787	0.0000	0.0000	0.0000
3.50	0.0703	0.0754	0.0000	0.0000	0.0000
4.00	0.0601	0.0678	0.0000	0.0004	0.0000
4.50	0.0506	0.0500	0.0000	0.0000	0.0000
5.00	0.0507	0.0500	0.0000	0.0004	0.0000
5.50	0.0503	0.0499	0.0000	0.0000	0.0000
6.00	0.0507	0.0506	0.0000	0.0000	0.0000
7.00	0.0507	0.0500	0.0000	0.0000	0.0000
8.00	0.0503	0.0507	0.0000	0.0004	0.0000
9.00	0.0503	0.0503	0.0000	0.0004	0.0000
10.00	0.0503	0.0506	0.0000	0.0000	0.0000
11.00	0.0507	0.0503	0.0000	0.0000	0.0000
12.00	0.0503	0.0503	0.0000	0.0000	0.0000
13.00	0.0500	0.0500	0.0000	0.0000	0.0000
14.00	0.0500	0.0500	0.0000	0.0000	0.0000
15.00	0.0500	0.0507	0.0000	0.0000	0.0000
16.00	0.0503	0.0500	0.0000	0.0000	0.0000
17.00	0.0503	0.0503			

Air velocity: 0.66 m/s

Main drying temperature: 69.5 °C

Mean ambient temperature: 26.3 °C

Mean ambient relative humidity: 75.1%

Table B.10. Results of drying test 31

Time (hour)	Dry basis moisture content		Dry basis solid concentrations		
	Measured	Simulated	Clara seed	Lucas seed	Lucas seed
0.00	0.2152	0.2152	0.0042	0.0042	0.0118
0.50	0.2158	0.0043	0.0055	0.0054	0.0116
1.00	0.0113	0.0042	0.0040	0.0073	0.0116
1.50	0.0190	0.0039	0.0049	0.0064	0.0109
2.00	0.0072	0.0034	0.0053	0.0067	0.0105
2.50	0.0111	0.0036	0.0035	0.0066	0.0101
3.00	0.0106	0.0046	0.0073	0.0060	0.0108
3.50	0.0072	0.0149	0.0058	0.0064	0.0049
4.00	0.0069	0.0172	0.0047	0.0068	0.0103
4.50	0.0064	0.0162	0.0013	0.0068	0.0117
5.00	0.0068	0.0171	0.0049	0.0068	0.0099
5.50	0.0048	0.0128	0.0050	0.0043	0.0097
6.00	0.0043	0.0049	0.0018	0.0041	0.0088
6.50	0.0060	0.0063	0.0049	0.0066	0.0087
7.00	0.0043	0.0044	0.0017	0.0043	0.0006
7.50	0.0047	0.0079	0.0045	0.0074	0.0003
8.00	0.0192	0.0016	0.0014	0.0079	0.0046
8.50	0.0092	0.0034	0.0048	0.0048	0.0119
9.00	0.0438	0.0446	0.0046	0.0043	0.0043
9.50	0.0111	0.0141	0.0049	0.0073	0.0041
10.00	0.0018	0.0019	0.0046	0.0059	0.0058
10.50	0.0014	0.0041	0.0041	0.0038	0.0083
10.55	0.0432	0.0006	0.0049	0.0048	0.0047
11.00	0.0071	0.0116	0.0042	0.0047	0.0093
11.50	0.0049	0.0019	0.0034	0.0079	0.0005
12.00	0.0040	0.0047			
12.50	0.0040	0.0047			

Air velocity: 0.11 m/s

Inlet drying air temperature: 30 °C

Inlet seedbed temperature: 20 °C

Inlet seedbed relative humidity: 64.1%

Table B.10 Results of drying test 12.

Time (min)	Dry basis moisture content		Dry basis solid concentrations		
	Measured	Simulated	Chloric acid	Lactic acid	Acetic acid
0:00	1.3458	1.3458	0.0076	0.0088	0.0138
0:30	1.3307	1.3307	0.0078	0.0090	0.0139
1:00	1.3149	1.3154	0.0082	0.0094	0.0137
1:30	0.8923	0.8348	0.0093	0.0096	0.0146
2:00	0.7449	0.6983	0.0047	0.0079	0.0118
2:30	0.6729	0.5847	0.0044	0.0067	0.0139
3:00	0.5361	0.3798	0.0064	0.0090	0.0130
3:30	0.4115	0.4038	0.0077	0.0088	0.0117
4:00	0.4387	0.4117	0.0053	0.0090	0.0139
4:30	0.3917	0.3833	0.0073	0.0073	0.0113
5:00	0.5398	0.3304	0.0066	0.0078	0.0041
5:30	0.3368	0.3114	0.0048	0.0078	0.0077
6:00	0.3035	0.2961	0.0044	0.0058	0.0017
6:30	0.2408	0.2134	0.0038	0.0064	0.0008
7:00	0.2362	0.2348	0.0044	0.0064	0.0006
7:30	0.2027	0.2016	0.0049	0.0049	0.0034
8:00	0.1714	0.1719	0.0053	0.0054	0.0047
8:30	0.1488	0.1536	0.0047	0.0077	0.0034
10:30	0.1390	0.1348	0.0034	0.0048	0.0019
12:30	0.1084	0.1134	0.0016	0.0051	0.0006
13:30	0.0941	0.1047	0.0030	0.0064	0.0015
14:30	0.0838	0.0906	0.0018	0.0049	0.0007
15:30	0.0737	0.0831	0.0044	0.0077	0.0006
16:30	0.0545	0.0779	0.0043	0.0073	0.0017
17:30	0.0540	0.0649			

Air velocity: 0.30 m/s

Inlet drying air temperature: 90.5 °C

Inlet ambient temperature: 24.8 °C

Inlet ambient relative humidity: 79.3%

Table B-3B: Results of drying test 22.

Time (hour)	Dry basis moisture content		Dry basis solid concentrations		
	Measured	Standard	Clonal solid	Lactate solid	Protein solid
0.00	0.3362	0.3362	0.0058	0.0079	0.0142
0.50	0.3113	0.3268	0.0045	0.0043	0.0163
1.00	0.3323	0.3118	0.0064	0.0093	0.0138
1.50	0.3134	0.3038	0.0088	0.0093	0.0139
2.00	0.3044	0.3042	0.0054	0.0076	0.0134
2.50	0.3149	0.3157	0.0073	0.0079	0.0146
3.00	0.3133	0.3138	0.0048	0.0071	0.0137
3.50	0.3000	0.3139	0.0041	0.0074	0.0141
4.00	0.3008	0.3361	0.0048	0.0074	0.0138
4.50	0.3362	0.3438	0.0040	0.0087	0.0136
5.00	0.3063	0.3323	0.0056	0.0077	0.0139
5.50	0.3117	0.3185	0.0068	0.0068	0.0138
6.00	0.3118	0.3337	0.0043	0.0073	0.0098
6.50	0.4873	0.4819	0.0054	0.0093	0.0134
7.00	0.4374	0.4421	0.0054	0.0091	0.0147
10.00	0.4119	0.4048	0.0037	0.0084	0.0139
11.00	0.3847	0.3823	0.0047	0.0047	0.0138
12.00	0.3349	0.3382	0.0049	0.0073	0.0135
13.00	0.3026	0.3033	0.0046	0.0093	0.0137
14.00	0.2384	0.2384	0.0068	0.0088	0.0140
15.00	0.2432	0.2397	0.0053	0.0079	0.0163
16.00	0.2364	0.2300	0.0044	0.0093	0.0139
18.00	0.2394	0.2139	0.0088	0.0093	0.0137
19.00	0.2812	0.2971	0.0047	0.0096	0.0173
17.00	0.3040	0.3043	0.0043	0.0071	0.0138
30.00	0.3748	0.3833	0.0050	0.0098	0.0144
34.00	0.3173	0.3163	0.0056	0.0100	0.0134
40.00	0.3317	0.3291	0.0049	0.0101	0.0145
46.33	0.3363		0.0047	0.0105	0.0137

Air velocity: 0.66 m/s

Inlet drying air temperature: 60 °C

Inlet ambient temperature: 24.3 °C

Inlet ambient relative humidity: 62.3%

Table B.34. Results of drying run 34

Time (min)	Dry basis ashless extract		Dry basis acid concentrations		
	Measured	Supplied	Chloric acid	Carbonic acid	Sulfuric acid
0.00	1.1365	1.1365	0.0014	0.0007	0.0268
0.30	1.1040	1.1040	0.0014	0.0008	0.0252
1.00	0.9768	1.0079	0.0048	0.0046	0.0242
1.30	0.9177	0.9223	0.0041	0.0046	0.0235
2.00	0.7418	0.7607	0.0040	0.0071	0.0220
2.30	0.6637	0.6874	0.0010	0.0090	0.0211
2.60	0.5970	0.5821	0.0015	0.0074	0.0201
2.90	0.5388	0.5268	0.0020	0.0066	0.0219
3.00	0.4934	0.4818	0.0044	0.0088	0.0232
4.00	0.4400	0.4432	0.0017	0.0077	0.0232
5.00	0.4132	0.4109	0.0024	0.0074	0.0234
5.30	0.3834	0.3826	0.0049	0.0079	0.0214
6.00	0.3618	0.3479	0.0048	0.0081	0.0232
7.00	0.3385	0.3149	0.0030	0.0087	0.0208
8.00	0.2944	0.2779	0.0049	0.0100	0.0234
9.00	0.2524	0.2601	0.0042	0.0100	0.0238
10.00	0.2361	0.2330	0.0034	0.0085	0.0219
11.00	0.2023	0.2010	0.0047	0.0100	0.0230
12.00	0.1828	0.1849	0.0040	0.0090	0.0200
13.00	0.1679	0.1679	0.0044	0.0110	0.0230
14.00	0.1317	0.1334	0.0017	0.0100	0.0230
15.00	0.1175	0.1400	0.0040	0.0087	0.0215
16.00	0.1240	0.1291	0.0032	0.0095	0.0234
17.00	0.1126	0.1288	0.0015	0.0108	0.0206
20.00	0.0804	0.0752	0.0030	0.0095	0.0219

Air velocity: 0.12 m/s

Mass drying air temperature: 65.1 °C

Mass ambient temperature: 25.2 °C

Mass ambient relative humidity: 78.8%

Table D.20 Results of drying test (3)

Time (hour)	Dry basis moisture content		Dry basis ash concentrations		
	Measured	Simulated	Crystalline	Amorphous	Partial amorphous
0:00	1.3356	1.3356	0.0048	0.0107	0.0313
0:30	1.2317	1.2501	0.0044	0.0129	0.0278
1:00	1.0383	1.0389	0.0034	0.0100	0.0266
1:30	0.9331	0.9339	0.0049	0.0097	0.0272
2:00	0.7906	0.7913	0.0068	0.0098	0.0259
2:30	0.7013	0.6719	0.0063	0.0100	0.0278
3:00	0.5975	0.5988	0.0047	0.0087	0.0236
3:30	0.5413	0.5279	0.0049	0.0112	0.0365
4:00	0.4930	0.4936	0.0032	0.0107	0.0233
4:30	0.4343	0.4407	0.0032	0.0108	0.0241
5:00	0.4268	0.4327	0.0043	0.0097	0.0276
5:30	0.3844	0.3838	0.0039	0.0040	0.0133
6:00	0.3413	0.3361	0.0060	0.0100	0.0233
7:00	0.2968	0.2978	0.0032	0.0097	0.0230
8:00	0.2634	0.2632	0.0032	0.0104	0.0236
9:00	0.2384	0.2379	0.0032	0.0090	0.0231
10:00	0.2368	0.2366	0.0032	0.0101	0.0235
11:00	0.1941	0.1942	0.0032	0.0092	0.0230
12:00	0.1767	0.1767	0.0040	0.0079	0.0219
13:00	0.1377	0.1382	0.0033	0.0088	0.0239
14:00	0.1378	0.1475	0.0041	0.0100	0.0233
15:00	0.1237	0.1236	0.0032	0.0111	0.0232
16:00	0.1136	0.1248	0.0044	0.0114	0.0249
17:00	0.1043	0.1145	0.0035	0.0093	0.0232

Air velocity: 0.89 m/s

Mean drying air temperature: 60.8 °C

Mean ambient temperature: 23.4 °C

Mean ambient relative humidity: 77.3%

Table D.34. Results of drying run 36

Time (Days)	Dry basis moisture content		Dry basis acid concentrations		
	Measured	Estimated	Chloric acid	Lactic acid	Acetic acid
0.00	1.3163	1.3163	0.0034	0.0000	0.0000
0.50	1.2513	1.2591	0.0048	0.0130	0.0078
1.00	1.2173	1.2609	0.0078	0.0100	0.0065
1.50	1.1833	1.2432	0.0049	0.0097	0.0072
2.00	1.0783	1.0830	0.0069	0.0098	0.0039
2.50	0.9943	1.0048	0.0061	0.0100	0.0078
3.00	0.9033	0.9641	0.0047	0.0087	0.0056
3.50	0.8440	0.9014	0.0039	0.0112	0.0065
4.00	0.7930	0.8391	0.0032	0.0107	0.0038
4.50	0.7684	0.7889	0.0017	0.0100	0.0041
5.00	0.6756	0.7633	0.0043	0.0097	0.0038
6.00	0.5866	0.6807	0.0039	0.0081	0.0038
7.00	0.5066	0.6047	0.0060	0.0100	0.0032
8.00	0.4736	0.4733	0.0017	0.0090	0.0030
9.00	0.4090	0.4073	0.0032	0.0068	0.0036
10.00	0.4071	0.4060	0.0032	0.0098	0.0031
11.00	0.3878	0.3864	0.0062	0.0101	0.0038
12.00	0.3330	0.3341	0.0063	0.0090	0.0030
13.00	0.3027	0.2871	0.0040	0.0099	0.0039
14.00	0.2689	0.2636	0.0033	0.0088	0.0039
15.00	0.2687	0.2461	0.0061	0.0108	0.0038
16.00	0.2336	0.2333	0.0032	0.0118	0.0032
17.00	0.2111	0.2049	0.0068	0.0138	0.0049
18.00	0.1908	0.1936	0.0033	0.0098	0.0032
19.00	0.1872	0.1742	0.0046	0.0130	0.0030
20.00	0.1631	0.1548			
20.75	0.1432				
44.00	0.1088	0.1078			

Air velocity: 0.21 m/s

Mass drying air temperature: 40.0 °C

Mass ambient temperature: 21.0 °C

Mass ambient relative humidity: 78.7%

APPENDIX E FORTRAN PROGRAM FOR SIMULATING TRANSPORT PHENOMENA IN THE DRYING OF FULLY EXPOSED CARCASS MEATS

The computer program was written in FORTRAN 77 with some implementations of FORTRAN 90 to simulate temperature and mass concentration profiles, as well as angles for linear slice geometries. It consists of a main module and four major subroutines which constitute the core of the program. The main program is basically used for process data input, to call the major subroutines and to output computed results. Three of the subroutines were developed for solving the partial-differential equations of the drying model. The fourth subroutine was developed to generate three-dimensional grid for finite slices. Several auxiliary modules were also included to compute the physical properties of the product, ambient and drying air. Four subroutines of the Mathcad Recipe Software package (Press et al., 1992) were incorporated in the subroutines written for estimating mass diffusivity. These subroutines were used as provided or with the introduction of some minor modifications. Their names are listed at the end of this appendix.

SAMPLE OF INPUT FILE TEST 02

```

DRYING, MEAN AMBIENT AND WET BULB TEMPERATURES (C),
AND AIR VELOCITY (M/S)
READUNIT=1 FMT=(3F10.2,3F10.2,A,TW,YA)
    08.45  26.23  25.55  1.55
PRODUCT TEMPERATURE (C), MOISTURE AND ACID CONTENTS (G/G), DEN
READUNIT=1 FMT=(3,F10.2,3F10.4),(F8.3,8G3.0,AC)
    26.30  1.0000  0.4073  0.0880
PROCESS DURATION (H) AND TIME INCREMENT (S)
READUNIT=1 FMT=(3,F10.2,3F10.2)
    16000 00  0.25
NUMBER OF SPACE SUBINTERVALS (X, Y AND Z DIRECTIONS)
READUNIT=1 FMT=(3,I30)X,MY,NZ
    5  5  5
PRINTING STEP IN TIME (S) AND SPACE (UNITS - X, Y, Z DIRECTIONS)
READUNIT=1 FMT=(3,F10.2,3,F10.2,3,F10.2,F10.2,F10.2)
    128 00  3  3  3
8      1.0000  26.2  24.4
600    0.0035
900    0.0141  26.2  24.4
1800   0.042  26.7  24.9
3600   0.0697  26.7  25.3
5400   0.0885  26.8  25.5
7200   0.0978  26.8  25.6
9000   0.0985  26.5  25.3
10800  0.1064  26.5  25.5
12600  0.1093  26.5  25.1
14400  0.1097  26.5  25.5
16200  0.109  26.5  26.0
18000  0.1094  26.0  26.0
21400  0.1002  26.0  26.2
27000  0.113  26.6  25.5
30600  0.119  26.5  25.2
34200  0.1734  25.5  25.8
41400  0.1397  26.0  25.6
45000  0.129  27.0  26.3
48600  0.1115  27.4  25.5
52200  0.0889  27.0  25.4
55800  0.0871  27.0  25.1
59400  0.0812  26.8  25.3

```

LIST OF REFERENCES

- Ahney, T.S. 1994. The effect of pod storage on the sprout of dry cocoa beans. *Indonesian Publication (Indonesian)* 22: 137-145.
- Ames, W.F. 1977. *Numerical Methods for Partial Differential Equations*. Academic Press, Inc., New York.
- Anderson, D.A., J.C. Tannehill, R.W. Fletcher. 1984. *Computational Fluid Mechanics and Heat Transfer*. Taylor & Francis, Bristol, PA.
- Aris, R. 1962. *Vectors, Tensors and the Basic Equations of Fluid Mechanics*. Dover Publications, Inc., New York.
- Balaban, M. 1989. Effect of volume change in foods on the temperature and moisture content predictions of simultaneous heat and moisture transfer models. *Journal of Food Process Engineering* 12: 45-60.
- Balaban, M.G., C.A. Zorita, R.P. Singh and E.-I. Heykkanen. 1987. Estimation of heat of moisture sorption and improved criteria for evaluating moisture sorption isotherm equations for foods. *Journal of Food Process Engineering* 10: 53-70.
- Barbier, P.R.P. 1979. Contribuicao para o conhecimento dos aspectos compositionais da semente e do mel de cacau. *Revista Brasileira (Brazil)* 9: 53-61.
- Barbier, P.R.P. and A.S. Lopes. 1979. The effect of bean moisture content on the susceptibility of seeds to contamination by insects. Unpublished internal report. CRIPLAN/IBRAC. Brazilian-Cocoa Research Center, Maracá, PA, Brazil.
- Bal, B., R. Mayas, G. Cross, L. Pullman and M.B. Reid. 1989. Chemical and physical changes in the pulp during ripening and post-harvest storage of cocoa pods. *Journal of the Science of Food and Agriculture* 48: 189-204.
- Diri, R.S., W.E. Howard and E.N. Legidoon. 1968. *Transport Phenomena*. John Wiley & Sons, New York.
- Bloomfield, E. 1994. Cocoa: costs of production in various producing countries. *Cocoa Grower's Bulletin* 22: 9-11.
- Datta, A. and D.R. McGee. 1971. Packed bed drying characteristics of cocoa beans. *West Indian Journal of Engineering* 2: 3-12.

- Brown, A. and D. R. McGee. 1978. Fundamental wetland drying characteristics of cocon (braz). *Tropical Agriculture (Trinidad)* 55: 385-400.
- Devender, D. B., F. W. Buhner, Adams and C. W. Hall. 1990. *Drying and storage of grains and seeds*. Van Nostrand Reinhold, New York.
- CEPLAC. 1982. *Atlas do bico-de-coco*. Brazilian Coconut Research Center (Ilheus, BA, Brazil).
- CEPLAC. 1984. *Processos internacionais do coco*. Brazilian Coconut Research Center (Ilheus, BA, Brazil).
- Cook, L. R. 1975. *Chocolate Production and Use*. Books for Industry, Inc. New York.
- Crank, J. 1975. *The Mathematics of Diffusion*. Clarendon Press, Oxford.
- Cunha, J. 1980. *Respostas de variedades de coco relacionadas as variáveis de manejo em cultura irrigada*. *Revista Theobroma (Brazil)* 13: 43-48.
- Cunha, J. 1989. *Resposta de coco para o preparo produtivo*. 663-676. In: *Proceedings of the 9th International Coconut Research Conference* Rome, Italy.
- Cunha, J. 1990. *Desenvolvimento de variedades Tabular, com ventilação forçada em variegas de coco*. *Agrotopos (Brazil)* 3: 39-45.
- Cunha, J. and E. S. Sereyde. 1991. *Tecnologia disponível para o beneficiamento e armazenamento do coco*. *Boletim Técnico ITD*. Brazilian Coconut Research Center (CEPLAC/CIPEC) Ilheus (BA, Brazil).
- De Zure, 1974. *Product grade - coconut powder*. *Canalizador De Zure B.V.* (Kong nam de Zure, Holland).
- Dias, J. C. and M. G. M. Avela. 1988. *Influência de período de pre-secagem do fruto no tempo de beneficiamento e acidez do coco*. *Agrotopos (Brazil)* 2: 142-150.
- Dias, J. C. and M. G. M. Avela. 1990. *Influence of the drying process on the acidity of coconut husk*. *Agrotopos (Brazil)* 3: 19-24.
- Duane, R. J. B., G. Godfrey, T. H. Yip, G. L. Penzance and T. Thanasangkul. 1989. *Improvement of Malagasy-coconut from Brevia by modification of harvesting, fermentation and drying methods-the Ilheus-Culbury process*. Technical report of

the joint Project Suez-Darby Plastics and Calfrop Ltd., Kuala Lumpur, Malaysia.

Draper, A.G. 1974. *Processos de Secagem*. Medellin, Colombia.

Fiksen, R.W. 1983. *Fundamentals of Transport Phenomena*. McGraw-Hill Book Company, New York.

Furrow, S.J. 1982. *Partial Differential Equations for Scientists and Engineers*. Dover Publications, Inc., New York.

Furlayson, H.A. 1980. *Nonlinear Analysis in Chemical Engineering*. McGraw-Hill International Book Company, New York.

Forland, K.S., T. Forland, and S.K. Rindge. 1988. *Irreversible Thermodynamics: Theory and Applications*. John Wiley & Sons Ltd., Chichester, UK.

Forsyth, W.G.C. and V.C. Quastel. 1963. Mechanisms of coxal curing. *Advances in Enzymology* 23: 437-492.

Forras, M. and M.R. Olson. 1989. Drying kinetics: thermodynamic and hydrodynamic as applied to foods and grains. 115-134. In: *Advances in Drying*. Volume 1. Mujumdar, A.S. (ed.) Hemisphere Publishing Corporation, New York.

Forras, M. and M.R. Olson. 1991a. A non-equilibrium thermodynamic approach to integrated phenomena in capillary porous media. *Transactions of the ASAE* 34: 756-760.

Forras, M. and M.R. Olson. 1991b. Non-equilibrium thermodynamic approach to heat and mass transfer in capillary media. *Transactions of the ASAE* 34: 761-769.

Forras, M., M.R. Olson and F.R. Durrant Jr. 1991. Heat and mass transfer analysis of integrated solvent drying and roasting. *Journal of Agricultural Engineering Research* 50: 209-225.

Freese, E.B., J. Cuello and F.J.R. Paoletti. 1985. Tercer de un ensayo para desarrollar técnicas para curar. *Revista Têxtil (Belo)* 14: 293-304.

Freese, E.B., R.F. Schwan and J. Cuello. 1992. Caracterização, armazenamento e classificação do cacau. 33-39. In: *Seminário de Processos de Curar no Armazenamento de Alimentos*. A.P.S., M.W. Idalberto and M.R.M. Stanton. (eds.) Fundação Coordenação de Aperfeiçoamento de Pessoal de Nível Superior (CNPq/CEPEC). Belo Horizonte, Brazil.

- Freitas, E.R., A.P. Simões, P.T. Feres, F.L. Pinna, E.C. Marins, R.F. Salazar, A. Lacerda, B.E. Chaput, M.B.S. Santos and H.J.S. Feres. 1999. Uses of residues and by-products of cocoa. Brazilian Cocoa Research Center (CEPLAC/CEPEC), Ilheus, BA, Brazil.
- Furland, G.D. 1969. A survey of recent Soviet research on the drying of solids. *The Canadian Journal of Chemical Engineering* 47: 378-388.
- Furt, T. and K.-J. Hignallaw. 1992. Heat and moisture transfer with thermodynamically irreversible flows I. Mathematical model development and numerical solution. *Transactions of the ASAE* 35: 1537-1546.
- Gleick, B.M. 1970a. A new drying system for cocoa beans. *Agricultural Engineering* 53: 16.
- Gleick, B.M. 1970b. Engineering aspects of cocoa drying in Brazil. *Revista Brasileira (Brazil)* 2: 23-37.
- Gleick, B.M. 1970c. Drying cocoa beans by gas. *Worldscope* 15: 232-235.
- Gleick, B.M. 1970d. Physical properties of cocoa beans. *Turkische (Cocoa Bean)* 23: 433-440.
- Gleick, B.M. 1976. The shape and size of cocoa beans. *Turkische (Cocoa Bean)* 26: 134-138.
- Gleick, B.M. and J. Corbin. 1975. Effect of process on wet drying of cocoa beans in Brazil. *Turkische (Cocoa Bean)* 25: 586-603.
- Godiva Chocolonier, Inc. (United). A brief history of chocolate. Godiva/DeLiax Home Page. <http://www.godiva.com>. Internet.
- Guimarães, I.C.P., A.E.R. Magno, B.P. Mendonça and A. Minato. 1992. Cultura e beneficiamento do cacau no Brasil. Brazilian Cocoa Research Center (CEPLAC/CEPEC). Ilheus, BA, Brazil.
- Hall, C.W. 1969. Editorial. *Drying Technology* 1: 1-2.
- Hess, A.C. and R.M. Maddox. 1963. *Mass Transfer: Fundamentals and Applications*. Prentice-Hall, Englewood Cliffs, N.J.
- Henderson, D. and L. Gosw. 1983. Thin layer wet drying of soybeans and wheat beans. *Journal of Food Technology* 18: 587-603.

- ICCQ: 1993. Quarterly Bulletin of cocoa statistics of the International Cocoa Organisation, 20(1).
- Incropera, F.P. and D.P. Dewitt, 1990. Fundamentals of Heat and Mass Transfer. Wiley & Sons, Inc. New York.
- Jeyen, D.S., S. Cankowala, S. Patil and W.E. Muir, 1981. Review of thin-layer drying and wetting equations. Drying Technology 9, 319-333.
- Jung, S. and P.S. Dirlich, 1981. Effect of roasting on solids transformation of cocoa beans. Journal of the Institute of Food and Agriculture 54, 317-321.
- Justi, E.L. and S.G. Justi, 1984. Fermentations involved in the production of cocoa, coffee and tea. Progress in Industrial Microbiology 19 411-458.
- Kaplan, W. 1991. Advanced Calculus. Addison-Wesley Publishing Company, Inc. Reading, Mass.
- Katchalsky, A. and P.F. Curran, 1967. Nonequilibrium Thermodynamics in Biophysics. Harvard University Press, Cambridge, Mass.
- Kear, R.B. 1993. Drying: Principles and Practice. Pergamon Press Ltd., Oxford.
- Kear, R.B. 1998. Theoretical foundations of drying theories: 1-30. In: Advances in drying. Volume 8. Mujumdar, A.S. (ed.) Hemisphere Publishing Corporation, New York.
- Knap, A.W. 1957. Cocoa Fermentation. John Ede, Sons and Cussons Ltd. London.
- Kreith, F. and W.Z. Black, 1980. Basic Heat Transfer. Harper & Row, Publishers, New York.
- Lang, S. 1994. Calculus of Several Variables. Springer-Verlag, New York.
- Lau, S.A. 1993. Editorial. Cocoa Currents Bulletin 47, 1.
- Latham, D.W. and C.L. Peterson, 1981. Cocoa fermentation. Biotechnology 5, 129-133.
- Lee, H.T.L. 1978. The criteria and mechanism for the removal of cocoa bean acidity. 425-439. In: Proceedings of International Conference of Cocoa and Chocolate. Kuala Lumpur.

- Lislefield, J.B. and M.R. Olsen: 1992 Moisture diffusivity in pasta during drying. *Journal of Food Engineering* 17: 117-142.
- Lotell, R.C., Freund, R.J. and Spearot, P.C.: 1981 *SAS System for Linear Models: SAS Series in Statistical Applications*. SAS Institute Inc., Cary, NC.
- Lopez, A.S.: 1985 Factors associated with cocoa bean acidity and the possibility of its reduction by improving fermentation. *Revista Brasileira (Brasil)* 13: 233-244.
- Lopez, A.S.: 1986 Chemical changes occurring during the processing of cocoa. 15-33. In: *Proceedings of the Cocoa Biotechnology Symposium*. Danish, P.S. (ed.), Pennsylvania State University, State College.
- Lopez, A.S. and C.R. McDonald: 1981 Definición de normas a nuevos estudios en equilibrio de los valores de chocolate con tests de degustación. *Revista Brasileira (Brasil)* 11: 268-277.
- Martynenko, G.D., N.V. Polyakovich and G.I. Rudin: 1980 Mathematical methods and kinetics of heat and mass transfer with phase change in porous media. 103-118. In: *Advances in drying*. Vol. 1. Mujumdar, A.S. (ed.) Hemisphere Publishing Corporation, New York.
- Meat, P. and M. Eves: 1988 Modelling grape-drying kinetics. 283-313. In: *Proceedings of the International Symposium of Fermentation and Drying of Foods*. Peiris, S. (ed.) Amsterdam, Holland.
- McDonald, C.R.: 1981 The drying of cocoa and yellow peas. Unpublished project report. Brazilian Cocoa Research Center (CEPLAC/CEPEC), Ilheus, BA, Brazil.
- McDonald, C.R., J. Cunha and E.S. Peire: 1988 Estado da arte da tecnologia de secagem. *Comunicado Técnico: perspectivas para melhoria de sua desenvolvimento*. Boletim Técnico 94. Brazilian Cocoa Research Center (CEPLAC/CEPEC), Ilheus, BA, Brazil.
- McDonald, C.R. and E.S. Peire: 1981 Cocoa drying in a platform type dryer with and without drying air recirculation. *Tropical Agriculture (Trinidad)* 58: 283-285.
- McDonald, C.R. and E.S. Peire: 1982 Investigation of the characteristics of a traditional natural convection cocoa-drier. *Tropical Agriculture (Trinidad)* 59: 25-32.
- McDonald, C.R., B.A. Lam and A.S.F. Lopez: 1981 Cocoa drying: a review. *Cocoa (Gainesville Bulletin)* 31: 3-43.

- Merson, A.S. and A.S. Mujumdar. 1983. Drying of solids: principles, classification, and selection of dryer. 3-46. In: *Handbook of Industrial Drying*. Mujumdar, A.S. (ed.) Marcel Dekker, Inc., New York.
- Mittelman, H.D. and M.H. Grook. 1984. *Unified Analysis and Solutions of Heat and Mass Diffusion*. Wiley & Sons, Inc., New York.
- Mooreau, H.J. 1970. *Entropy for Biologists: An Introduction to Thermodynamics*. Academic Press, Inc., New York.
- Mujumdar, A.S. 1980. *Advances in Drying*. Volume I. Hemisphere Publishing Company, New York.
- Perry, J.L. 1985. Mathematical modelling and computer simulation of heat and mass transfer in agricultural grain drying. *American Journal of Agricultural Engineering Research* 32: 1-26.
- Park, M. 1998. A theoretical model for thin-layer grain drying. *Drying Technology* 8: 401-423.
- Park, M. and I. Dapuntovic. 1998. Diffusion coefficient for corn drying. *Transactions of the ASAE* 31: 1655-1656.
- Pereira, F.F.V. and F.M.L. Pereira. 1995. Considerações sobre parâmetros de dissecação de produtos para armazenamento de grãos submetidos à secagem. *Boletim Técnico IGT-CR/PLACEPEC*. Ilheus, BA, Brazil.
- Peterson, G. and W.H. Corwin. 1948. Turbulent heat and mass transfer from stationary particles. *Canadian Journal of Chemical Engineering* 26: 35-42.
- Powell, B.D. 1981. The quality of cocoa beans-the needs of the manufacturer. 751-758. In: *Proceedings of the 8th International Cocoa Research Conference*, Cartagena, Colombia.
- Prado, E.F., T. Haru, J.B. Pinheiro, and F.T.L. Thibaut. 1981. Possibilidade de armazenamento de castor durante o processo de secagem, em câmaras fixas, a 60 e 80°C. *Revista Brasileira de Engenharia* 11: 125-130.
- Press, W.H., S.A. Teukolsky, W.T. Vetterling, and B.P. Flannery. 1992. *Numerical Recipes in FORTRAN: The Art of Scientific Computing*. Cambridge University Press, New York.

- Quemel, F.C. 1965. Agents inducing the death of cancer cells during fermentation. *Journal of the Science of Food and Agriculture* 15:441-443.
- Rakusandj, D.A. 1959. *Handbook of Nonlinear Regression Models*. Marcel Dekker, Inc., New York.
- Ribeiro, M.C. de A. 1984. Características físico-químicas das amostras de carne de *Amazona domestica*. 789-793. In: *Proceedings of the 10th International Cancer Research Conference, Santo Domingo, Dominican Republic*.
- Rosen, J.B. and K.-I. Popelarsen. 1977. Simultaneous heat and moisture transfer in dehydrated food - a review of theoretical models. *AIChE Symposium Series* 73: 75-84.
- Saizawa, J.S. 1984. Análises de propriedades físicas e curvas de ressecamento, em carnes de frango, de amostras de carne (*Thermoderma vacca* L.). Unpublished MS thesis. Universidade Federal de Viçosa, Brazil.
- Schwan, R.F. 1984. Variação na natureza do processo (mecanismo) de fermentação de carne na Índia: e identificação das espécies de bactérias envolvidas nesse processo. Unpublished MS thesis. Universidade Federal de Viçosa, Brazil.
- Schwan, R.F., A. Lopez, D.G. Silva and M.C.D. Vargas. 1990. Influência da frequência e intensidade de transferência sobre a fermentação de carne e qualidade da charque. *Aplicaciones (Brazili)* 2: 23-31.
- Shelton, B. 1967. Artificial drying of meat loaves. *Tropical Agriculture (Trinidad)* 44: 125-132.
- Singh, A.A., E. Leonard and G.B. Thorpe. 1993. A solution procedure for the equations that govern three-dimensional free convection in bulk mixed gases. *Transactions of the ASME* 115: 1109-1113.
- Stern, L.B. and D.B. Peis. 1972. *Elements of Transport Phenomena*. McGraw-Hill Book Company, New York.
- Stefan, A.H.P. 1945. *Differential Mass Transfer*. R.E. Krieger Pub. Co., Mishaw, Pa.
- Stellary, J.C. 1967. General balance equations for a phase interface. *Industrial & Engineering Chemistry, Fundamentals* 6: 304-115.
- Stellary, J.C. 1968. *Momentum, Energy and Mass Transfer in Continua*. Krieger Publishing Company, Huntington, N.Y.

- Smith, G. B. 1978. *Numerical Solution of Partial Differential Equations: Finite Difference Methods*. Clarendon Press, Oxford.
- Smith, R. W. 1994. Cocoa production systems: options and constraints. *Cocoa Grower's Bulletin* 47: 39-46.
- Soltanpour, S. 1987. Drying fundamentals. 817-854. In: *Handbook of Industrial Drying*. Mujumdar, A.S. (ed.). Marcel Dekker, Inc., New York.
- Standart, G. 1964. The mass, momentum and energy equations for heterogeneous flow systems. *Chemical Engineering Science* 19: 223-253.
- Stewart, J. F. 1982. *Mathematical Modeling of Transport Phenomena*. Prentice Hall, Englewood Cliffs, New Jersey.
- Stenlund, C. and C. Lopez-Camacho. 1983. Energy aspects in drying. 433-462. In: *Handbook of Industrial Drying*. Mujumdar, A. S. (ed.). Marcel Dekker, Inc., New York.
- Stenlund, C. and T. Kärén. 1984. *Drying: Principles, Applications and Design*. Gordon and Breach Science Publishers, Yverdon, Switzerland.
- Sun, De-Wen and J. L. Woods. 1994. Low temperature moisture transfer characteristics of barley: thin-layer models and equilibrium isotherms. *Journal of Agricultural Engineering Research* 58: 273-283.
- Taylor, R. and R. Krishna. 1993. *Multicomponent Mass Transfer*. John Wiley & Sons, Inc., New York.
- Tong, C. H. and D. B. Lund. 1990. Effective moisture diffusivity in porous materials as a function of temperature and moisture content. *Biotechnology Progress* 6: 47-59.
- Wagman, G. E., D. Mannes-Kramer, and G. D. Barrow. 1996. An analysis of mass transfer in air-drying of foods. *Drying Technology* 14: 323-342.
- van Arman, J. 1983. *Food Dehydration*, Vol. 1. AVI Publishing Company, Inc., Westport, Conn.
- van Doikal, J. and P. M. Hoorigan. 1994. Analysis of diffusion in macroporous media in terms of a porosity, a tortuosity and a convective factor. *International Journal of Heat and Mass Transfer* 17: 1093-1103.

- Vincent, L.-C. and P. Doley. 1983. *Étude des sources et modes d'enrichissement pour la fermentation des froms de caes*. Technical Report. IRCCADIRSAT, Montpellier, France.
- Wakeling, S.A. 1994. Review of production, consumption, stocks and prices. *Cocoa*. *Cocoa's Bulletin* 42: 2-8.
- Wexler, A. and L. Ginzburg. 1975. Vapor pressure equation for water in the range of 0 to 100°C. *NBS Journal of Research* 75A: 231-239.
- Wilhelm, L.R. 1976. Numerical calculation of psychrometric properties in SI units. *Transactions of the ASHRAE* 79: 318-321, 325.
- Wilkinson, A.P. 1985. Marketing, 331-342. In *Cocoa*. Wood, G.A.R. and R.A. Lutz (eds.) Longman, London.
- Winnacker, S., R. Badermeier and R. Neumann. 1978. *Thermodynamics of Monoglyceride Processes*. Polish Scientific Publishers, Warsaw.
- Wood, G.A.R. 1971. Cocoa drying. *The Planter* 47: 449-457.
- Wood, G.A.R. and R.A. Lutz. 1980. *Cocoa*. Longman Int., New York.

BIOGRAPHICAL SKETCH

Ernesto José Freire was born at São João do Jacaré (Serra da Capim), State of Minas Gerais, Brazil, in 1933. He completed his elementary and secondary education in his home village. In 1955, he received his Bachelor of Science degree in Agronomy from the Federal University of Viçosa, Minas Gerais State, Brazil. He joined the staff of the Brazilian-Corn Research Center (CEPLAC/CEPEC), Bahia State, Brazil, in 1956. For three years he served as the Brazilian counterpart on a joint R&D program on corn-drying between the British and Brazilian governments, under the supervision of Dr. Oliver Richard McDonald. In 1959, he started a Master of Science program at National College of Agricultural Engineering, at Solihull, England, sponsored by the British Council, returning to CEPLAC/CEPEC in 1961. A fellowship was granted to him in 1961, by the Brazilian Government through the National Research Council (CNPq), to pursue his doctoral degree in the Agricultural and Biological Engineering Department, University of Florida.

I certify that I have read this study and that in my opinion it conforms to acceptable standards of scholarly presentation and is fully adequate, in scope and quality, as a thesis for the degree of Doctor of Philosophy



Kiar Yun-Chan, Chairman
Professor of Agricultural and Biological
Engineering

I certify that I have read this study and that in my opinion it conforms to acceptable standards of scholarly presentation and is fully adequate, in scope and quality, as a thesis for the degree of Doctor of Philosophy



C. David Baird
Professor of Agricultural and Biological
Engineering

I certify that I have read this study and that in my opinion it conforms to acceptable standards of scholarly presentation and is fully adequate, in scope and quality, as a thesis for the degree of Doctor of Philosophy



Michael G. Selenko
Associate Professor of Food Science
and Human Nutrition

I certify that I have read this study and that in my opinion it conforms to acceptable standards of scholarly presentation and is fully adequate, in scope and quality, as a thesis for the degree of Doctor of Philosophy



Arthur A. Trevisan
Professor of Agricultural and Biological
Engineering

I certify that I have read this study and that in my opinion it conforms to acceptable standards of scholarly presentation and is fully adequate, in scope and quality, as a thesis for the degree of Doctor of Philosophy



Stephen A. Harrison
Professor Chemical
Engineering

This dissertation was submitted to the Graduate Faculty of the College of Engineering and to the Graduate School and was accepted as partial fulfillment of the requirements for the degree of Doctor of Philosophy

December 1995



W. M. Phillips
Dean, College of
Engineering

Karen A. Holbrook
Dean, Graduate School